Effect of environmental conditions on deformation of thin composite laminates made by 4D printing

Alan Victor Alfred Raju

A Thesis

in

The Department

of

Mechanical and Industrial Engineering

Presented in Partial Fulfillment of the Requirements

for the Degree of Master of Applied Science (Mechanical Engineering)

at

Concordia University

Montreal, Quebec, Canada

July 2018

CONCORDIA UNIVERSITY
SCHOOL OF GRADUATE STUDIES

This is to certify that the thesis prepared,

By: **Alan Victor Alfred Raju**

Entitled: "**Effect of environmental conditions on deformation of thin composite laminates made by 4D printing.**"

and submitted in partial fulfillment of the requirements for the degree of

Master of Applied Science (Mechanical Engineering)

complies with the regulations of this University and meets the accepted standards with respect to originality and quality.

Signed by the Final Examining Committee:

_____ Chair
Dr. Ayhan Ince

_____ Examiner
Dr. Maria Elektorowicz

_____ Examiner
Dr. Tsz Ho Kwok

_____ Supervisor
Dr. S. V. Hoa

Approved by

_____
Dr. Mamoun Medraj Graduate Program Director

_____
Dean Amir Asif Faculty of Engineering & Computer Science

Date: _____

ABSTRACT

The process of 4D printing of composites (4DPC) can make curved laminates without the need for curved molds. This is due to the use of unsymmetric laminates. Stacks of laminates with specified layup sequence (for thin composite laminates) are deposited on to flat molds using an automated fiber placement machine (AFP). On curing, the laminate takes a curved shape which can be determined by laminate theory. The factors that contribute to the curvature of the samples are the difference in coefficients of thermal contraction and shrinkage of the resin during curing.

When a thin composite laminate made by 4DPC is placed in room conditions, it is observed to open up and changes its radius of curvature over time. This is due to the absorption of moisture from the surroundings thuough diffusion.

This research aims to find the effect of the contribution of temperature, resin shrinkage and moisture absorption on the radius of curvature of the samples.

To analyze the contribution of difference in coefficients of thermal contraction and resin shrinkage on the curvature of the samples, the samples were first completely desorbed of moisture by desorption test and then a temperature cycling test is carried out. The results obtained from temperature cycling test are compared with the theoretical results generated using the MATLAB program. To study the effect of moisture on the thin composite samples, moisture absorption tests were performed to determine the change in radius and weight of samples over the course of time.

Acknowledgment

First and foremost, I would like to highly appreciate my supervisor Dr. Suong Van Hoa for his invaluable guidance from the beginning of the work as well as unwavering support, encouragement and continuous patience throughout the research. I am sincerely grateful to him for giving me the opportunity to get such a precious experience.

It is an honor to express my gratitude to the committee members who devoted their time to the detailed review of my thesis.

I would also like to acknowledge Dr. Daniel Rosca for his technical support and practical guidance, which facilitated this research. I also wish to express my gratitude to my friend Jeffrey Fortin Simpson who helped me with sample preparation during the early stages of this research.

I wish to express my special thanks to all the technical and administrative staff of Mechanical, Industrial and Aerospace Engineering Department for their excellent assistance.

The final recognition goes to my parents and my sister, who have truly inspired me and shown care for success in all aspects of my life. I feel very fortunate to have them in my life, and I owe then for all the things that they have done for me. Their love, support, and understanding kept me moving throughout this journey.

Last but not the least I would like to thank my friends Jana, Kire, Nikola, Dilani, Deepak, Sonu, Mithun, Melvin, Chaithin, Kamal, Urvi, Assad, Thomas, Aby, Amar, Aravind and Rassal for supporting me with their constant companionship.

CONTENTS

LIST OF FIGURES

LIST OF TABLES

LIST OF NOMENCLATURE

a	= Length of material.
Δa	= Change in length of material.
A, B & D	= A, B, D matrix of laminate
b	= Breadth of material.
Δb	= Change in width of material.
D	= diffusion coefficient.
E_1, E_2, G_{12}	= Elastic moduli of the material.
Δh	= Change in thickness of material
H	= Thickness of laminate
K_x, K_y & K_{xy}	= Curvature in x, y and xy directions.
M_m	= Maximum moisture content.
ΔC	= Moisture content (%).
M_x^T, M_y^T & M_{xy}^T	= Thermal moment resultants
M_x^S, M_y^S & M_{xy}^S	= Moment resultants due to shrinkage.
M_x^H, M_y^H & M_{xy}^H	= Moment resultants due to moisture.
N_x^T, N_y^T & N_{xy}^T	= Thermal stress resultants.
N_x^S, N_y^S & N_{xy}^S	= Stress resultants due to shrinkage.
N_x^H, N_y^H & N_{xy}^H	= Stress resultants due to moisture.
t	= Thickness of material.
ΔT	= Difference in temperature (C)
W	= Weight of the sample at given time.
W_d	= Weight of the dry sample.
V_{12} And V_{21}	= Poisson ratios of respective layers of lamina.
z	= length in the thickness direction.
θ	= Angle between fiber direction and x-coordinate axis of the laminate
$\varepsilon_x^*, \varepsilon_y^*$ & ε_{xy}^*	= In plane strain.
$\varepsilon_x^s, \varepsilon_y^s$ & ε_{xy}^s	= off axis strain due to shrinkage.
ε_H	= Hygroscopic Strain
β_H	= Coefficient of moisture expansion (/%).
β_1	= Coefficient of moisture expansion in the longitudinal direction (/%).
β_2	= Coefficient of moisture expansion in the transverse direction (/%).

CHAPTER 1: INTRODUCTION & LITERATURE REVIEW

Use of composite materials has increased in recent years because of their high mechanical strength combined with their lightweight. Composite materials are a compelling choice for aerospace industry manufacturer since their primary aim is to reduce the weight of the overall aircraft. Composites also have been used in making automobiles and wind turbine blades.

1.1 Composite materials and their manufacturing

Composite materials are manufactured by combining two or more different materials with different physical properties usually known as matrix and reinforcements. Figure 1.1 shows steps in the manufacturing of composites. Reinforcements for composite material are in the form of fibers, particles or flakes that provide the mechanical strength of the material [1].

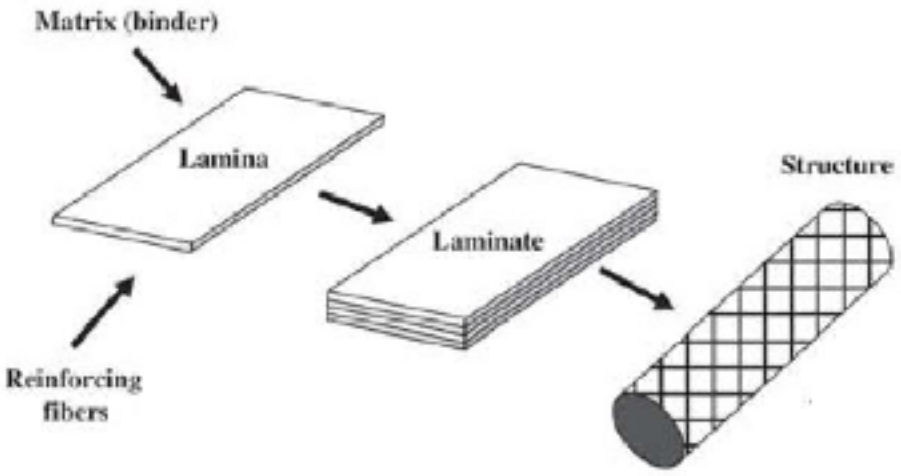

Figure 1.1 Manufacturing of composite materials [1]

The composite structure is usually a laminate made up of layers of composite materials with various fiber orientations. These structures are classified as thin and thick laminates depending on their thickness of complete structure and number of layers present in the structure.

1.1.1 Fibers

Reinforcing fibers are known as bones of composite materials as they provide the characteristic mechanical properties of the composites. These fibers have high strength and modulus [4]. They show high resistance to solvents and temperatures. The composites are well known for weight sensitive applications, the primary reason behind this is the density of the fibers which is low when compared to other reinforcing materials. Typical fiber reinforcements include carbon fibers, glass fibers, Kevlar and thermoplastic fibers [1].

1.1.2 Matrix

Matrix act as binders for the composite materials since they hold the reinforcements and help to distribute the stress more equally. Resins are mainly classified into Thermoset and Thermoplastic Matrix [1].

1.1.2.1 Thermoset resins

These resins have the property of irreversibility, once these resins are cured they become infusible and insoluble. The reason behind this is the formation of a covalently crosslinked and thermally stable three-dimensional network. The short molecular chains are also the reason for inhibition of movements of molecules [4]. Unlike thermoplastics, these resins are formed from low molecular weight liquid with low viscosity. Some of the typical resin systems are epoxy resins, polyimides, and polyurethanes.

1.1.2.2 Thermoplastic resins

The thermoplastic polymers are known for their linear structure in the molecules without any linking between them. The bonds present between the individual molecules are Vander walls and hydrogen bonding. Heating can remove these bonding forces. When the resin is subjected to heat, the molecules tend to move to new positions. On cooling the resin these molecules freeze in their new positions. This is the reason why the thermoplastic resin can be reused and recycled. Some of the advantages of thermoplastic resin over thermoset resin are their unlimited storage time at room temperature, ease of handling, recyclability and short fabrication time [4]. Typical thermoplastic resins are nylons, polyolefin, and polycarbonates.

1.1.3 Manufacturing Techniques

The composite structures can be manufactured using a variety of techniques such as Manual hand layup and autoclave processing, Filament Winding, Fiber Placement, Pultrusion, Liquid Composite Molding [1]. Manufacturing of composites is an important factor which determines the cost of the final product. Hence the selection of perfect manufacturing technique is highly critical. Some of the manufacturing techniques are explained below.

1.1.3.1 Hand Lay Up technique

This technique involves manually laying up of layers by hand and then curing them in an oven or autoclave using their respective curing cycle. The process for curing the material is shown in figure 1.2. The primary limitation of this process is the low volume manufacturing of the final product since this process takes a lot of time for large-scale production.

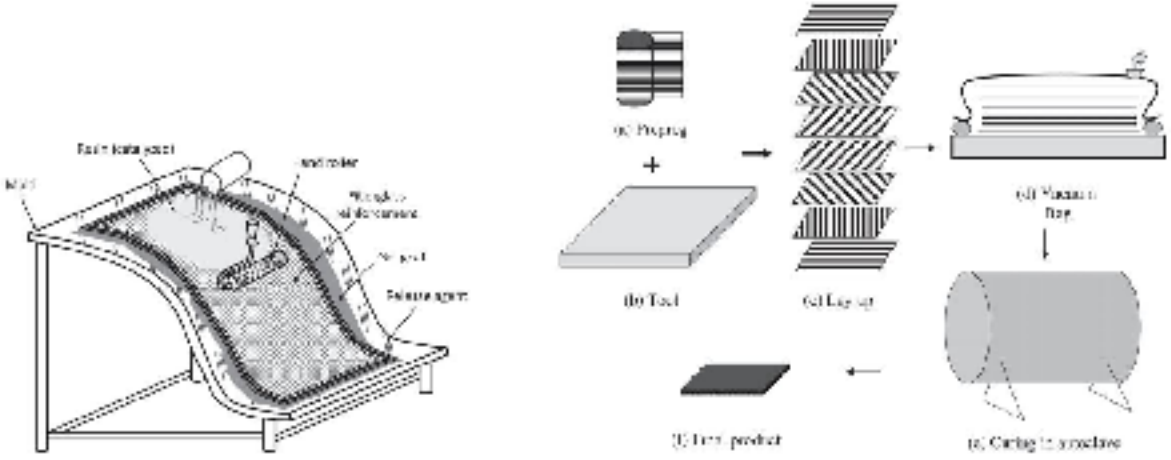

Figure 1.2 Hand layup technique and processing method of curing in an oven [1]

1.1.3.2 Filament winding and Fiber Placement

Filament winding is a process used to make composite structures such as pressure vessels, storage tanks, and pipes [1]. This technique is used to make composite structures of cylindrical shape. This is the primary limitation of the filament winding process that it is limited to manufacturing products of a specific

shape. Fiber placement is similar to filament winding in which fibers are placed on to the surface with application of heat.

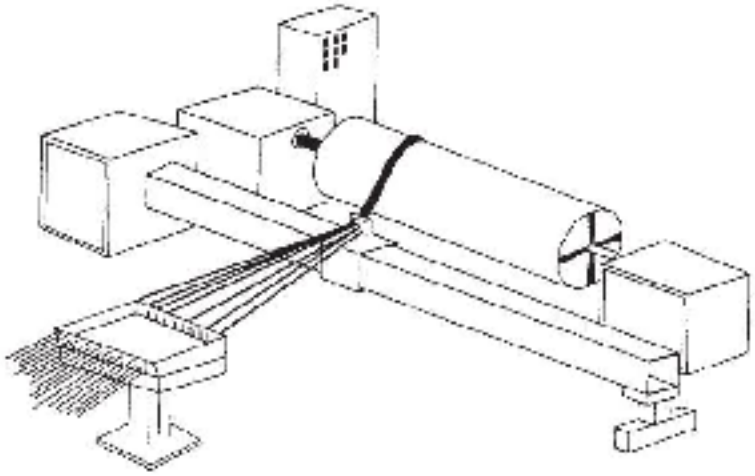

Figure 1.3 Schematic representation of filament winding [1]

1.1.3.3 Pultrusion

Pultrusion is a manufacturing process in which fibers are drawn from fiber tows and passed through a resin bath for impregnation, After that the fibers are collimated into an aligned bundle before entering into the heated die. A pictorial representation is shown in figure 1.4.

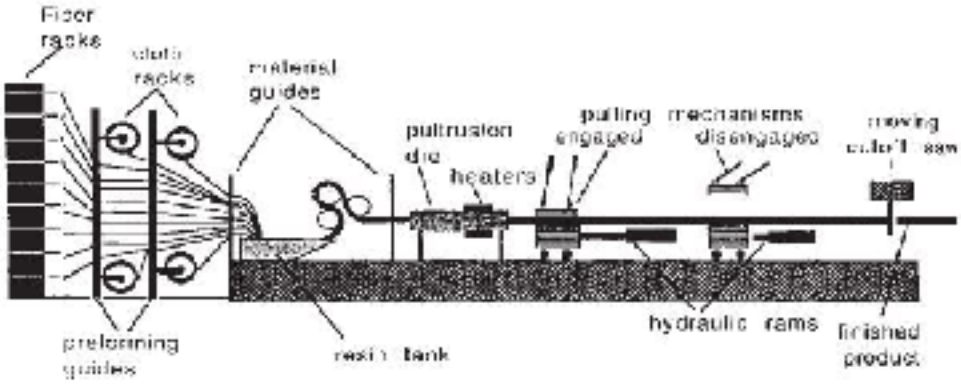

Figure 1.4 Schematic representation of pultrusion process [1]

1.1.3.4 Liquid composite molding

Liquid composite molding (LCM) is a process in which a preform is made using dry fibers. Compression molding, braiding or knitting can be used to make the preform. Later this preform is placed inside the tool into which resin is infused along with catalyst required for curing. After curing the resin, the product is de-molded as shown in figure 1.5.

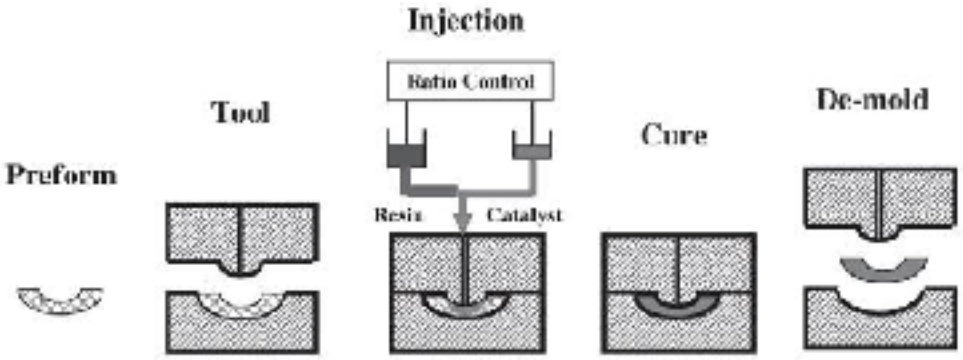

Figure 1.5 Schematic representation of Liquid composite molding (LCM) process [1]

All the manufacturing processes mentioned above have various limitations such as:

- Some of the techniques require prepreg, which usually has a low shelf life which leads to a time constraint.
- Some of the processes require autoclave hence for manufacturing large parts such as turbine blades, or a boat will be practically impossible.
- For processes like liquid composite molding (LCM), the preform needs to be held with the help of binders, and the dimensional accuracy of the preform is very critical.

1.2 3D Printing Technology

3D printing, also known as the additive manufacturing (AM), rapid prototyping (RP), or solid freeform (SFF) is defined as the process of joining materials to produce an object using 3D model data, usually layer by layer [5]. The 3D printing was first explained by Charles Hull in 1986 [6]. This process is carried out by meshing a 3D computer model using a computer-aided design (CAD) software. Later on, an STL (Surface Tessellation Language) file is created in which the 3D mesh data will be slotted down to 2D build file for each layer [5]. This file is sent to a 3D printing machine. Different types of 3D printing technologies are classified as follows:

1. **Light polymerization:** Parts are build using light to selectively curing layers of material in vat of photopolymer. Some of the process used are Digital Light Processing(DLP) and Stereolithography (SLA) [7][8].
2. **Material jetting:** Build parts by set down of small droplets of the filament and then these parts are cured exposing by UV light [7][8].
3. **Binder jetting:** Creating object by joining the powdered material through jet deposition of binding agents.[7][8]
4. **Material extrusion:** This is also known as Fuse Deposition Modeling (FDM). Objects are created by depositing material through heated nozzle each layer is placed layer by layer until final product is made [7][8][9]. The process is shown in figure 1.6.

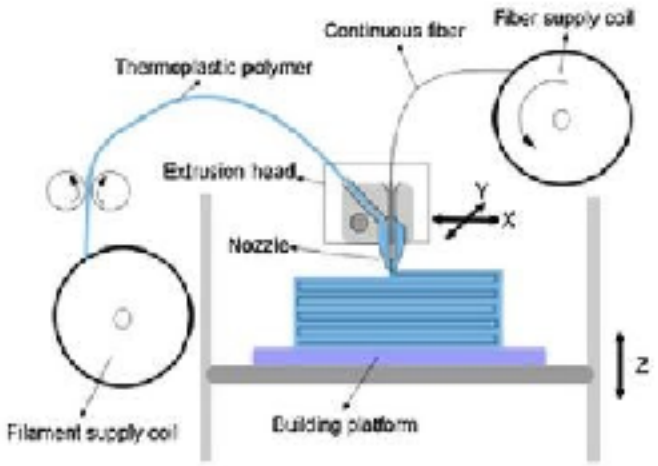

Figure 1.6 Graphical representation of 3D printing of composites [5]

5. **Powder bed fusion:** Uses thermal energy to fuse regions on a power bed [7][8]. This process uses high powered laser for this process some of the commom processes are Direct Metal Laser Sintering (DMLS), Election Neam Melting (EBM), Selective Heat Sintering (SHS), Selective Laser Melting (SLM), and Selective Laser Sintering (SLS).
6. **Sheet lamination:** In this process metal sheets are bound together by using external force. Metal sheets are welded using ultrasonic welding in layers.[8]
7. **Directed energy deposition:** Focused thermal energy is used for fusing material while depositing on the substrate. [7][8]

The materials involved in the 3D printing of polymer composites are Iron/ ABS, Copper/ ABS, Alumina/UV-sensitive resin and many more.

Advantages:

- The significant advantage of this process is that the final product is made up of soft particles hence they can be compressed to obtain a specific shape.
- Another significant advantage is the minimal material loss when compared to other manufacturing techniques

Disadvantages:

- The 3D printing technology for composites is limited to the number of materials that can be used. Currently, only thermoplastic polymers with low glass transition temperature and suitable viscosity are used. Some powdered formed materials and few photopolymers can also be used [5].
- The material made using the 3D printing technology has low mechanical properties when compared to the structures made by other manufacturing techniques. Hence structures require additional post-treatments such as infiltration or consolidation to improve their properties. This makes the whole process of making a composite structure more expensive than other processes [5].
- Since the 3D printing process is done layer by layer, the time consumed for fabricating the part is much higher when compared with other techniques.

Since there are many limitations which need to be corrected, even though the 3D printing technology already develops fast in recent years, there is need of new manufacturing technique which addresses the limitations of 3D printing technology along with the limitations of conventional manufacturing techniques. This led to the evolution of a new manufacturing technique which is called 4D printing.

1.3 4D Printing

4D printing was first studied, initiated and termed by Tibbits [10]. The 4D printing technique is inspired by the self-folding origami structures (as shown in figure 1.7), these structures can change in the configuration under certain stimulating conditions [11]. Origami studies focus on paper crafting, which mainly deals with the folding of 2-dimensional (2D) paper into 3-dimensional (3D) structure along the pre-defined hinge patterns [11]. The stimulating conditions include infrared (IR) lights, heat or moisture.

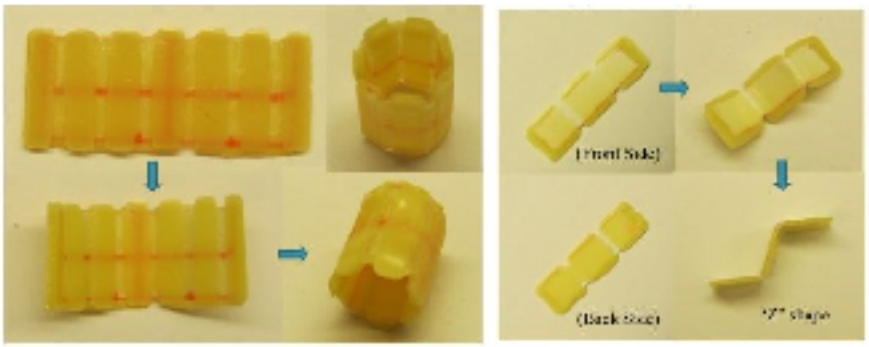

Figure 1.7 Self-folding origami structures [11]

The 4D printing technique is an evolution of 3D printing technology regarding shape, property, and functionality [12]. 4D printing is not a replacement for 3D printing technology, it is kind of technology which can be used to manufacture certain type of products. The conventional 4D printing technology exploits the properties of materials such as swelling ratio, thermal coefficient of expansion [12].

When a 2-dimensional smart material with known properties, predefined material structure (volume fractions of fibers, matrix, filament size, anisotropy, etc.) is subjected to stimulating conditions such as temperature, light intensity, water, etc. it transforms into a 3D structure. This process of manufacturing is known as 4D printing technique. The process also involves the use of mathematical models to determine the desired shape [12].

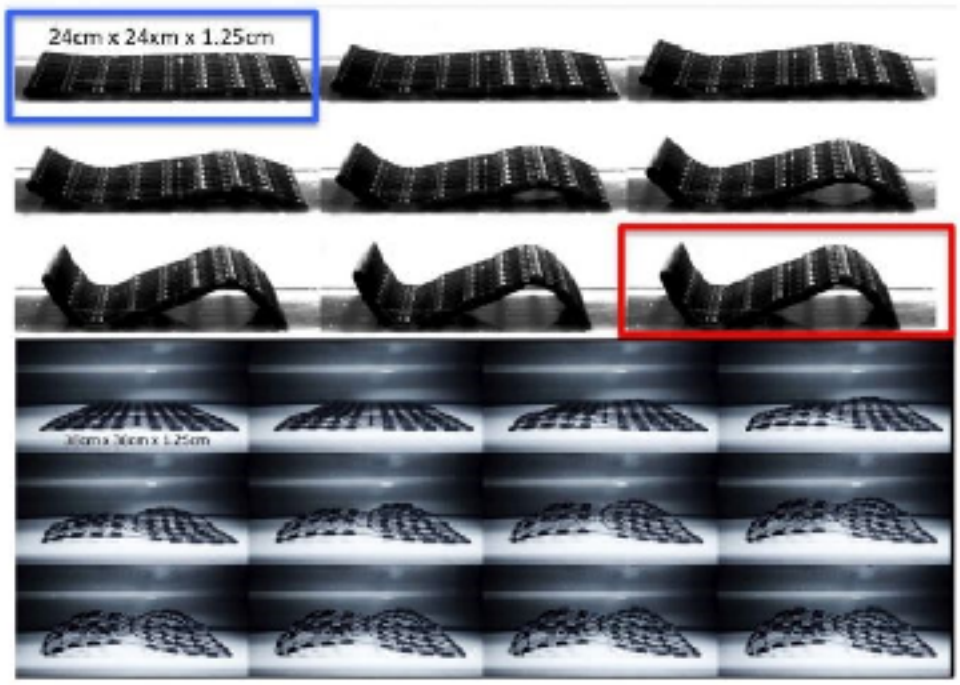

Figure 1.8 Transformation of 2D material to a 3D structure using 4D printing technique [12] [13]

Different types of 4D printing method was developed over the years, some of them are

1. **Multi-Material 4D printing**: This process includes use of multiple polymer combination with precise geometric distribution and configurations enabled by 3D printing.[14] Some of the examples are Hydrogel-based Shape Changing , SMPs-based Shape Changing [14].
2. **Single Material 4D printing**: This process directly prints the active material as the final product. Some examples of this type of processing are Photopolymerization-based Printing and Extrusion-based Printing.[14]

Advantages:

- 4D printing manufacturing technique is a form of mold-less manufacturing technique, hence avoids the cost and time required for making molds.
- Dimensional accuracy: with the proper implementation of a mathematical model, one can obtain high dimensional accuracy in the final structure.

- Time and cost involved in making a 4D printed structure are decidedly less when compared to conventional manufacturing techniques.

Disadvantages

Even though a 4D printing technique comes with numerous advantages over conventional manufacturing technique it also has few drawbacks.

- The materials used for 4D printing are usually soft plastic with a special property. Hence it is limited to a few materials [2].
- The 4D printed structure tends to degrade after a certain number of shape-shifting cycles and is non-recoverable [12][13].

In 2017, Hoa [2] introduced the concept of 4D printing of composites (4DPC).

1.4 Introduction to the 4D printing of composites (4DPC)

Many industrial parts are made using a mold of the respective shape. The designing and making of molds take a lot of time and money. Also after using the mold for manufacturing, the molds may be sent for recycling or demolishing. Introduction of 4D printing in the world of manufacturing of composites can reduce the cost and time required to make a product, as the primary cost and time are involved in making and designing of mold.

Hoa [2] has defined the various factors affecting the 4DPC. The process defines a method of automated composite manufacturing using automated fiber placement (AFP) and later on curing in an autoclave [2]. Hoa used CYCOM 977-2 prepreg tows in automated fiber placement (AFP) machine and laid up unsymmetrical laminates consisting of [0/90] and placed inside the autoclave. Upon curing, the flat laminate gets reconfigured and takes a curved shape. The reconfiguration of the composite structure depends on various parameters, such as the material properties, the layup sequence, fiber orientation, thickness and the strategic position of laminae with different orientation [2]. An example of a 4DPC laminate manufactured using the process explained above is shown in figure 1.9.

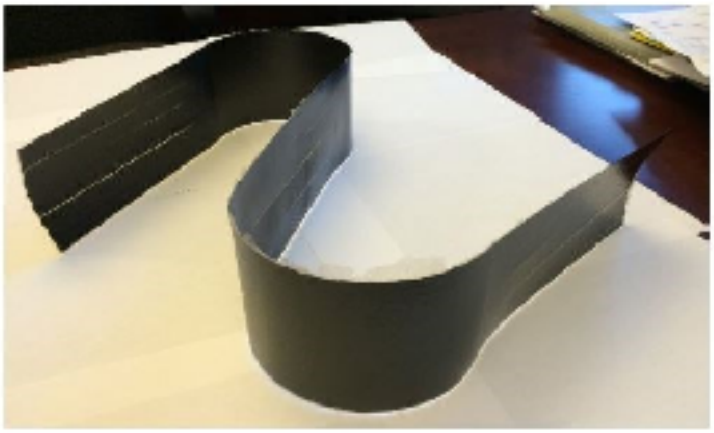

Figure 1.9 Composite piece made using 4D printing [2]

The factors affecting 4DPC were calculated using the laminate theory [15]. When the unsymmetrical composite laminate consisting of 0° & 90° layers is cured, it tends to curl up and acquire a radius of curvature. According to Hoa [2], the two primary factors that affect the stress resultants and moment resultants in the material which are responsible for the curling of the material are difference in coefficients of thermal contraction and resin shrinkage. The effects of difference in coefficients of thermal contraction and resin shrinkage on the stress resultants and moment resultants on the material are explained below.

Laminate theory

The laminate theory equations involved in finding the A, B and D matrix, are given by equations (1.1), (1.2) & (1.3) [2]

$$A_{ij} = \int \overline{Q_{ij}}\, dz \qquad B_{ij} = \int \overline{Q_{ij}}\, z\, dz \qquad D_{ij} = \int \overline{Q_{ij}}\, z^2\, dz \qquad \ldots\ldots\ldots (1.1)$$

Where i, j=1, 2, 6.

And

$$\bar{Q}_{11} = Q_{11}m^4 + 2(Q_{12} + 2Q_{66})n^2m^2 + Q_{22}n^4$$

$$\bar{Q}_{12} = (Q_{11} + Q_{22} - 4Q_{66})n^2m^2 + Q_{12}(n^4 + m^4)$$

$$\bar{Q}_{16} = (Q_{11} - Q_{12} - 2Q_{66})nm^3 + (Q_{12} - Q_{22} + 2Q_{66})n^3m$$

$$\bar{Q}_{22} = Q_{11}n^4 + 2(Q_{12} + 2Q_{66})n^2m^2 + Q_{22}m^4$$

$$\bar{Q}_{26} = (Q_{11} - Q_{12} - 2Q_{66})n^3m + (Q_{12} - Q_{22} + 2Q_{66})nm^3$$

$$\bar{Q}_{66} = (Q_{11} + Q_{22} - 2Q_{12} - 2Q_{66})n^2m^2 + Q_{66}(n^4 + m^4) \quad \ldots\ldots\ldots (1.2)$$

Where,

$$Q_{11} = \frac{E_1}{1 - V_{12}V_{21}}$$

$$Q_{12} = \frac{V_{12}E_2}{1 - V_{12}V_{21}} = \frac{V_{21}E_1}{1 - V_{12}V_{21}}$$

$$Q_{22} = \frac{E_2}{1 - V_{12}V_{21}}$$

$$Q_{66} = G_{12} \quad \ldots\ldots\ldots (1.3)$$

Where,

Q_{ij} = on axis stiffness

$\bar{Q}_{ij}$ = reduced stiffness

And $E_1, E_2, G_{12} V_{12}$ and V_{21} are moduli and Poisson ratios of a layer respectively and also $m = \cos\theta$ and $n = \sin\theta$, where θ is the angle between the fiber direction in the layer relative to the x coordinate axis of the laminate.

1.4.1 Effect of Temperature

A composite consists of fibers and resins, one has to heat up the laminate for curing the resin in the laminate to form a composite structure. Subsequently, they need to be cooled down to room temperature. While cooling down thermal coefficient of contraction takes effect in the composite laminate. The thermal coefficient of contraction of material is responsible for the thermal stresses in the material which results in curling up of flat unsymmetrical laminate. Thermal stresses are caused not only by the uneven temperature field but also due to the anisotropy of properties [16]. Stresses and moments contribution due to temperature while cooling down from curing temperature to room temperature can be calculated using equation (1.4) [2], [15].

$$\begin{bmatrix} N_x^T \\ N_x^T \\ N_x^T \\ M_x^T \\ M_y^T \\ M_{xy}^T \end{bmatrix} = \begin{bmatrix} A_{11} & A_{12} & A_{16} & B_{11} & B_{12} & B_{16} \\ A_{12} & A_{22} & A_{26} & B_{12} & B_{22} & B_{26} \\ A_{16} & A_{26} & A_{66} & B_{16} & B_{26} & B_{66} \\ B_{11} & B_{12} & B_{16} & D_{11} & D_{12} & D_{16} \\ B_{12} & B_{22} & B_{26} & D_{12} & D_{22} & D_{26} \\ B_{16} & B_{26} & B_{66} & D_{16} & D_{26} & D_{66} \end{bmatrix} \begin{bmatrix} \overset{\circ}{\varepsilon_x} \\ \overset{\circ}{\varepsilon_y} \\ \overset{\circ}{\gamma_{xy}} \\ K_x \\ K_y \\ K_{xy} \end{bmatrix} \quad \ldots\ldots\ldots (1.4)$$

And

$$\begin{bmatrix} \overset{\circ}{\varepsilon_x} \\ \overset{\circ}{\varepsilon_y} \\ \overset{\circ}{\gamma_{xy}} \\ K_x \\ K_y \\ K_{xy} \end{bmatrix} = \begin{bmatrix} a_{11} & a_{12} & a_{16} & b_{11} & b_{12} & b_{16} \\ a_{12} & a_{22} & a_{26} & b_{12} & b_{22} & b_{26} \\ a_{16} & a_{26} & a_{66} & b_{16} & b_{26} & b_{66} \\ b_{11} & b_{12} & b_{16} & d_{11} & d_{12} & d_{16} \\ b_{12} & b_{22} & b_{26} & d_{12} & d_{22} & d_{26} \\ b_{16} & b_{26} & b_{66} & d_{16} & d_{26} & d_{66} \end{bmatrix} \begin{bmatrix} N_x^T \\ N_y^T \\ N_{xy}^T \\ M_x^T \\ M_y^T \\ M_{xy}^T \end{bmatrix} \quad \ldots\ldots\ldots (1.5)$$

$$N_x^T = \int_{\frac{-H}{2}}^{\frac{H}{2}} (\bar{Q}_{11}\alpha_x^T + \bar{Q}_{12}\alpha_y^T + \bar{Q}_{16}\alpha_{xy}^T)\Delta T \, dz \quad \ldots\ldots\ldots (1.6)$$

$$N_y^T = \int_{\frac{-H}{2}}^{\frac{H}{2}} (\bar{Q}_{12}\alpha_x^T + \bar{Q}_{22}\alpha_y^T + \bar{Q}_{26}\alpha_{xy}^T)\Delta T \, dz \quad \ldots\ldots\ldots (1.7)$$

$$N_{xy}^T = \int_{\frac{-H}{2}}^{\frac{H}{2}} (\bar{Q}_{16}\alpha_x^T + \bar{Q}_{26}\alpha_y^T + \bar{Q}_{66}\alpha_{xy}^T)\Delta T \, dz \quad \ldots\ldots\ldots (1.8)$$

$$M_x^T = \int_{\frac{-H}{2}}^{\frac{H}{2}} (\bar{Q}_{11}\alpha_x^T + \bar{Q}_{12}\alpha_y^T + \bar{Q}_{16}\alpha_{xy}^T)\Delta T z \, dz \quad \ldots\ldots\ldots (1.9)$$

$$M_y^T = \int_{\frac{-H}{2}}^{\frac{H}{2}} (\bar{Q}_{12}\alpha_x^T + \bar{Q}_{22}\alpha_y^T + \bar{Q}_{26}\alpha_{xy}^T)\Delta T z \, dz \quad \ldots\ldots\ldots (1.10)$$

$$M_{xy}^T = \int_{\frac{-H}{2}}^{\frac{H}{2}} (\bar{Q}_{16}\alpha_x^T + \bar{Q}_{26}\alpha_y^T + \bar{Q}_{66}\alpha_{xy}^T)\Delta T z \, dz \quad \ldots\ldots\ldots (1.11)$$

Where α's are the off-axis coefficients of thermal contraction and are given as,

$$\alpha_x = \alpha_1 m^2 + \alpha_2 n^2 \ , \ \alpha_y = \alpha_1 n^2 + \alpha_2 m^2 \ , \alpha_{xy} = 2(\alpha_1 - \alpha_2)mn \quad \ldots\ldots\ldots (1.12)$$

α_1 and α_2 are on-axis coefficients of thermal contraction of a particular layer and m= cos θ and n=sin θ. [7] [8]

Where,

N_x^T, N_y^T & N_{xy}^T= Thermal stress resultants.

M_x^T, M_y^T & M_{xy}^T=Thermal moment resultants

ε_x°, ε_y° & ε_{xy}°= In plane strain

K_x, K_y & K_{xy}= curvature.

ΔT = Difference in temperature

H = Thickness of laminate.

1.4.2 Effect of shrinkage

The shrinkage of the composite material is due to resin shrinkage. For curing of thermoset resin, the liquid resin transforms into a solid as a result of chemical reaction between the molecules [2]. This transformation can take place at different temperatures depending upon the type of resin. For matrix such as polyester, the liquid to solid transformation occurs at room temperature whereas for resin such as epoxy the transformation occurs at a higher temperature (about 180 ^{0}C). [2]. The temperature at which a significant amount of transformation takes place is known as cure temperature.

According to Bogetti and Gillespie [17], the process of resin cure and modulus development includes three phases. Phase 1 is when the modulus of resin is zero because the resin is liquid. As the liquid resin gels, the degree of cure increases to a value denoted by α_{gel}^{mod}. During Phase 2 the resin transforms into the solid state from the gel state and degree of cure changes from α_{gel}^{mod} to α_{diff}^{mod} [17]. The shrinkage effect in the material occurs during this phase. Finally, the phase 3 is the saturated phase where resin is completely cured and no more further shrinkage or modulus development take place. When shrinkage occurs at an early stage, when the material is still soft, the shrinkage during this stage may not contribute to the reconfiguration or curling of the material. Once the modulus of resin reaches α_{diff}^{mod}, making the resin solid and stiff, the shrinkage that occurs during this stage results in reconfiguration or curling of the material.

The effect of shrinkage coefficient on the net stress and net moments are calculated using equation (1.13-1.14) [2][15].

$$\begin{bmatrix} N_x^S \\ N_x^S \\ N_x^S \\ M_x^S \\ M_y^S \\ M_{xy}^S \end{bmatrix} = \begin{bmatrix} A_{11} & A_{12} & A_{16} & B_{11} & B_{12} & B_{16} \\ A_{12} & A_{22} & A_{26} & B_{12} & B_{22} & B_{26} \\ A_{16} & A_{26} & A_{66} & B_{16} & B_{26} & B_{66} \\ B_{11} & B_{12} & B_{16} & D_{11} & D_{12} & D_{16} \\ B_{12} & B_{22} & B_{26} & D_{12} & D_{22} & D_{26} \\ B_{16} & B_{26} & B_{66} & D_{16} & D_{26} & D_{66} \end{bmatrix} \begin{bmatrix} \overset{*}{\varepsilon}_X \\ \overset{*}{\varepsilon}_Y \\ \overset{*}{\gamma}_{xy} \\ K_x \\ K_y \\ K_{xy} \end{bmatrix} \quad \ldots\ldots\ldots (1.13)$$

And

$$\begin{bmatrix} \overset{*}{\varepsilon}_X \\ \overset{*}{\varepsilon}_Y \\ \overset{*}{\gamma}_{xy} \\ K_x \\ K_y \\ K_{xy} \end{bmatrix} = \begin{bmatrix} a_{11} & a_{12} & a_{16} & b_{11} & b_{12} & b_{16} \\ a_{12} & a_{22} & a_{26} & b_{12} & b_{22} & b_{26} \\ a_{16} & a_{26} & a_{66} & b_{16} & b_{26} & b_{66} \\ b_{11} & b_{12} & b_{16} & d_{11} & d_{12} & d_{16} \\ b_{12} & b_{22} & b_{26} & d_{12} & d_{22} & d_{26} \\ b_{16} & b_{26} & b_{66} & d_{16} & d_{26} & d_{66} \end{bmatrix} \begin{bmatrix} N_x^S \\ N_y^S \\ N_{xy}^S \\ M_x^S \\ M_y^S \\ M_{xy}^S \end{bmatrix} \quad \ldots\ldots\ldots (1.14)$$

$$N_x^S = \int_{\frac{-H}{2}}^{\frac{H}{2}} (\bar{Q}_{11}\varepsilon_x^s + \bar{Q}_{12}\varepsilon_y^s + \bar{Q}_{16}\varepsilon_{xy}^s)\, dz \quad \ldots\ldots\ldots (1.15)$$

$$N_y^S = \int_{\frac{-H}{2}}^{\frac{H}{2}} (\bar{Q}_{12}\varepsilon_x^s + \bar{Q}_{22}\varepsilon_y^s + \bar{Q}_{26}\varepsilon_{xy}^s)\, dz \quad \ldots\ldots\ldots (1.16)$$

$$N_{xy}^S = \int_{\frac{-H}{2}}^{\frac{H}{2}} (\bar{Q}_{16}\varepsilon_x^s + \bar{Q}_{26}\varepsilon_y^s + \bar{Q}_{66}\varepsilon_{xy}^s)\, dz \quad \ldots\ldots\ldots (1.17)$$

$$M_x^S = \int_{\frac{-H}{2}}^{\frac{H}{2}} (\bar{Q}_{11}\varepsilon_x^s + \bar{Q}_{12}\varepsilon_y^s + \bar{Q}_{16}\varepsilon_{xy}^s)\Delta T z\ dz \quad \ldots\ldots\ldots (1.18)$$

$$M_y^S = \int_{\frac{-H}{2}}^{\frac{H}{2}} (\bar{Q}_{12}\varepsilon_x^s + \bar{Q}_{22}\varepsilon_y^s + \bar{Q}_{26}\varepsilon_{xy}^s)\Delta T z\, dz \quad \ldots\ldots\ldots (1.19)$$

$$M_{xy}^S = \int_{\frac{-H}{2}}^{\frac{H}{2}} (\bar{Q}_{16}\varepsilon_x^s + \bar{Q}_{26}\varepsilon_y^s + \bar{Q}_{66}\varepsilon_{xy}^s)\Delta T z\, dz \quad \ldots\ldots\ldots (1.20)$$

Where ε_x^s , ε_y^s, ε_{xy}^s are the off-axis strains due to resin shrinkage and are given as,

$$\varepsilon_x^s = \varepsilon_1^s m^2 + \varepsilon_x^s n^2 \ , \ \varepsilon_y^s = \varepsilon_1^s n^2 + \varepsilon_2^s m^2 \ , \ \varepsilon_{xy}^s = 2(\varepsilon_1^s - \varepsilon_2^s)mn \quad \ldots\ldots\ldots (1.21)$$

Where ε_1^s and ε_2^s are the strain due to shrinkage of a unidirectional layer, along with the fiber direction, and transverse to the fiber direction respectively and m= cos θ and n= sin θ. [1][2][18]

N_x^S, N_y^S & N_{xy}^S= Stress resultants due to shrinkage.

M_x^S, M_y^S & M_{xy}^S=Moment resultants due to shrinkage.

$\varepsilon_x^s, \varepsilon_y^s$ & ε_{xy}^s= off axis strain due to shrinkage.

$\varepsilon_x^*, \varepsilon_y^*$ & ε_{xy}^*= in plane strains.

K_x, K_y & K_{xy}= curvatures.

ΔT = Difference in temperature

H = Thickness of laminate

1.4.3 Effect of moisture

The laminate theory corresponding to the effect of moisture is given by the following equations from 1.22 -1.30.

$$\begin{bmatrix} N_x^H \\ N_x^H \\ N_x^H \\ M_x^H \\ M_y^H \\ M_{xy}^H \end{bmatrix} = \begin{bmatrix} A_{11} & A_{12} & A_{16} & B_{11} & B_{12} & B_{16} \\ A_{12} & A_{22} & A_{26} & B_{12} & B_{22} & B_{26} \\ A_{16} & A_{26} & A_{66} & B_{16} & B_{26} & B_{66} \\ B_{11} & B_{12} & B_{16} & D_{11} & D_{12} & D_{16} \\ B_{12} & B_{22} & B_{26} & D_{12} & D_{22} & D_{26} \\ B_{16} & B_{26} & B_{66} & D_{16} & D_{26} & D_{66} \end{bmatrix} \begin{bmatrix} \varepsilon_x^* \\ \varepsilon_y^* \\ \gamma_{xy}^* \\ K_x \\ K_y \\ K_{xy} \end{bmatrix} \quad \ldots\ldots\ldots (1.22)$$

And

$$\begin{bmatrix} \varepsilon_x^* \\ \varepsilon_y^* \\ \gamma_{xy}^* \\ K_x \\ K_y \\ K_{xy} \end{bmatrix} = \begin{bmatrix} a_{11} & a_{12} & a_{16} & b_{11} & b_{12} & b_{16} \\ a_{12} & a_{22} & a_{26} & b_{12} & b_{22} & b_{26} \\ a_{16} & a_{26} & a_{66} & b_{16} & b_{26} & b_{66} \\ b_{11} & b_{12} & b_{16} & d_{11} & d_{12} & d_{16} \\ b_{12} & b_{22} & b_{26} & d_{12} & d_{22} & d_{26} \\ b_{16} & b_{26} & b_{66} & d_{16} & d_{26} & d_{66} \end{bmatrix} \begin{bmatrix} N_x^H \\ N_y^H \\ N_{xy}^H \\ M_x^H \\ M_y^H \\ M_{xy}^H \end{bmatrix} \quad \ldots\ldots\ldots (1.23)$$

$$N_x^H = \int_{-\frac{H}{2}}^{\frac{H}{2}} (\bar{Q}_{11}\beta_x^H + \bar{Q}_{12}\beta_y^H + \bar{Q}_{16}\beta_{xy}^H)\Delta C dz \quad \ldots\ldots\ldots (1.24)$$

$$N_y^H = \int_{-\frac{H}{2}}^{\frac{H}{2}} (\bar{Q}_{12}\beta_x^H + \bar{Q}_{22}\beta_y^H + \bar{Q}_{26}\beta_{xy}^H)\Delta C\, dz \quad \ldots\ldots\ldots (1.25)$$

$$N_{xy}^{H} = \int_{-\frac{H}{2}}^{\frac{H}{2}} (\bar{Q}_{16}\beta_x^H + \bar{Q}_{26}\beta_y^H + \bar{Q}_{66}\beta_{xy}^H)\Delta C \, dz \qquad \ldots\ldots\ldots (1.26)$$

$$M_x^H = \int_{-\frac{H}{2}}^{\frac{H}{2}} (\bar{Q}_{11}\beta_x^H + \bar{Q}_{12}\beta_y^H + \bar{Q}_{16}\beta_{xy}^H)\Delta C z \, dz \qquad \ldots\ldots\ldots (1.27)$$

$$M_y^H = \int_{-\frac{H}{2}}^{\frac{H}{2}} (\bar{Q}_{12}\beta_x^H + \bar{Q}_{22}\beta_y^H + \bar{Q}_{26}\beta_{xy}^H)\Delta C z \, dz \qquad \ldots\ldots\ldots (1.28)$$

$$M_{xy}^H = \int_{-\frac{H}{2}}^{\frac{H}{2}} (\bar{Q}_{16}\beta_x^H + \bar{Q}_{26}\beta_y^H + \bar{Q}_{66}\beta_{xy}^H)\Delta C z \, dz \qquad \ldots\ldots\ldots (1.29)$$

Where β's are the off-axis coefficients of moisture expansion and are given as,

$$\beta_x = \beta_1 m^2 + \beta_2 n^2 \;,\; \beta_y = \beta_1 n^2 + \beta_2 m^2 \;,\; \beta_{xy} = 2(\beta_1 - \beta_2)mn \qquad \ldots\ldots\ldots (1.30)$$

β_1 and β_2 are on-axis coefficients of moisture expansion of a particular layer and m= cos θ and n=sin θ.

Where β_1 and β_2 are given by equation 1.31 & 1.32 [19].

$$\beta_1 = 0 \qquad \ldots\ldots\ldots (1.31)$$

$$\beta_2 = \beta_m (1 - \sqrt{v_f}) \left[1 + \frac{\sqrt{v_f}(1-\sqrt{v_f})E_m}{\sqrt{v_f}E_2 + (1-\sqrt{v_f})E_m}\right] \qquad \ldots\ldots\ldots (1.32)$$

Where,

β_m = Isotropic matrix moisture expansion coefficient (β_m= 0.004 [20])

v_f = fiber volume fraction (Assumed to be 0.6).

E_m= modulus of the isotropic matrix.

E_2 = Elastic modulus of the unidirectional composite.

N_x^H, N_y^H & N_{xy}^H= stress resultants due to moisture.

M_x^H, M_y^H & M_{xy}^H= moment resultants due to moisture

$\varepsilon_x^*, \varepsilon_y^*$ & ε_{xy}^*= In plane strain

K_x, K_y & K_{xy}= curvature.

ΔC = Moisture content in (%)

H = Thickness of laminate

Using the equations 1.22 - 1.29, the stress resultant and moment resultants due to moisture absorption are calculated.

The stress resultants and moment resultants due to moisture causes the composite laminate made by 4DPC to open up when placed at room conditions.

After calculating the net stress and net moments resultants due to difference in coefficient of thermal contraction, resin shrinkage and moisture absorption, the radius of curvature of the samples can be calculated using the equations (1.33 and 1.34) [2]

$$R_x = \frac{1}{K_x} \qquad \ldots\ldots\ldots (1.33)$$

$$R_y = \frac{1}{K_y} \qquad \ldots\ldots\ldots (1.34)$$

$$K_x = \frac{1}{B_{11}}[N_x^T + N_x^s - N_x^H - A_{11}\varepsilon_x^\circ - A_{12}\varepsilon_y^\circ] \qquad \ldots\ldots\ldots (1.35)$$

$$K_y = \frac{1}{B_{22}}[N_y^T + N_y^s - N_x^H - A_{12}\varepsilon_x^\circ - A_{22}\varepsilon_y^\circ] \qquad \ldots\ldots\ldots (1.36)$$

$$\varepsilon_x^\circ = \frac{Y_2\left(M_x^T + M_x^S - M_x^H - X_3\right) - X_2\left(M_y^T + M_y^s - M_y^H - Y_3\right)}{Y_2X_1 - Y_1X_2} \qquad \ldots\ldots\ldots (1.37)$$

$$\varepsilon_y^\circ = \frac{Y_1\left(M_x^T + M_x^S - M_x^H - X_3\right) - X_1\left(M_y^T + M_y^s - M_y^H - Y_3\right)}{Y_1X_2 - Y_2X_1} \qquad \ldots\ldots\ldots (1.38)$$

Where,

$$X_1 = B_{11} - \frac{D_{11}}{B_{11}}A_{11} - \frac{D_{12}}{B_{22}}A_{12}$$

$$X_2 = -\frac{D_{11}}{B_{11}}A_{12} - \frac{D_{12}}{B_{22}}A_{22} \qquad \ldots\ldots\ldots (1.39)$$

$$X_3 = \frac{D_{11}}{B_{11}}\left(N_x^T + N_x^s - N_x^H\right) - \frac{D_{12}}{B_{22}}\left(N_y^T + N_y^s - N_y^H\right)$$

$$Y_1 = -\frac{D_{11}}{B_{11}}A_{11} - \frac{D_{22}}{B_{22}}A_{12}$$

$$Y_2 = B_{22} - \frac{D_{12}}{B_{11}}A_{12} - \frac{D_{22}}{B_{22}}A_{22} \qquad \ldots\ldots\ldots (1.40)$$

$$Y_2 = \frac{D_{12}}{B_{11}}(N_x^T + N_x^s - N_x^H) - \frac{D_{22}}{B_{22}}(N_y^T + N_y^s - N_y^H)$$

Where,

N_x^T, N_y^T & N_{xy}^T= Thermal stress resultants. (Refer equations 1.4 - 1.12)

M_x^T, M_y^T & M_{xy}^T=Thermal moment resultants (Refer equations 1.4 - 1.12)

N_x^S, N_y^S & N_{xy}^S= Stress resultants due to shrinkage. (Refer equations 1.13 - 1.21)

M_x^S, M_y^S & M_{xy}^S=Moment resultants due to shrinkage. (Refer equations 1.13 - 1.21)

N_x^H, N_y^H & N_{xy}^H= stress resultants due to moisture. (Refer equations 1.22 – 1.29)

M_x^H, M_y^H & M_{xy}^H= moment resultants due to moisture (Refer equations 1.22 – 1.29)

$\varepsilon_x^*, \varepsilon_y^*$ & ε_{xy}^*= In plane strain

K_x, K_y & K_{xy}= curvature.

R_x, R_y = radius of the sample in x and y direction respectively.

Also A_{ij}, B_{ij}, D_{ij} are A,B,D matrix calculated using equation (1.1)[2].

1.5 Effect of moisture

When the composite material is exposed to its surrounding after curing, the sample tends to absorb moisture through diffusion from the surrounding atmosphere. This process is mainly dependent on the diffusivity of the moisture into the material.

The moisture present in the material can be in two different states which are free moisture and bound moisture.

- Free moisture is state of the water molecules that are unbound and mobile within the material.
- Bound moisture is defined as the moisture in which the water molecules are immobilized and bound by other molecules in the polymer.

When moisture diffuses into the samples, there is a change in the net weight of the samples and swelling occurs. This leads to change in strain in material and change in the radius of the sample. The moisture absorption in the material leads to change in the glass transition temperature (Tg) [21]. Moisture absorption

occurs at a different rate for different temperature, so the diffusion coefficient changes with temperature for the same relative humidity (RH%) [21].

Moisture diffusion into the resin leads to a reduction of glass transition temperature and softening of the resin system, which results in degradation of stiffness and strength [22][23]. The moisture enters into locations where there are loose ends inside the cured composite. Loose ends inside the composites are the locations where the samples are not entirely cured. Once the moisture enters this region, it may swell and plasticise that region. Hence the moisture content (ΔC) in composite materials is significant for calculations of stresses involved.[23] Diffusion of moisture to a condition of spatial uniformity can take months, even years, depending on the thickness of the laminate [18].

To understand the individual effect of moisture in composite materials, a detailed study of both absorption and desorption of moisture on the composite samples made using 4DPC needs to be performed. Analogous to the effect of resin shrinkage, the coefficient of moisture expansion of the material is required to calculate the net stress and net moments.

The moisture content in a sample is calculated using equation 1.41. [22]

$$\Delta C = \frac{W - W_d}{W_d} X\ 100 \qquad \ldots\ldots\ldots (1.41)$$

W = weight of the sample at given time.

W_d = Weight of the dry sample.

1.5.1 Coefficient of moisture expansion

The effect of moisture on a composite material can be found by determining hygroscopic strain due to the change in moisture content inside the material. This can be used to calculate the coefficient of hygroscopic swelling. Then the stress resultants and moment resultants are determined. These then are used to determine the radius of the 4D printed unsymmetrical laminate after moisture absorption.

When moisture diffuses into the matrix, it may lead to swelling and plasticizing of fiber – matrix network and decreases the strength of interface[23]. A decrease of 17% in transverse strength can be seen due to degradation of the interface (results through SEM analysis [23]), So material failure is seen to change from matrix cracking to interface fracture due to the decrease in residual compressive stress. Hence it can be concluded that both temperature and swell stress lead to a decrease in residual compressive stress.

There are various effects when moisture diffuses into composite laminate such as reduction in glass transition temperature and softening of the material resulting in the degradation of stiffness and strength [23]. To find the effect of moisture content (ΔC), it is necessary to find the coefficient of moisture expansion.

The strain due to the coefficient of moisture expansion (β_H) is given by the following equation [18]

$$\varepsilon_H = \beta_H x \Delta C \qquad \ldots\ldots\ldots (1.42)$$

ε_H = Hygroscopic Strain.

β_H = Coefficient of moisture expansion (%).

ΔC = Moisture content (%).

The coefficient of moisture expansion along both longitudinal and transverse directions are given by equations 1.43 & 1.44 [19]

$$\beta_1 = 0 \qquad \ldots\ldots\ldots (1.43)$$

$$\beta_2 = \beta_3 = \beta_m(1-\sqrt{v_f})\left[1+\frac{\sqrt{v_f}(1-\sqrt{v_f})E_m}{\sqrt{v_f}E_2+(1-\sqrt{v_f})E_m}\right] \qquad \ldots\ldots\ldots (1.44)$$

Where,

β_m = Isotropic matrix moisture expansion coefficient

v_f = fiber volume fraction (Assumed to be 0.6).

E_m = modulus of the isotropic matrix.

E_2 = Elastic modulus of the unidirectional composite.

Hence by computing the coefficient of moisture expansion for each layer and using laminate theory, the stress resultant and moment result due to moisture can be calculated.

The thin solid composite laminates made using 4DPC were seen to be opening up once cured and left at room condition. This is due to moisture absorption into the material, this occurs in both thin and thick laminates, but the opening up is more in the thin laminates whereas the thick laminates do not undergo any significant change. The reason behind this is that the stiffness of the thick laminate is higher than the stiffness of the thin laminate. Hence the moisture has less effect of on the thick laminate than on thin laminate. Hence a detailed study of the effect of temperature & moisture in 4D printed composite thin composite laminates needs to be performed.

1.6 Research objective

The primary objective of this research is to study the effect of environmental conditions on the deformations of thin composite laminates made by the 4DPC. The research involves the following

- Effect of temperature on the curvature of the thin composite laminates. This study involves subjecting the thin composite laminate to temperature cycling (both heating up to curing temperature and then cooling down to room temperature)
- Effect of resin shrinkage of the material on the deformation of thin composite laminates.
- Effect of moisture on the curvature of the thin composite laminates. This part of the research mainly deals with the absorption and desorption of moisture through diffusion into the composite sample made using 4DPC. The research involves finding the coefficient of moisture expansion (β_H) of the material and calculating the stress resultant and the moment resultants due to moisture diffusion.
- To calculate the radius of curvature due to the stress resultants and moment resultants in the thin composite laminate due to the combined effect of temperature, shrinkage, and moisture and compare both theoretical and experimental results.

CHAPTER 2: SAMPLE PREPARATION

2.1 Sample preparation

For the experimental procedure, various samples were prepared for different experiments such as

1. Differential scanning calorimetry (DSC)
2. Temperature Cycling
3. Shrinkage Test
4. Moisture Absorption
5. Moisture Desorption

The samples prepared for the experiments above are different. Hence it is necessary to discuss the sample preparation methods.

2.1.1 Composite laminates made by 4D printing (4DPC)

A flat shaped composite laminate consisting of carbon epoxy (CYCOM 977-2) prepreg tow was manufactured using 4DPC via an automated fiber placement (AFP) machine at Concordia AFP lab (figure 2.1). At first, the machine bed is heated using a propane flame so that the prepreg does not slip away during the laying up process. A thermoset head is fixed to the machine. The layup sequence is shown in figure 2.2.

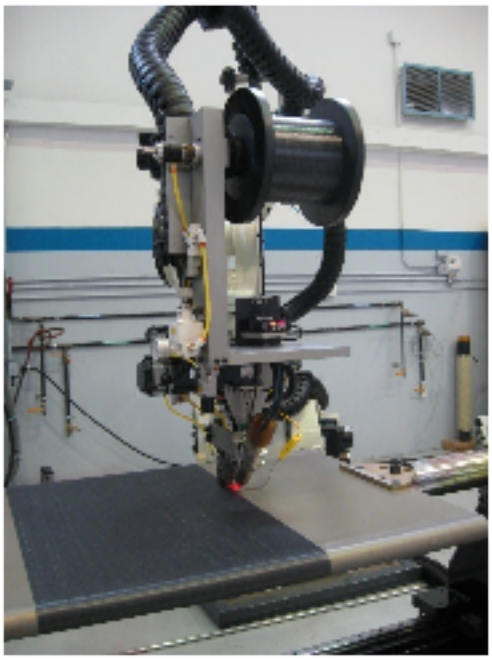

Figure 2.1 Automated Fiber Placement machine in the composite lab at Concordia (Photo courtesy: www.concordia.ca)

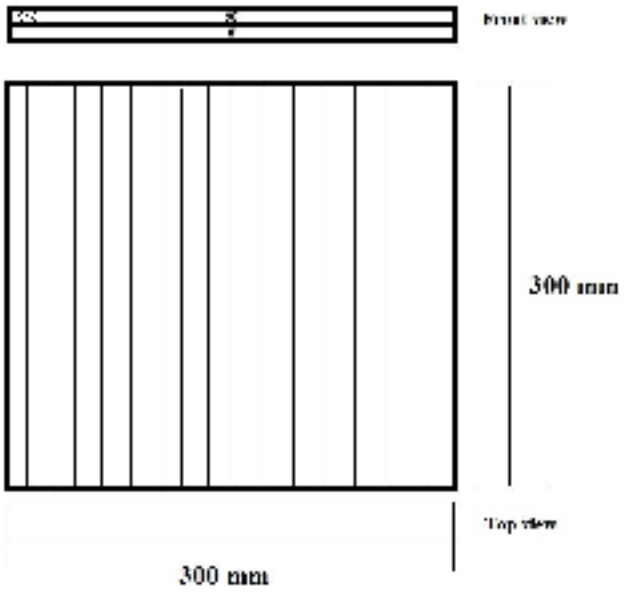

Figure 2.2 Layup sequence of the thin laminate using AFP machine

After all the prepregs have been laid (as shown in figure 2.2), they are vacuum bagged by the following steps below.

a. The tool is cleaned using a cleaner (LOCTITE PM cleaner). After the cleaning process, a releasing agent is applied so that the sample does not stick to the tool during the curing process. The release agent used for this process is shown in figure 2.3.

Figure 2.3 Release agent used for Vacuum bagging

b. After applying the release agent, the sample is placed on top of the tool for the bagging process. The release film is cut to required length and placed on top of the tool. The sample may stick to the breather material or the bagging material. As such another release film is used before placing the breather film. Before placing the vacuum bag, the base of the pressure valve is placed on top of the breather material at the edges to provide vacuum pressure throughout the sample equally. A schematic representation of bagging sequence is shown in figure 2.4.

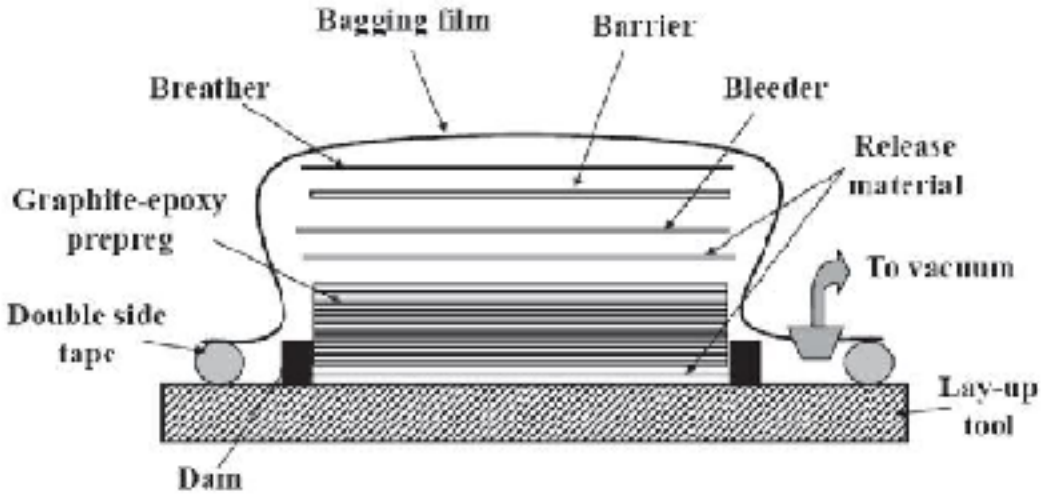

Figure 2.4 Schematic representation of Vacuum bagging [1]

c. The bagging is completed by using gum sealant tape placed at the edges and then tucking the vacuum bag tightly without leaving any allowance for air. The air inside the bag is removed using an external vacuum pump. After the bagging process, the efficiency of bagging or leakage test is checked using a vacuum pump. This is done by setting the vacuum at 15 Torr. Once the vacuum is reached the machine is turned off to check the variation in pressure. The final vacuum bagged sample is shown in figure 2.5

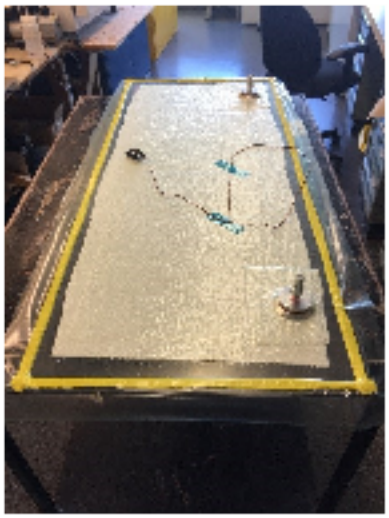

Figure 2.5 Vacuum bagged sample

d. The vacuum bagged sample is placed in an autoclave and is cured following the curing cycle as shown in figure 2.6. The sample after curing curls up as shown in figure 2.7.

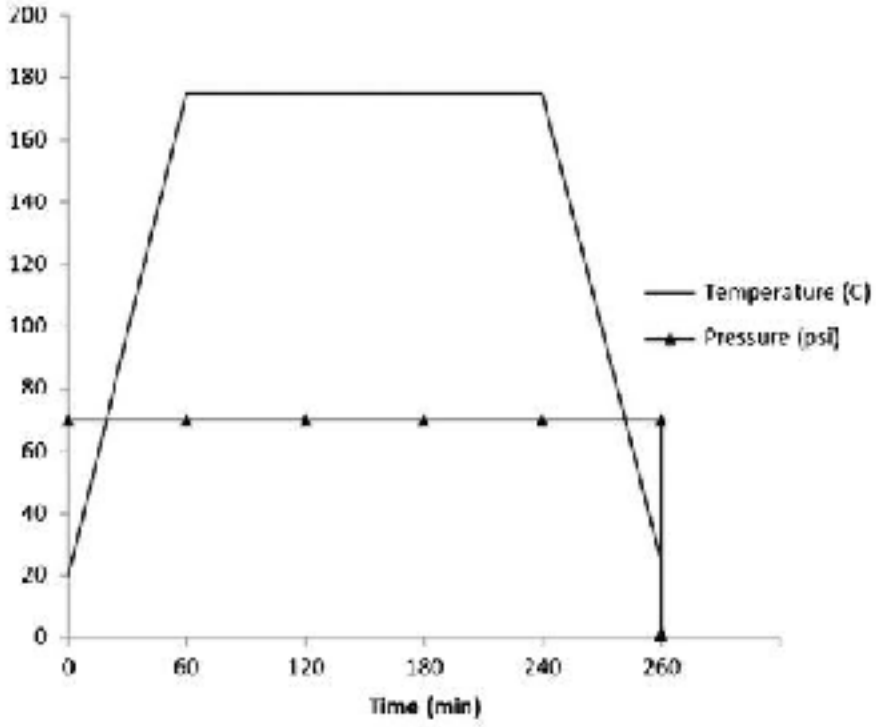

Figure 2.6 Curing cycle [2]

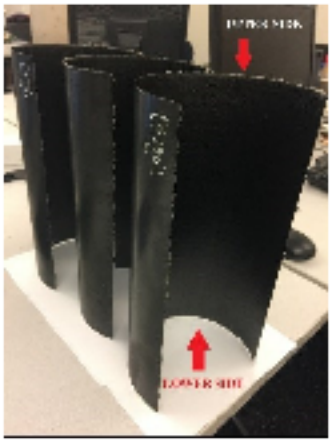

Figure 2.7 Final samples made by 4D printing

The samples after curing tend to curl up (refer figure 2.7). This is due to various contributions during curing such as

1. Tool- part interaction
2. Resin shrinkage [2]
3. The difference in coefficient of thermal contraction between the layers [2]
4. Moisture absorption by the samples

2.1.1.2 Effect of Tool-part interaction

A common phenomenon that is observed by composite manufactures while manufacturing composite parts is the shape change of the final product manufactured. The shape change is caused due to the arising of invariable residual stress, which causes deformation in the final product [24]. One of the reason for this arise of residual stress in the samples is due to the mismatch of the Coefficient of Thermal Expansion (CTE) between the tool and part [24] which is known as tool part interaction.

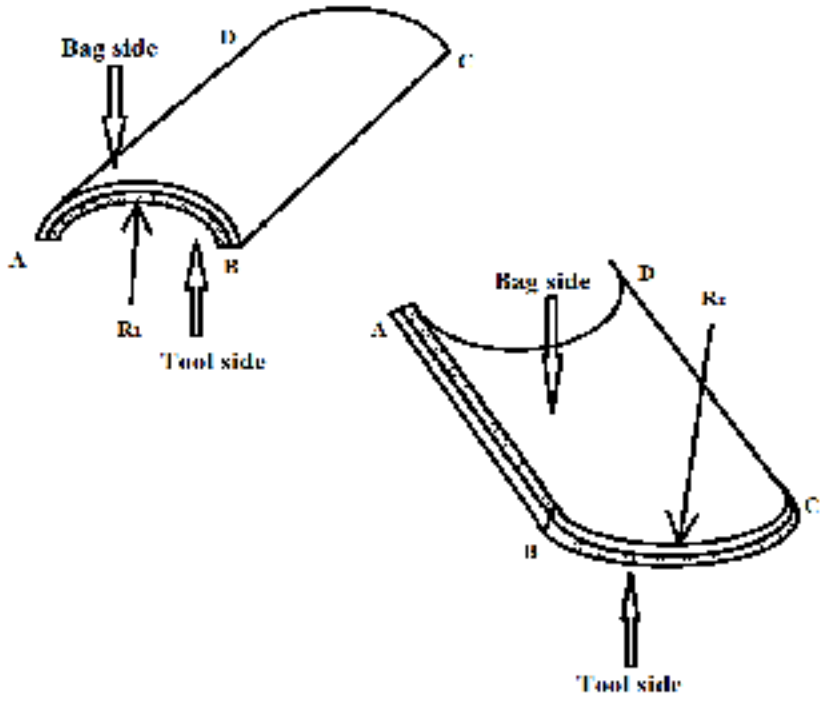

Figure 2.8 Radius of curvature of a sample for both the tool side and bag side

For determining the effect of tool-part interactions, 5 samples consisting of [0/90] of dimensions 6''x 6'' was made by 4DPC. By checking the radius of curvature of these samples (for method refer 2.3) for both directions i.e. R_1 the radius of curvature of tool side (part of composite laminate touching the tool surface) and R_2 the radius of curvature of Bag side (part of laminate facing away from the tool surface)(figure2.8). The difference in the radius values (as shown in table 2.1) will show the effect of part and tool interaction on the radius of curvature.

SAMPLE	**Average Radius of curvature of Tool side (R_1) (cm)**	**Average Radius of curvature of Bag side (R_2) (cm)**
SAMPLE A	6.4 $\pm$ 0.2	6.0 $\pm$ 0.1
SAMPLE B	6.3 $\pm$ 0.2	5.9 $\pm$ 0.1
SAMPLE C	6.5 $\pm$ 0.1	6.0 $\pm$ 0.0
SAMPLE D	6.5 $\pm$ 0.05	6.0 $\pm$ 0.05
SAMPLE E	6.7 $\pm$ 0.2	6.0 $\pm$ 0.25

Table 2.1 Radius of part of sample touching the tool & Radius of apart of sample away from the tool

From the values of the radii, it is clear that there is a small effect of part-tool interaction on the curvature of the samples. This is because the coefficient of steel (tool used) is 13.2 x 10^{-6}/°C whereas the coefficient of thermal expansion of CYCOM 977-2 (material used for 4DPC) along the transverse direction is 24.3 x 10^{-6}/°C. This difference in values of coefficients of thermal expansion (CTE) causes the mismatch between the tool and part. Hence the steel tool restricts the fibers touching the tool surface to shrink to its maximum expansion values and thereby forcing the composite face touching the tool surface to attain a slightly higher value.

Hence from this experiment, it is clear that part and tool interaction has a very small effect on the radius of curvature of the samples made by 4DPC.

2.1.1.1 Samples for a study on the effect of temperature and resin shrinkage

Three samples labeled as Sample 1, Sample 2 and Sample 3 were made by 4DPC with layup sequence [0/90] for performing the study on the effect of temperature and resin shrinkage. (Refer Chapter 3)

After cooling the samples to room temperature and placing them in room conditions, the samples tend to open up after some time. This opening may be due to the following reasons

- Continue curing of the samples at room temperature due to the incompleteness of the cure of the samples
- Stress relaxation due to the incompleteness of the cure of the samples
- Absorption of moisture

In order to see whether there is any incompleteness of the degree of cure in the samples, DSC tests need to be performed on the three samples.

2.2 Differential Scanning Calorimetry Test (DSC)

DSC test was conducted on the 4D printing samples to check whether the samples were cured entirely. This is done by checking the variation in the heat flow of the material for a particular temperature. When the sample absorbs heat (endothermic reaction) or releases heat (exothermic reaction), they show a peak in the graphs during the process.

2.2.1 Sample preparation

A small piece of more than 10 mg (for proper signals) is cut from the original composite samples made by 4DPC. The small piece was weighed in a weighing scale. The samples are placed in hermetic pans. The pans were closed using Hermetic lids (as shown in figure 2.9) and a hand press technique. The procedure mentioned above was done for three samples.

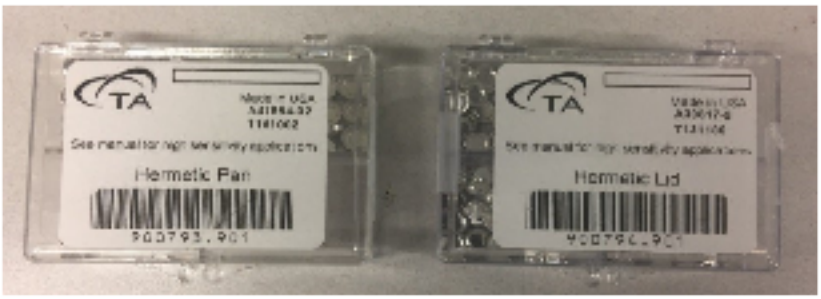

Figure 2.9 Hermetic Pan and Lid used for DSC test

2.2.2 Experimental Procedure

1. A DSC machine as shown in figure 2.10 is used for this experiment. Opening the nitrogen line then increase the pressure regulator to below 20 psi. The cooling device is switched on. In the software TA instrument explorer Control > event > on, to turn on cooling. Then to get the machine to standby temperature Control > go to standby temp.

Figure 2.10 DSC test machine (photo courtesy: www.google.ca)

2. DSC sample prepared as mentioned in section 2.2.1 was then placed into the machine by opening the lid of the machine using the machine software. An empty reference pan is also placed which stays near the wall. The pan with the sample is placed in the position closer to the user among the two positions to place the samples.

3. Fill in the summary tab (ramp option is most often used for the degree of cure, heat/cool/heat for glass transition temp). Set the temperature at 300°C to which the samples needed to be heated. Run the machine for the test and check for results.
4. Click Graph icon to start data logging. When the test is completed, go to Control > event > off. Turn off the cooling tower. Turn off nitrogen to avoid wastage of nitrogen.
5. The test was performed on three DSC coupons each from the samples made by 4D printing (Table 2.2), so in total nine coupons were used. A DSC test on the prepreg of CYCOM 977-2 was done to check the degree of cure before curing the prepregs.
6. The graphs plotted by the DSC machine is Heat flow (W/g) vs. Temperature from which degree of cure of the sample can be calculated using the variation in the heat flow in the graphs.

Samples made by 4D printing	DSC test samples
SAMPLE 1	COUPON 1.1
	COUPON 1.2
	COUPON 1.3
SAMPLE 2	COUPON 2.1
	COUPON 2.2
	COUPON 2.3
SAMPLE 3	COUPON 3.1
	COUPON 3.2
	COUPON 3.3

Table 2.2 Sample list for DSC test

2.2.3 Results and Discussion

This test was performed on nine samples as shown in Table 2.2. After performing a DSC test on each of the samples mentioned above, similar graphs (as shown in figure 2.10, 2.11 and 2.12) were obtained.

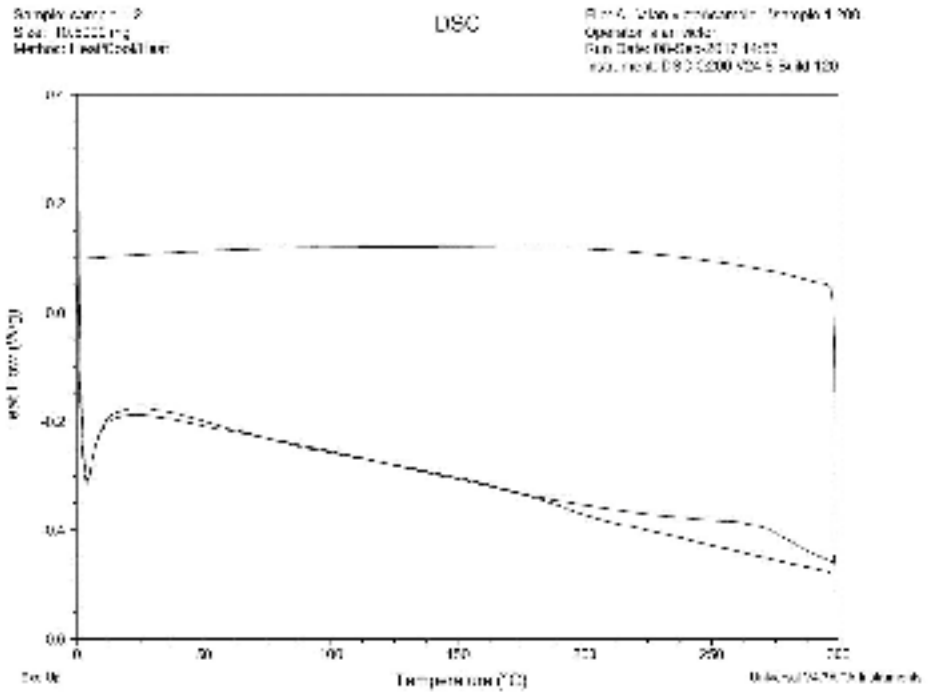

Figure 2.11 DSC graph obtained for Coupon 1.2

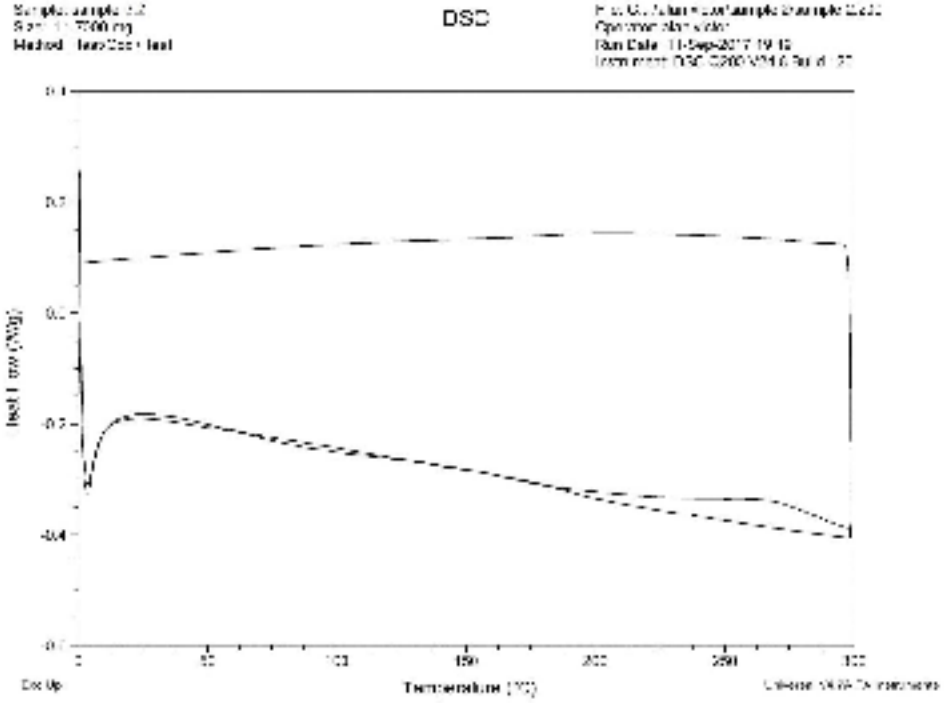

Figure 2.12 DSC graph obtained for Coupon 2.2

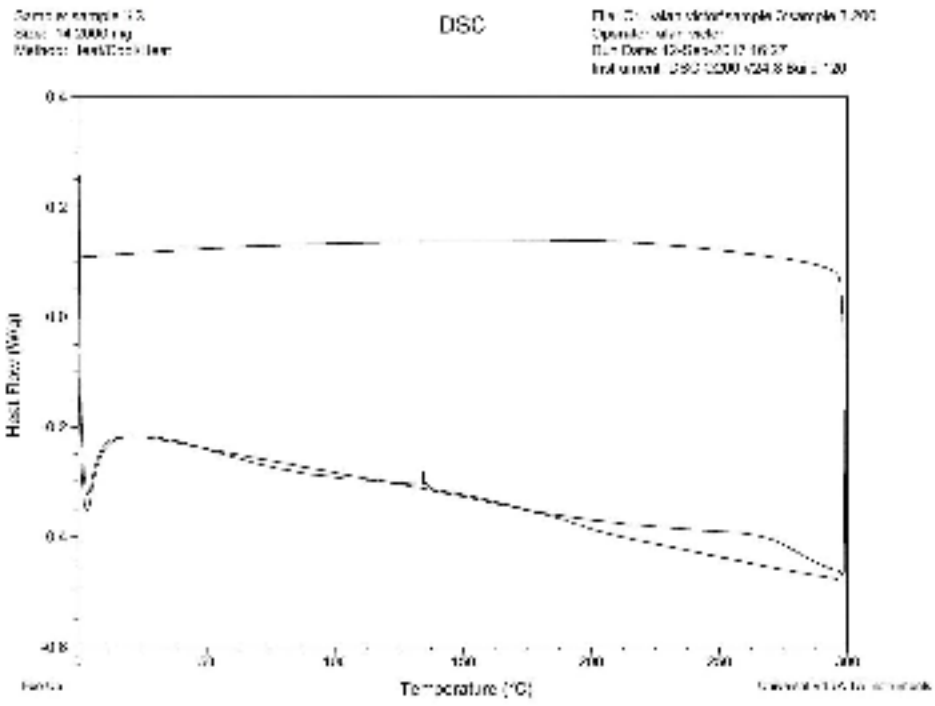

Figure 2.13 DSC graphs obtained for Coupon 3.2

All graphs for the rest of the coupons are shown in Appendix A. From the above graphs it is evident that the samples were completely cured.

For comparison, a DSC test was performed on the prepreg of CYCOM 977-2. Figure 2.13 shows the DSC graph for a prepreg of material CYCOM 977-2. The graph shows an exothermic peak, which shows that the sample of the prepreg is uncured and can be cured by following a curing cycle. So when we compare the graphs for the samples made by 4D printing (figure 2.10, 2.11 & 2.12) and the graph for prepreg material (figure 2.13), there are no visible peaks in the sample made by 4D printing. Hence they are proved to be completely cured samples.

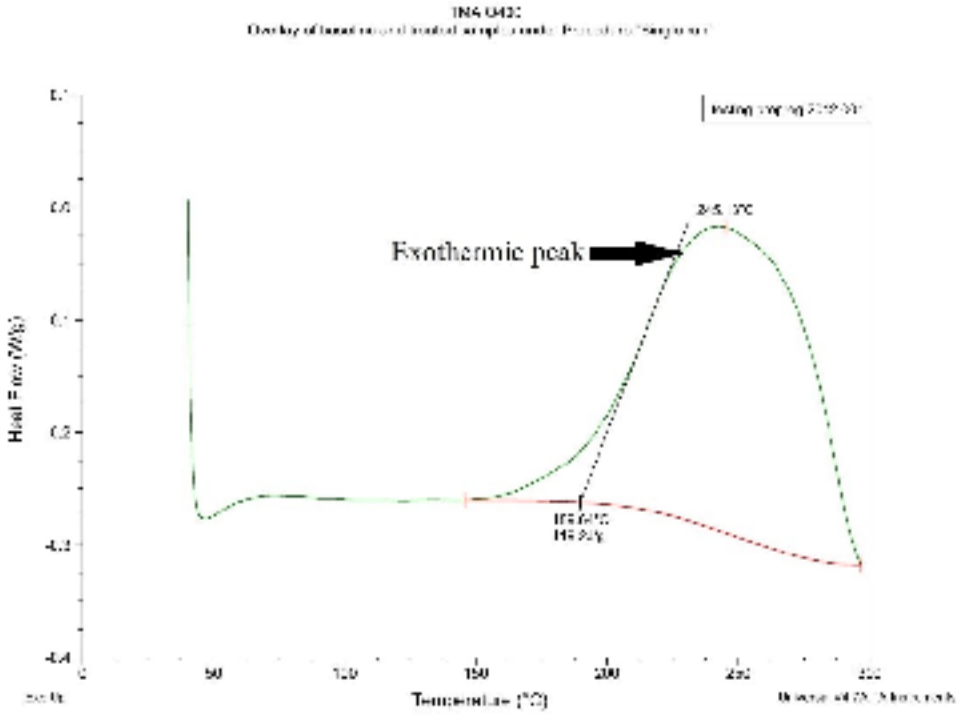

Figure 2.14 DSC graph for prepreg CYCOM977-2

Even when the samples were completely cured, they tend to open up when placed in room conditions. This opening up of samples (as shown in figure 2.15) was observed by measuring the radius using the radius measurement method explained in section 2.3. The primary reasons for this opening up of the samples may be due to the following factors

- Post-curing of the samples
- Stress relaxation in the samples
- Moisture absorption from the surroundings

Post curing and Stress relaxation factors can be eliminated because the results of the DSC test show that the samples are completely cured. This leaves to determine the effect of moisture on the curvature of samples.

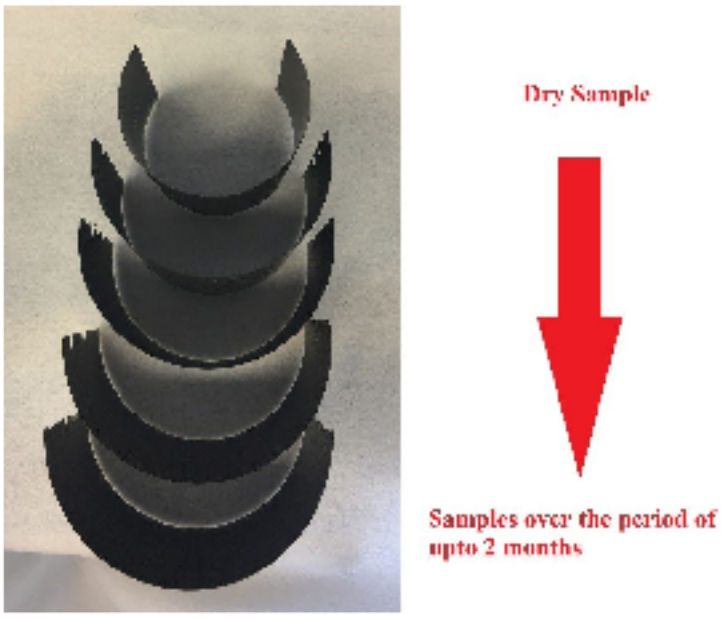

Figure 2.13 Openings up of the sample

2.3 Radius measurement and calculating methods

The arc or curve of the edge of the sample to be measured was physically traced on a piece of paper. The method adopted for calculating the radius of curvature is perpendicular bisector of chord method. The point of intersection of the perpendicular bisector 1 of the chord 1 and perpendicular bisector 2 of the chord 2 is the center of the arc, and the distance from the center of the arc to the arc gives the radius for the arc. This schematic representation is shown in figure 2.14.

During the radius measurement, the points for the chord are chosen from the middle of the arc length and not close to the edge. This is because the radius close to edges may be different from the radius at the middle of the arc length, due to tool-part interactions at the edges.

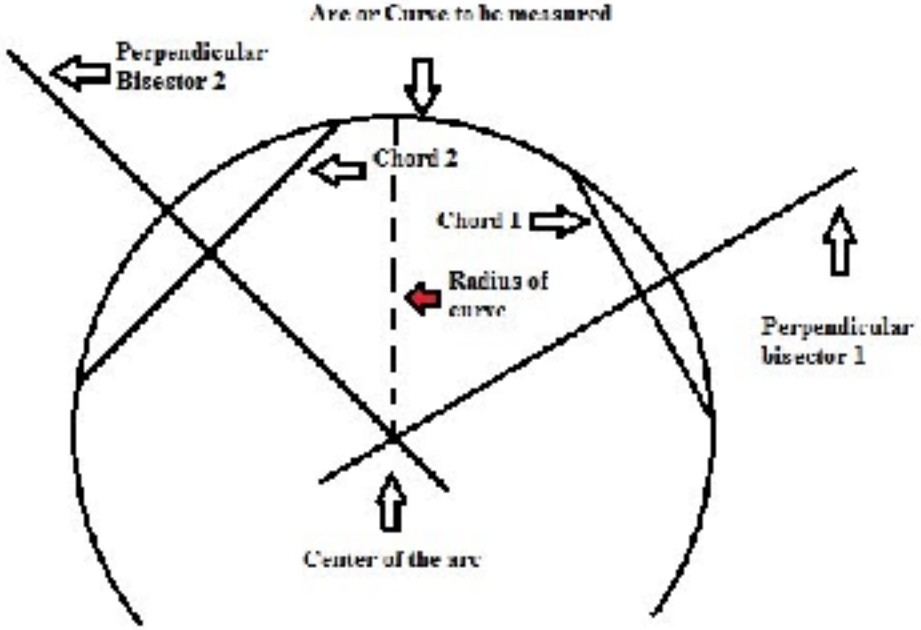

Figure 2.16 Schematic representation of finding the radius of curvature

CHAPTER 3: EFFECT OF TEMPERATURE & RESIN SHRINKAGE

The curvature of the sample made by 4D printing is due to the effect of resin shrinkage and the difference in coefficients of thermal contraction along different directions in a lamina. The effect of these can be investigated by doing thermal cycling tests. To do the thermal cycling tests, at first, the moisture present in the sample needs to be removed. Hence a desorption process is performed on the samples.

3.1 Moisture Desorption from samples for Thermal cycling experiment

Desorption is the process of removing the moisture from a material with the help of a desiccant. This is done by subjecting the material to a desiccant (A material that absorbs moisture from its surroundings). In this case, we use Anhydrous Calcium Sulfate.

The removal of moisture from the sample or material should result in the change in net strain in the material, as removal of moisture eliminates the net stress and net moment due to the moisture. This makes the sample to have a smaller radius than the one with moisture present.

3.1.1 Sample preparation

1. Three samples were manufactured using 4D printed technology in an autoclave by following a curing cycle as explained above in the section 2.1.1. These samples were left at room temperature for 840 h (35 days), and DSC test (refer 2.2) were performed to check for degree of cure of the samples. The temperature of room averages at 22°C and relative humidity at around 30%.
2. The three samples were cut in half (as shown in figure 3.1) and the edges of these samples were smoothened after cutting using a file and sandpaper. The samples were labeled as Sample 1A, Sample 1B, Sample 2A, Sample 2B, Sample 3A and Sample 3B. Each of these samples was marked upper

and lower regions for measuring the radius (figure 3.2). These samples are placed inside a desiccator for moisture description.

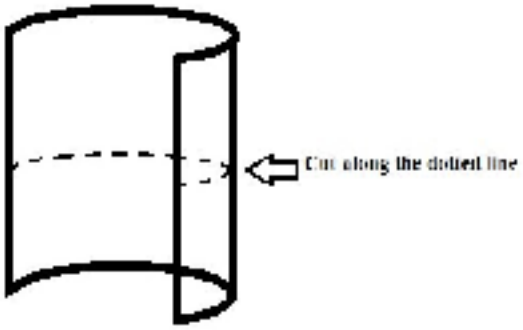

Figure 3.1 Sample cut for description test

3.1.2 Experimental Procedure

A. Removal of free moisture

Procedure

1. After conducting the DSC, the samples cut were cut in half along its length (explained in the section 3.1.1) as shown in figure 3.2.

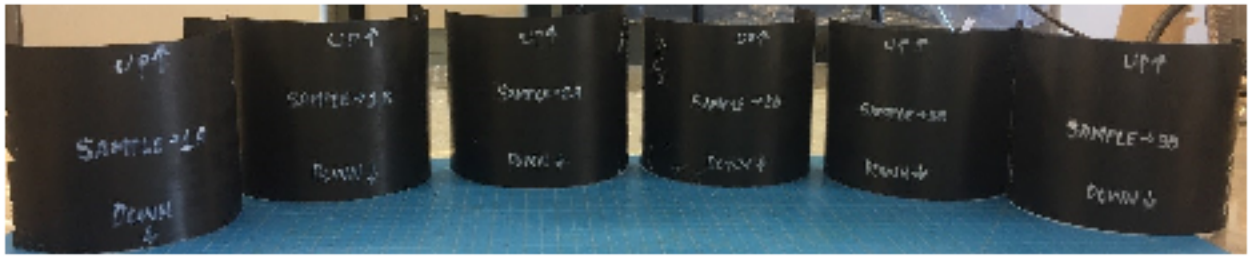

Figure 3.2 Description test samples

2. The samples were placed inside a desiccator (figure 3.3) under vacuum for various days until all the free moisture from samples is removed.

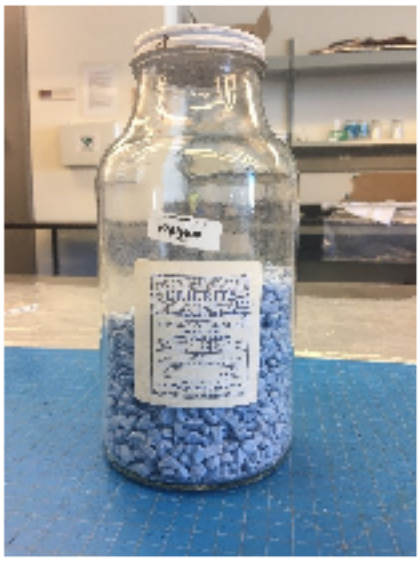

Figure 3.3 Desiccant: Anhydrous Calcium Sulfate

3. While the samples are placed inside the desiccator as shown in figure 3.4, they are checked for the radius (using perpendicular bisector chord method as explained in section 2.3) and weight (figure 3.5). This process was done for every 12h for the first five days and later when it stabilizes the readings were taken every 24 h.

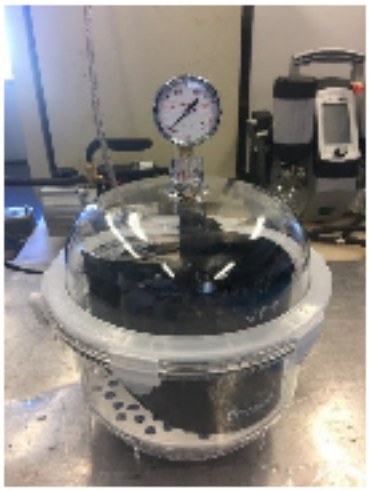

Figure 3.4 Samples placed inside the desiccator

4. From the values obtained for radius and moisture content (ΔC) (using the equation 1.30), graphs were plotted between Radius vs. Time & Moisture content (ΔC) vs. the square root of Time. This process is repeated for the six samples mentioned above.

B. Removal of bound moisture

Bound moisture present in samples was removed by heating up the sample to a temperature higher than 100 °C (temperature for water to evaporate) and checking for a change in weight.

Procedure

1. The samples were placed in the oven at 180 °C for 20 h and then checked for radius and weight change, Later it was again heated for 3h at the same temperature. This was done to confirm that there was no weight change after the initial heating.
2. During this experiment, both radius and weight (using a weighing scale shown in figure 3.5) of the sample was measured. This was repeated for the all the six samples on which free moisture removal test was performed.

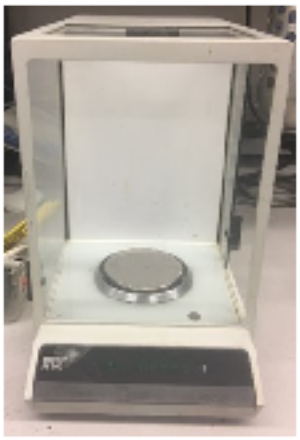

Figure 3.5 Weighing scale

3.1.3 Results and discussion

A. Removal of free moisture

a) Radius calculation

The radii measured at various time interval were plotted against time for all the six samples and the curvature shown in figures 3.6 – 3.11.

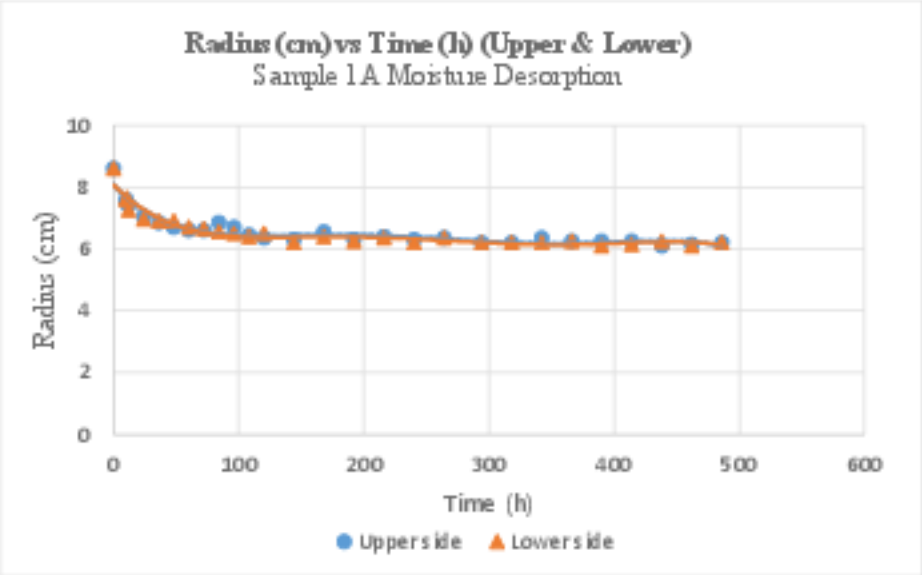

Figure 3.6 Radius (cm) vs Time (h) (Upper & Lower) for Sample 1A (Moisture Desorption)

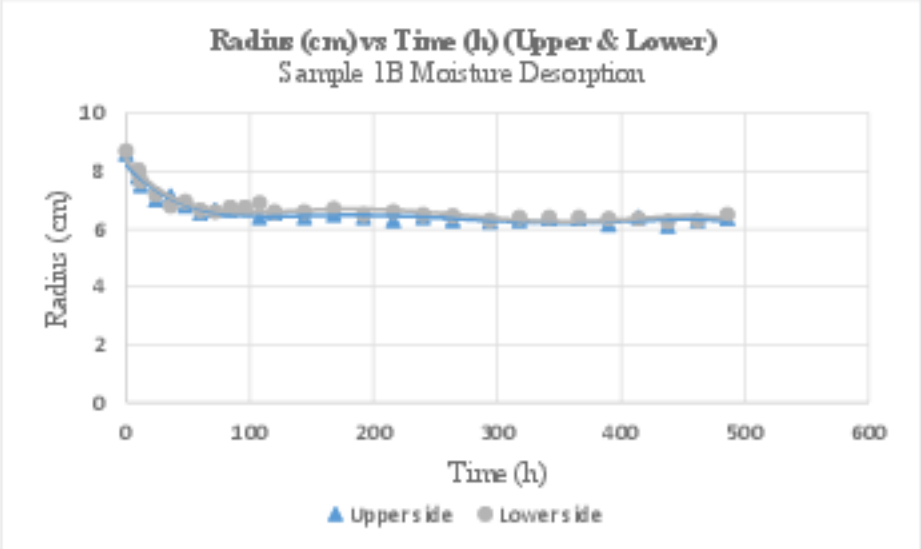

Figure 3.7 Radius (cm) vs Time (h) (Upper & Lower) for Sample 1B (Moisture Desorption)

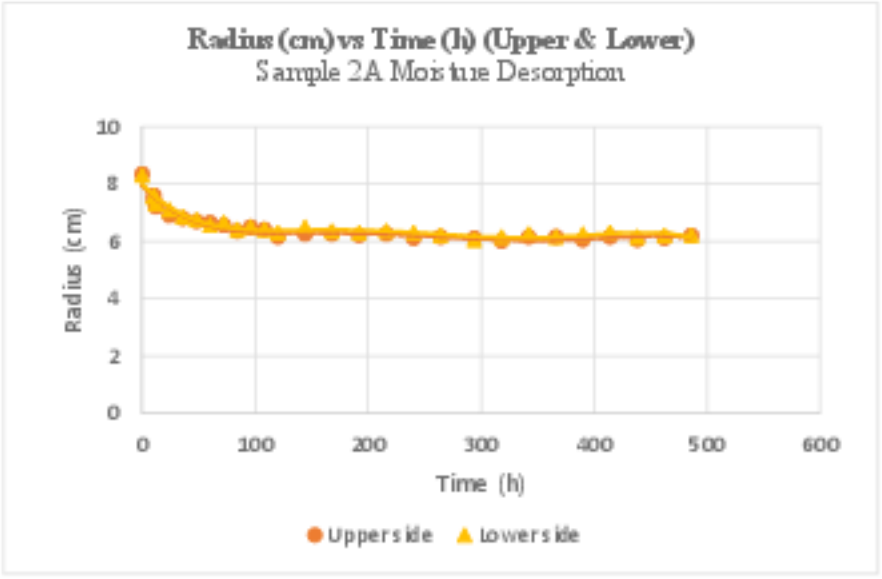

Figure 3.8 Radius (cm) vs Time (h) (Upper & Lower) for Sample 2A (Moisture Desorption)

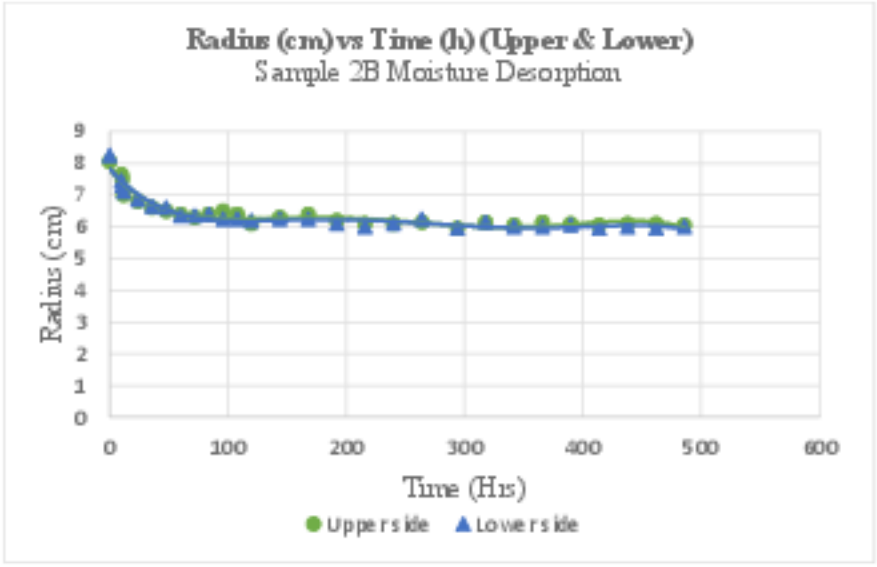

Figure 3.9 Radius (cm) vs Time (h) (Upper & Lower) for Sample 2B (Moisture Desorption)

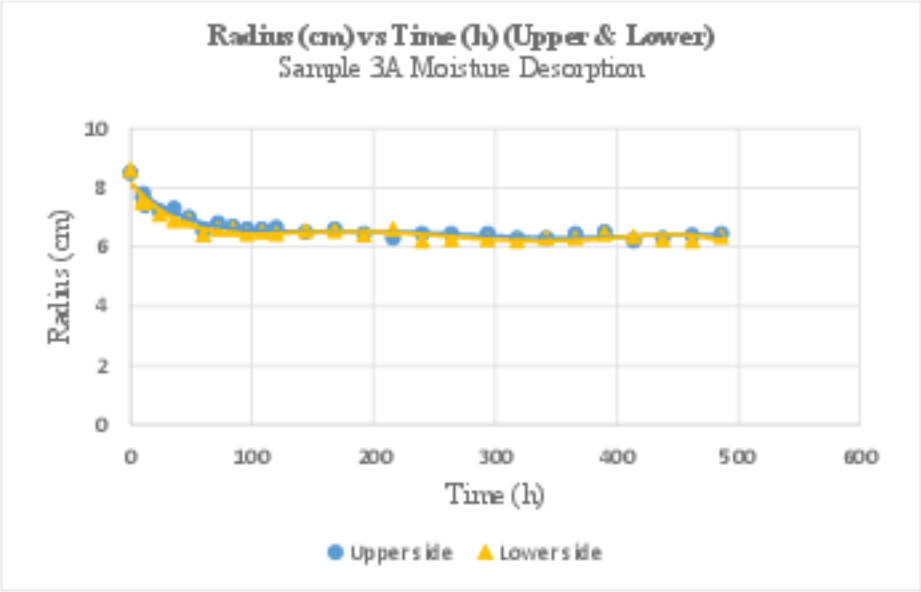

Figure 3.10 Radius (cm) vs Time (h) (Upper & Lower) for Sample 3A (Moisture Desorption)

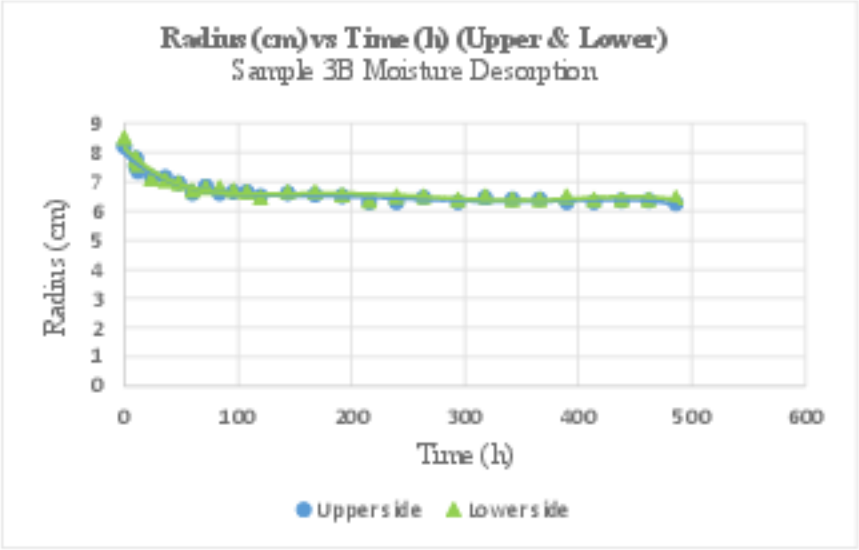

Figure 3.11 Radius (cm) vs Time (h) (Upper & Lower) for Sample 3B (Moisture Desorption)

From figures 3.6 to 3.11, it is clear that all samples follow the same pattern in a change in radius during moisture desorption. From the above the values of radii, an average value was calculated for each sample and was plotted against time as shown in figure 3.12.

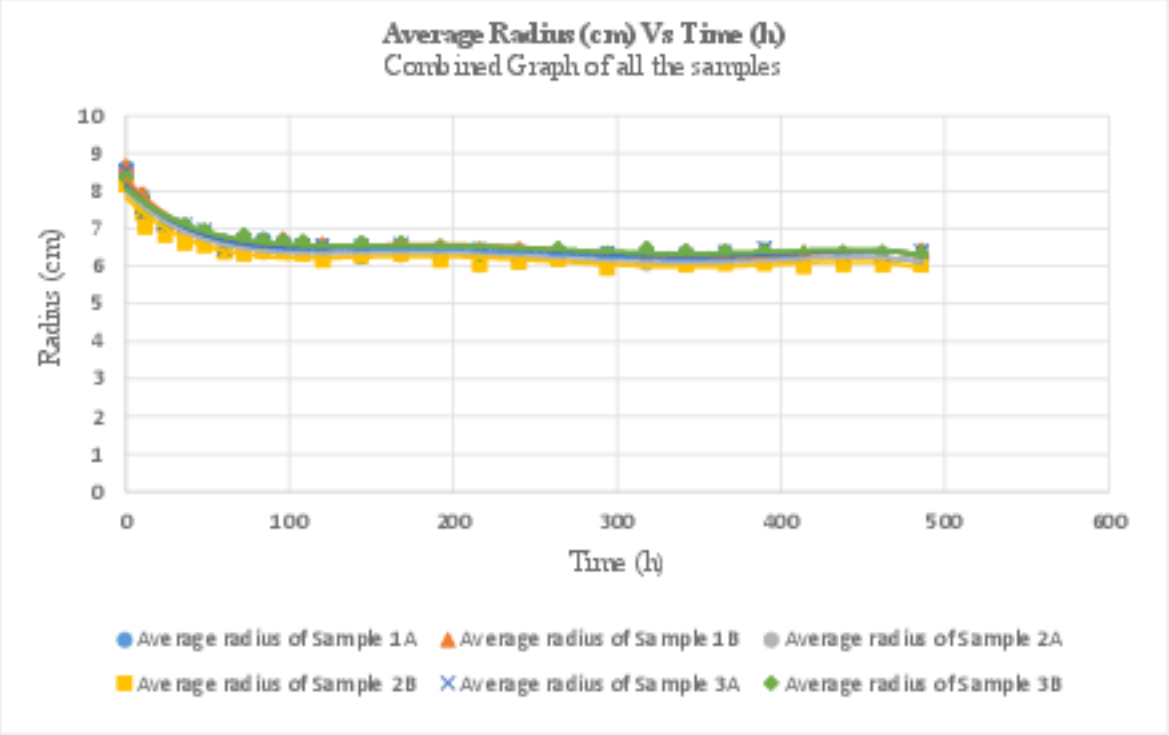

Figure 3.12 Average Radius (cm) vs. Time (h) Combined Graph of all the samples

From the above graph between Average Radius (cm) vs. Time (h), it can be concluded that all the samples tend to follow the same pattern once the moisture is removed and also the radius almost constant after 240 h. (14400 minutes). The final average radius values of all the sample curves as shown in table 3.1.

Sample Name	Average Radius (cm)
Sample 1A	6.19 ± 0.04
Sample 1B	6.31 ± 0.07
Sample 2A	6.12 ± 0.05
Sample 2B	6.03 ± 0.05
Sample 3A	6.30 ± 0.06
Sample 3B	6.36 ± 0.04

Table 3.1 Final average radius to which the samples curve up after desorption

When the samples were subjected to atmospheric conditions, the samples tend to absorb moisture from the surrounding, and this moisture diffuses into matrix region and plasticizes the material and swells the

polymer network leading to the increase of the free volume of polymer, which allows slight movements of polymer chains.

When the material is subjected to desorption, once the moisture is removed through a diffusion process, the free volume of the matrix region becomes empty and restricts any further movement, leading the polymer in the samples to return to their original positions (without moisture after curing). This is confirmed by the radius value calculated before the desorption test and at the end of the test as shown in table 3.3.

b) Weight Calculation

Removal of Free moisture

During the desorption test, the weight of each sample was also measured at the same time with the radius of the sample. The weight (g) vs. time (h) graphs are plotted as shown in figure 3.13 and all values are as shown in Appendix B.

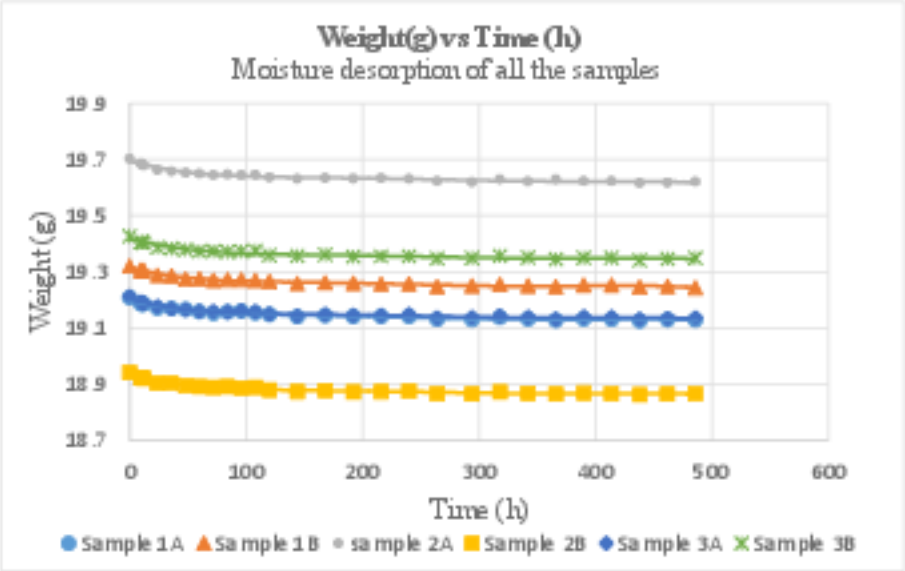

Figure 3.13 Weight (g) vs. Time (h) for all the samples

With the weight measurements tabulated, the Moisture content (ΔC) using equation (1.30) was calculated and plotted against the square root of time

The graphs are shown in figure 3.14-3.19.

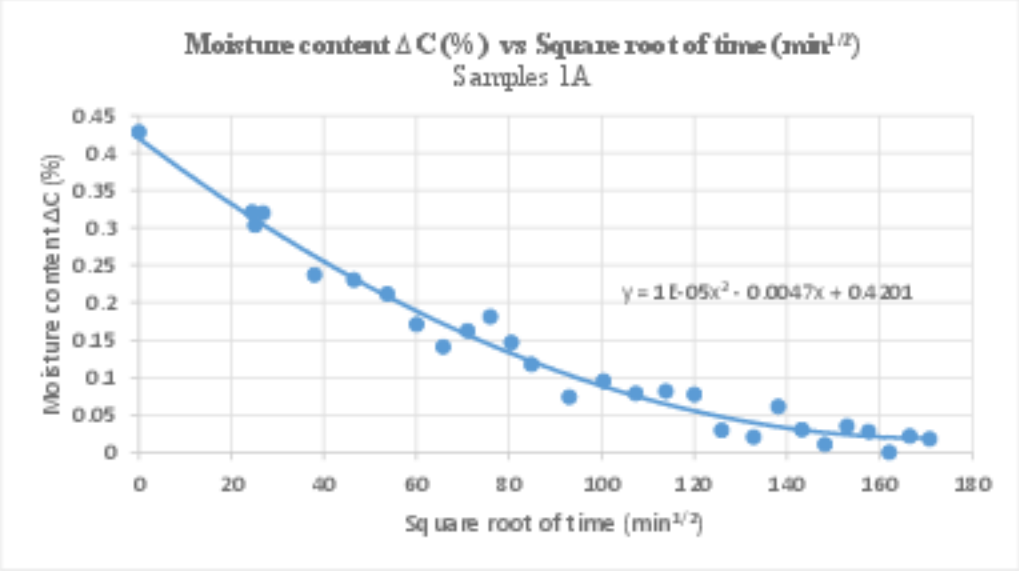

Figure 3.14 Moisture content (ΔC) (%) vs. Square root of time (min$^{1/2}$) for Sample 1A

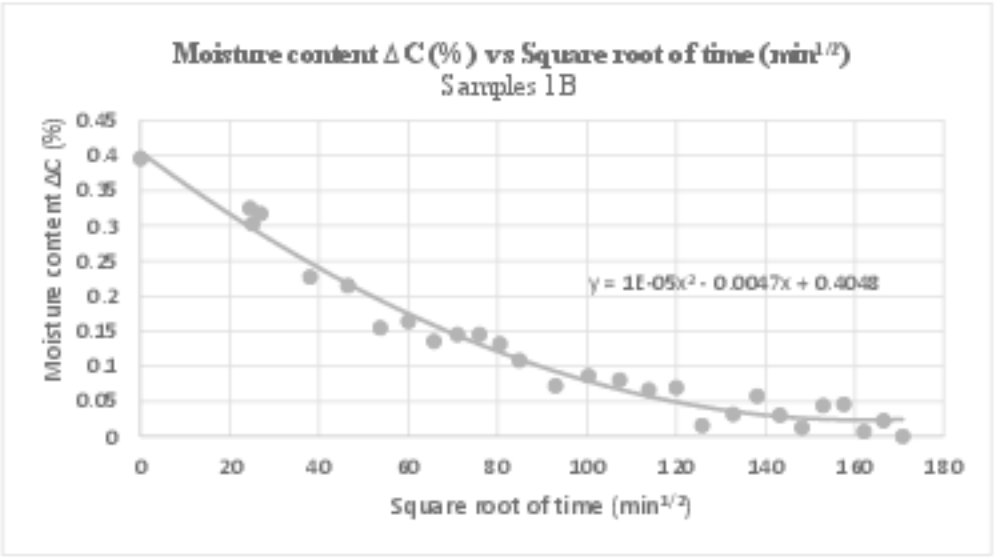

Figure 3.15 Moisture content (ΔC) (%) vs. Square root of time (min$^{1/2}$) for Sample 1B

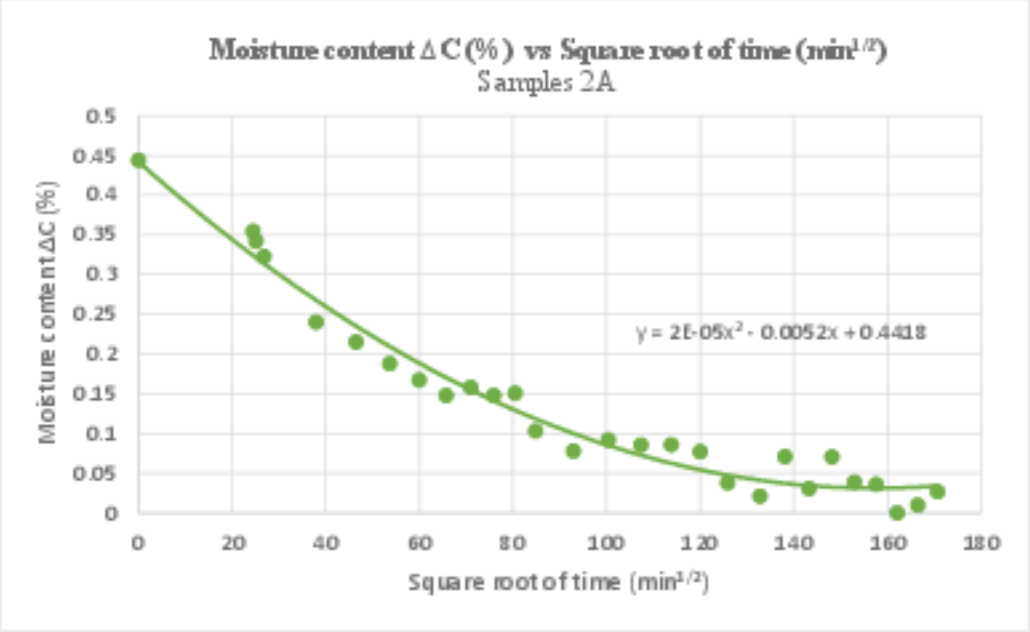

Figure 3.16 Moisture content (ΔC) (%) vs. Square root of time (min$^{1/2}$) for Sample 2A

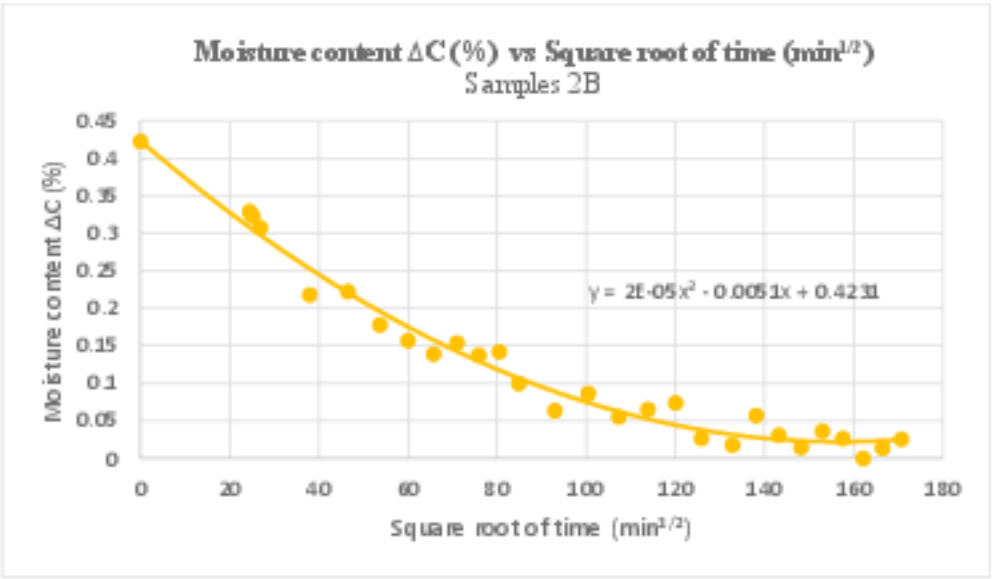

Figure 3.17 Moisture content (ΔC) (%) vs. Square root of time (min$^{1/2}$) for Sample 2B

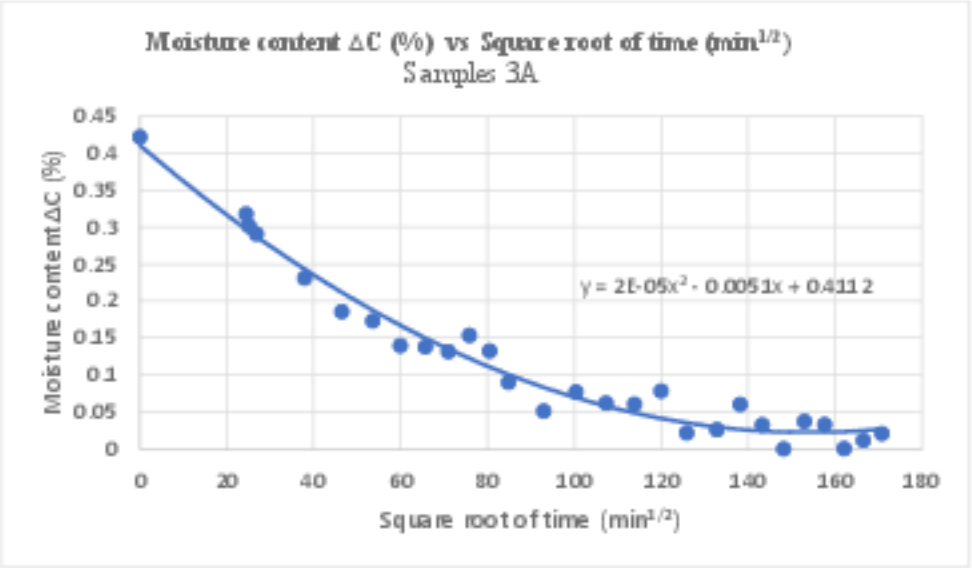

Figure 3.18 Moisture content (ΔC) (%) vs. Square root of time ($min^{1/2}$) for Sample 3A

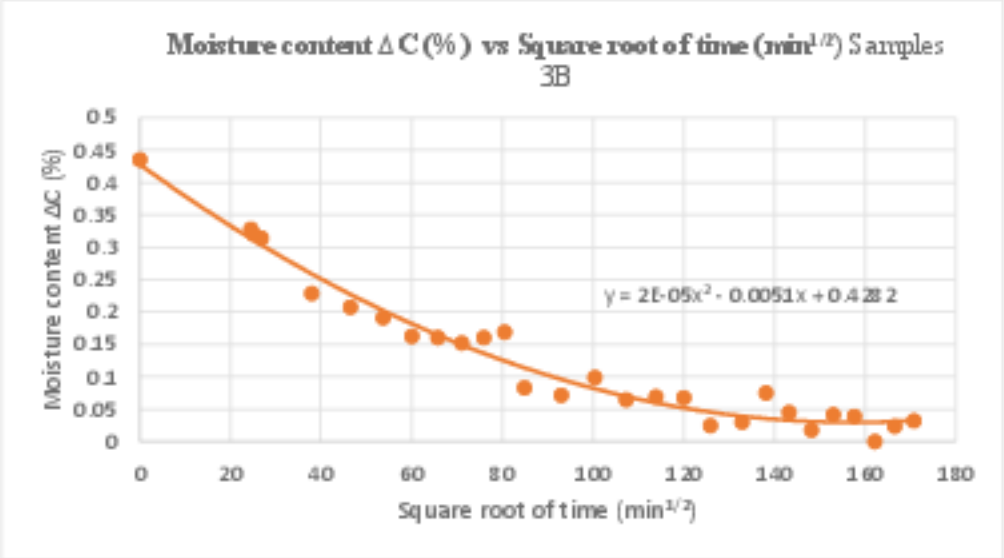

Figure 3.19 Moisture content (ΔC) C (%) vs. Square root of time ($min^{1/2}$) for Sample 3B

From figures 3.14-3.19, it is clear that the same follows Fick's law second law of diffusion as mentioned in equation 4.2.

Fick's second law can be written as [22]

$$\Delta C = \frac{4M_m}{h\sqrt{\pi}}\sqrt{t}\sqrt{D} \qquad \ldots\ldots\ldots (4.2)$$

M_m = Maximum moisture content.

D = diffusion coefficient.

t = conditioning time.

h= thickness of the sample.

The graph plotted for above equation increases or decreases (depending on absorption or desorption) linearly and then tend to reach asymptotic to a value [22] [25]

All the samples show the same variation as equation 4.2, hence they all follow the Fickian curve during diffusion.

A combined graph of all the samples above is plotted as shown in figure 3.20 for comparison.

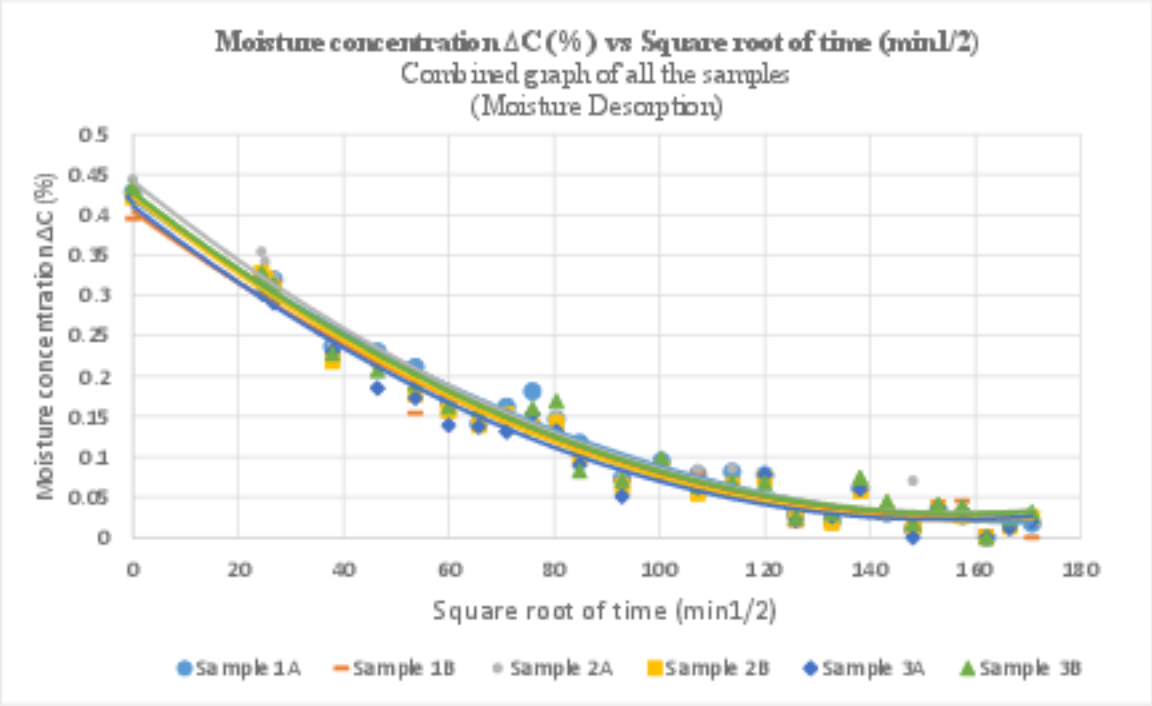

Figure 3.20 Combined graph of all the samples

From the graphs, it can be concluded that the moisture content (ΔC) tends to average about 0.35-0.4 (%) after 120 $min^{n1/2}$ or 240 h. This means that the samples had achieved asymptotic moisture content (ΔC) thuough diffusion between the materials and the desiccant. Hence all the samples follow the Fick's second law of diffusion as it follows the Fickian curve.

So from the radius calculation and weight calculation of moisture desorption, it is found that after 240 h the samples tend to be asymptotic and hence the radius and weight of the material reach the value at which the sample may be free from free moisture.

B. Removal of bound moisture

To remove the bound moisture, the sample was heated up to 180°C for 23 h and checked for weight (shown in Appendix B). It was found that weight of the sample remains constant after heating for 20 h and later it was again heated for 3h more. After the final heating for 3h, it was found to have reached a weight at which the samples were dry after curing as shown in table 3.2.

The temperature of 180°C was chosen randomly and it was seen that this temperature did not seem to degrade the material as the samples returned to state right after curing this can be seen in table 3.3.

Sample Name	Average Weight (g) (After Removal Free moisture)	Average Weight (g) (After Removal bound moisture)
Sample 1A	19.13 ± 0.003	19.12 ± 0.003
Sample 1B	19.25 ± 0.004	19.24 ± 0.004
Sample 2A	19.62 ± 0.005	19.61 ± 0.005
Sample 2B	18.87 ± 0.003	18.86 ± 0.003
Sample 3A	19.14 ± 0.003	19.13 ± 0.003
Sample 3B	19.35 ± 0.004	19.34 ± 0.004

Table 3.2 Weight of each sample after the removal of Free and Bound moisture

As the samples are almost dry, they are ready for the thermal cycling experiment. The radius and weight measurements before and after moisture removal are shown in table 3.3.

Sample Name	Average Radius (cm) (Before removal of moisture)	Average Radius (cm) (After removal of moisture)	Weight (g) (Before Removal moisture)	Average Weight (g) (After Removal moisture)
Sample 1A	8.6 ± 0.01	6.1 ± 0.03	19.21	19.12 ± 0.003
Sample 1B	8.65 ± 0.05	6.1 ± 0.04	19.32	19.24 ± 0.004
Sample 2A	8.33 ± 0.03	6 ± 0.04	19.70	19.61 ± 0.005
Sample 2B	8.15 ± 0.1	6 ± 0.03	18.94	18.86 ± 0.003
Sample 3A	8.55 ± 0.05	6.15 ± 0.01	19.21	19.13 ± 0.003
Sample 3B	8.35 ± 0.15	6.15 ± 0.04	19.43	19.34 ± 0.004

Table 3.3 Radius and weight measurements after removal of moisture

3.2 Contribution of the coefficient of thermal contraction

Thermal cycling is defined as the process of subjecting a material to various temperatures with sufficient dwell time at each temperature for attaining thermal equilibrium. The process is conducted gradually or slow pace so that there is no thermal shock induced in the material. (Thermal shock is defined by the large thermal gradient or variation in temperature inside the material).

3.2.1 Sample preparation.

After removing both free moisture and bound moisture, two samples were chosen, and thermal cycling experiment was performed in an oven as shown in figure 3.21. Among the six samples (refer section 3.1). two random samples, Sample 1A and Sample 3B, were chosen for the temperature cycling test. Only two samples were chosen because other samples were needed later for future experiments such as shrinkage test.

3.2.2 Experimental Procedure

1. The sample preparation for this experiment is explained in section 3.1.1. The samples chosen were Sample 1A and Sample 3B. The samples were subjected to various temperatures by placing them in an oven as shown in figure 3.21. The samples were heated up from 25°C to 40 °C, 60 °C, 80 °C, 100 °C, 120 °C, 140 °C, 160 °C, 180 °C & 190 °C.
2. The samples were also cooled after heating from 190 °C to 180 °C, 160 °C, 140 °C, 120 °C, 100 °C, 80 °C, 60 °C, 40 °C & 25°C. This is a step by step process.

Figure 3.21 Sample placed in an oven for temperature cycling

3. While placing the sample inside the oven, an actual ruler was placed along with samples. This ruler is used for radius measurement for the given scale in Digimizer (explained in section 3.1.3).
4. During both heating and cooling down processes, photographs of the sample for each particular temperature mentioned above were taken for measurement of the radius at that particular temperature.
5. The photographs taken were analyzed using Digimizer (an image analyzing software)[3] to calculate the radius. The process of analyzing the image for radius was explained in section 3.1.3.
6. The average radius values obtained from the measurement list in the Digimizer were tabulated, and graphs were plotted between Average Radius (cm) vs. temperature (°C) for both heating up and cooling down processes.

3.2.3 Image analysis

The image files were opened in this digimizer software, and the scale of the image was defined using the 'Unit' tool in the software. The method to set the scale of the image is by placing a ruler (as shown in figure 3.22) beside the sample and to define a length in the ruler by using 'Unit' tool. By this way, digimizer [3] calculates the number of pixels in the image and with the help of scale defined by the user (in this case scale is defined by marking a defined length on the ruler).

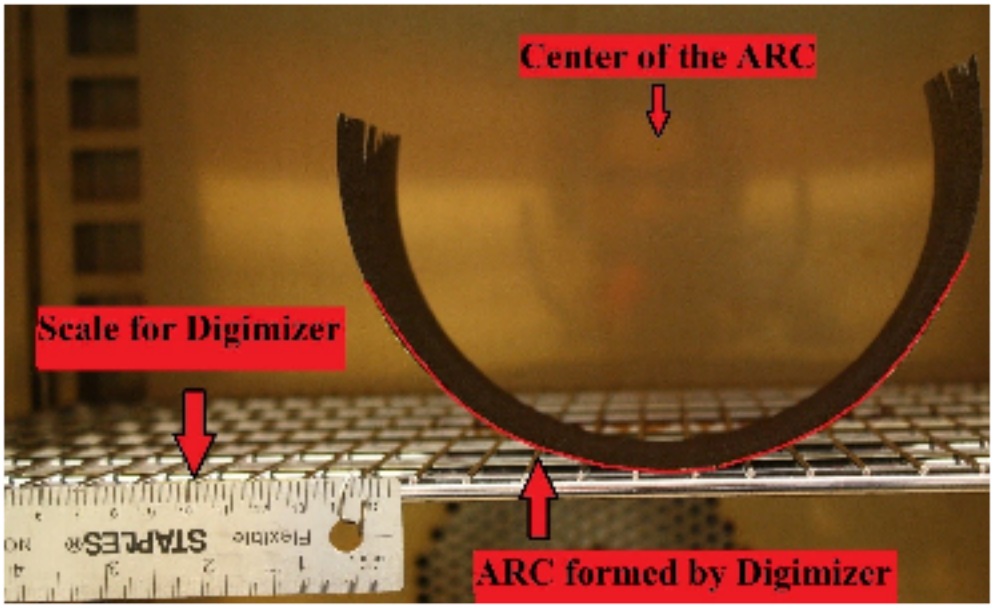

Figure 3.22 Finding center of arc using digimizer [3]

Now after defining the scale, the 'center of the circular path' tool in the software is used mark various points around the curvature of the samples in the image files. After marking the various points along the curvature of the samples, the software finds an average radius and center of the arc formed by the points around the curve. Checking the measurement list for each file gives the value of radius and location of the center of the curvature.

3.2.4 Results and Discussion

After analyzing the radii using Digimizer, for various temperatures mentioned in the temperature cycling experiment, a graph was plotted between Average Radius (cm) vs. Temperature (°C) for both Sample 1A and Sample 3B. The graphs plotted for heating up process are shown in figures 3.23 & 3.24.

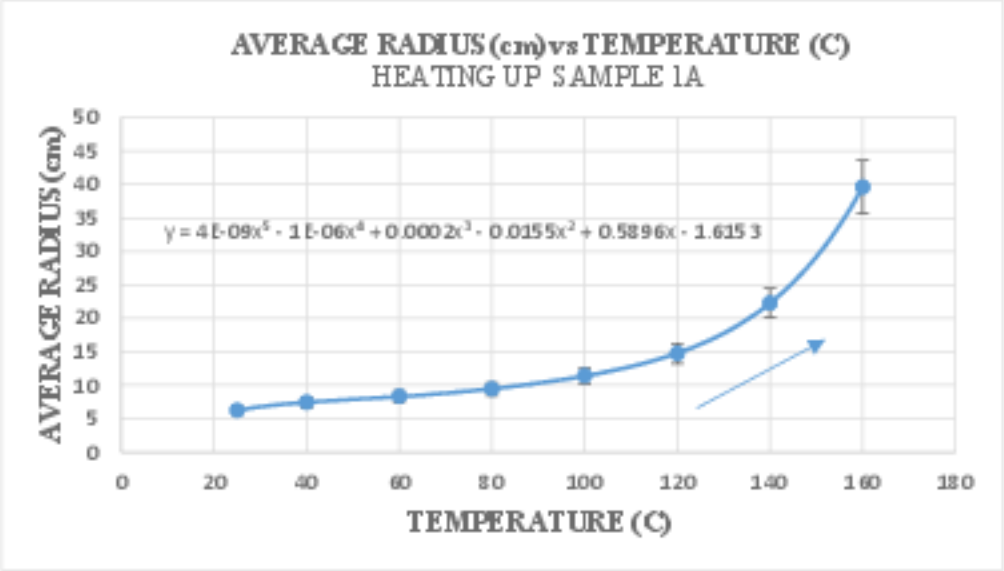

Figure 3.23 Average radius (cm) vs Temperature (C). Heating up of Sample 1A

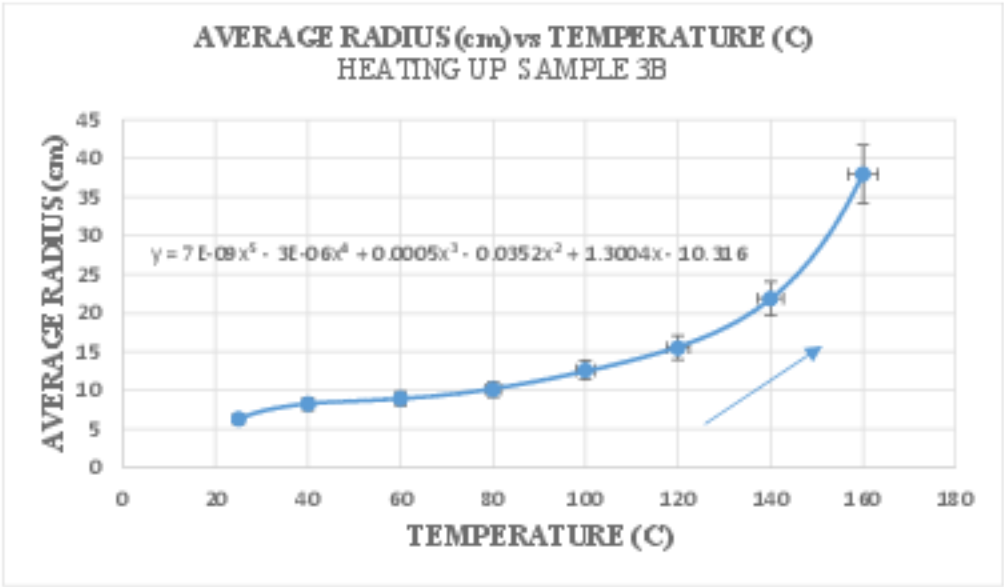

Figure 3.24 Average radius (cm) vs. Temperature (C). Heating up of Sample 3B

The graphs for cooling down of Sample 1A and Sample 3B during the temperature cycling are shown in figures 3.25 & 3.26. All the radius values for the respective temperatures from this experiment are given in Appendix C.

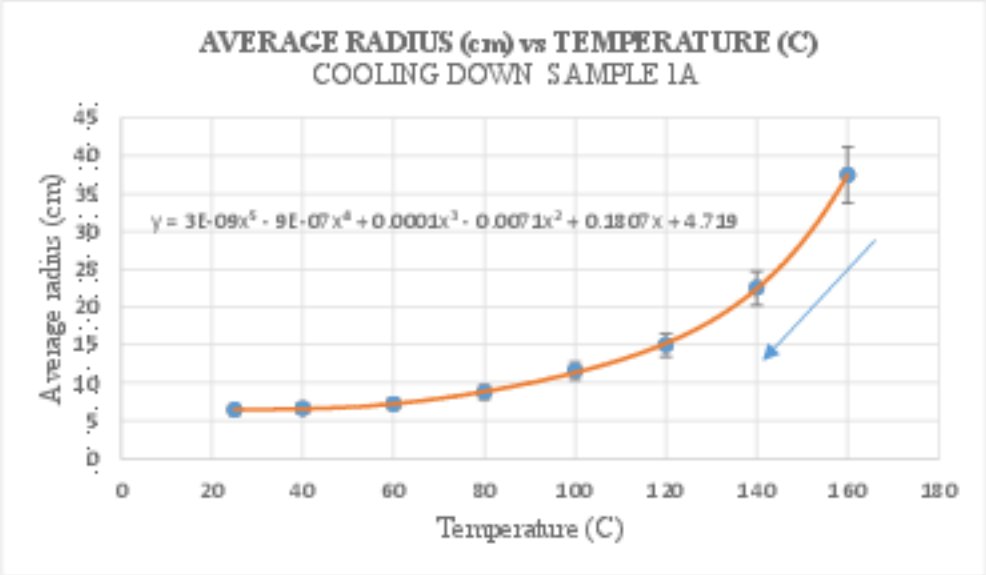

Figure 3.25 Average radius (cm) vs Temperature (C). Cooling down of Sample 1A

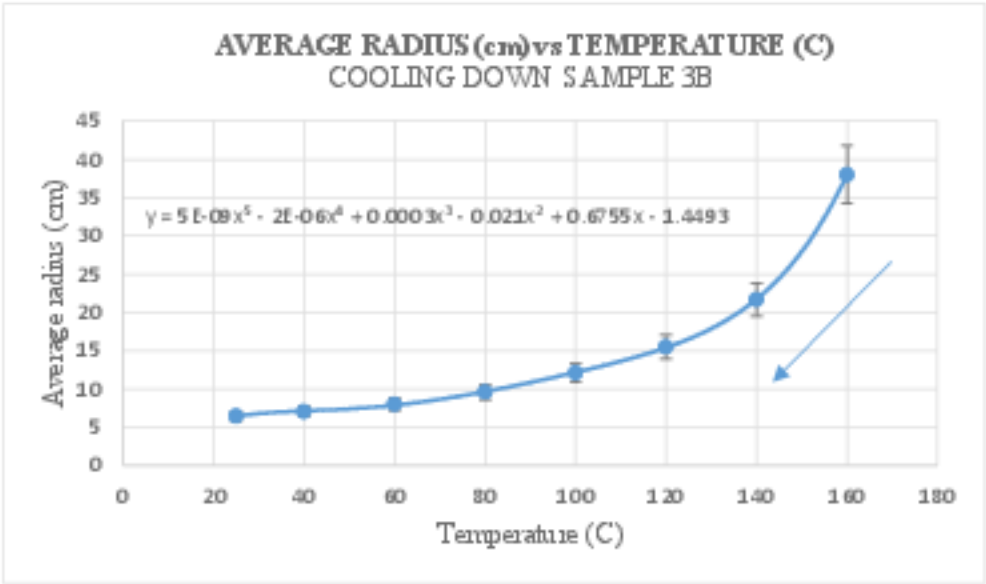

Figure 3.26 Average radius (cm) vs Temperature (C). Cooling down of Sample 3B

From the graphs (figure 3.23- 3.25), it can be concluded that the samples tend to follow the same pattern for change in radius for both heating up and cooling down. The graph is observed to stop at 160 °C because the sample at 180 °C is seen to be flat hence after radius is assumed to infinity. The sample at 180 °C even though looks flat but can still be part of a larger radius. This is explained in section 3.3. Error bars are shown in the graphs as average values are taken from three photographs analyzed at the same temperature.

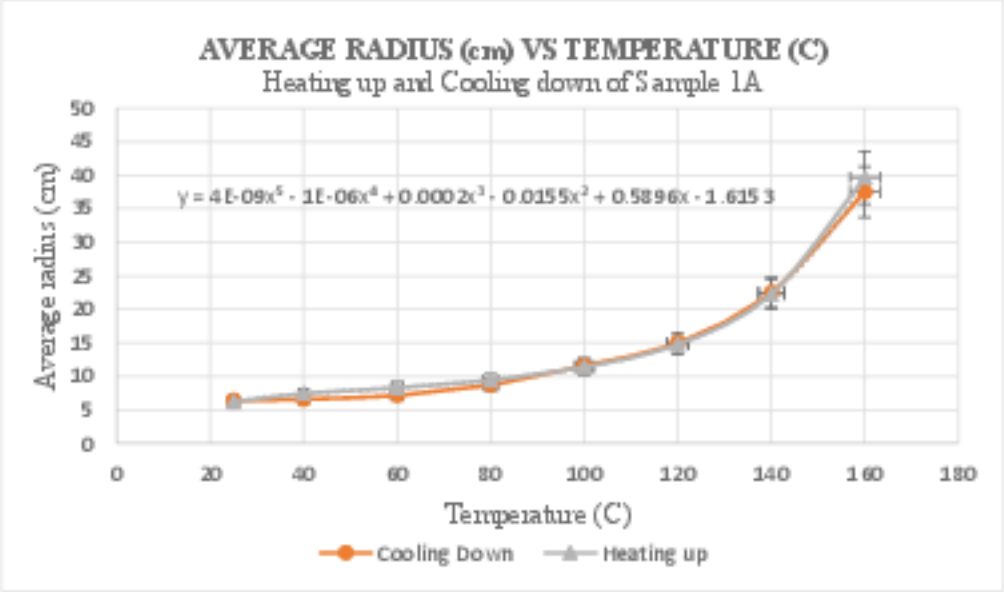

Figure 3.27 Average radius (cm) vs. Temperature (C). Heating up & cooling down of Sample 1A

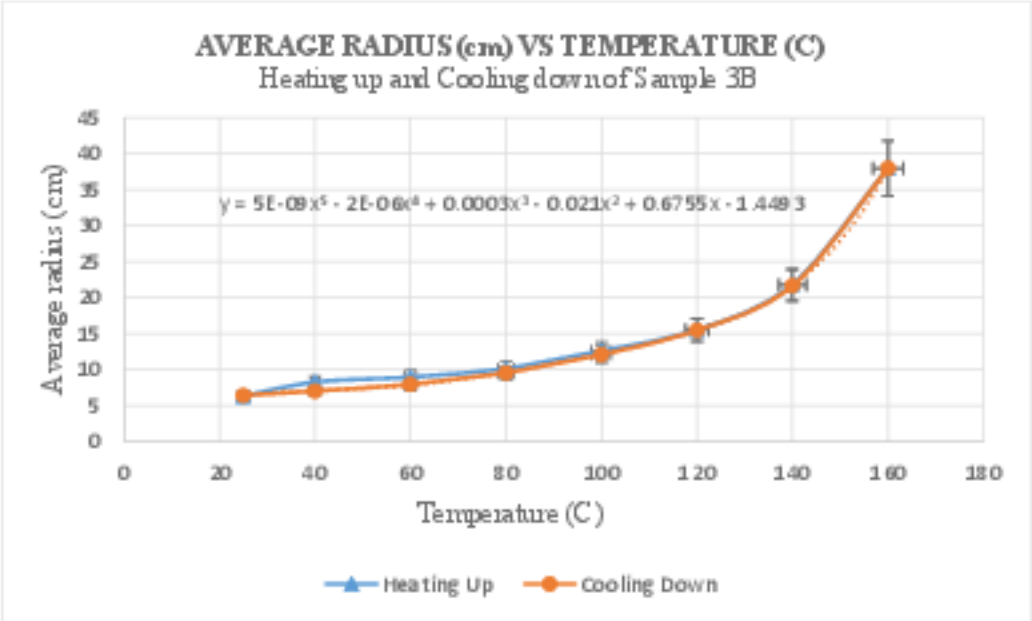

Figure 3.28 Average radius (cm) vs. Temperature (C). Heating up & cooling down of Sample 3B

From the combined graphs for heating up and cooling down of both the Samples 1A and 3B, it can be seen that the material follows non-linear variation with the 5th-degree polynomial equation. The equations of both the graphs are shown in figure 3.27 and 3.28.

Since this test was performed after the desorption of the sample, the radius that the samples are due to the effects of temperature and shrinkage. To compare the radius values obtained due to the effect of thermal coefficient of expansion/contraction of the material laminate theory was used [15]. A MATLAB program was written using the equation (1.1 to 1.29) and input parameters are given in table 3.4 (Refer appendix F).

The MATLAB program helps in generating the theoretical radius for 25 °C to 40 °C, 60 °C, 80 °C, 100 °C, 120 °C, 140 °C & 160 °C.

Modulus of Elasticity E_1 (GPA)	155
Modulus of Elasticity E_2 (GPA)	12.1
Shear Modulus G_{12} (GPA)	4.40
Poisson's ratio υ_{12}	0.248

On axis coefficient of thermal contraction α_1 (10^{-6} %/°C)	-0.018
On axis coefficient of thermal contraction α_2 (10^{-6} %/°C)	24.3
On-axis shrinkage coefficient ε_1^s (%)	0
On-axis shrinkage coefficient ε_2^s (%)	0.033

Table 3.4 Input parameters of material properties for the MATLAB program [2]

A comparison between the theoretical value of radius for their respective temperature and the experimental radius obtained using the MATLAB program is shown in figure 3.29.

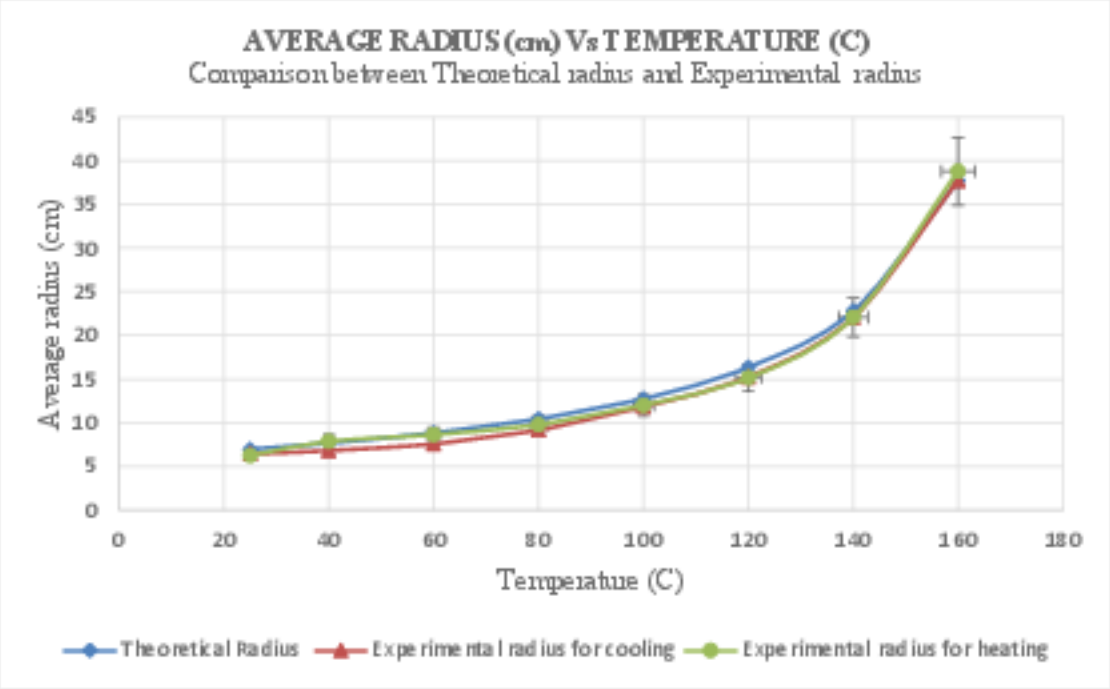

Figure 3.29 Average radius (cm) vs. Temperature (C). Comparison between the Theoretical radius and Experimental radius

From figure 3.29, the experimental and theoretical radius values agree with each other. The variation of radius for change in temperature is a curve of a 5th-degree polynomial equation. The graph (figure 3.29) shows that the contribution of the coefficient of thermal contraction is significant for the curvature change at various temperatures.

The curves show linear proportionality at lower temperatures and non-linear at higher temperatures. At lower temperatures, the value of ΔT is higher, hence the contribution of the coefficient of thermal contraction on radius of curvature is more significant when compared to other factors such as shrinkage and drop in elastic properties. The reason for nonlinearity at higher temperatures is explained in section 3.3.

Hence the contribution of the coefficient of thermal contraction to the curvature of the samples is clear from the above result, it is necessary to determine the contribution of shrinkage in the curvature of the samples.

3.3 Contribution of shrinkage

As we have seen that the samples open up over the course of time at room conditions. This opening up of the samples can be due to various reasons such as post-curing, stress relaxation, and moisture absorption. The effect of temperature change and contribution of the coefficient of thermal contraction is studied using temperature cycling experiment, so in order to find the effect of shrinkage, the following experiment needs to be performed.

The experiment mainly aims at finding the temperature at which the sample opens up entirely and difference from this temperature from the curing temperature (Tc).

3.3.1 Sample preparation

Now after the desorption test, three samples were chosen Sample 1A, Sample 1B, and Sample 3B among six from the desorption test samples (refer to section 3.1). For accounting, the effect of shrinkage, the samples were placed in the oven for heating up until the cure temperature. At cure temperature, if the sample still has some curvature present, this is due to the effect of resin shrinkage in the composite. Because at this temperature the contribution of the effect of difference in coefficient of thermal contraction between the layers is zero and the only factor responsible for the curvature is the resin shrinkage.

3.3.2 Experimental Procedure

1. To prepare the samples for the shrinkage test, the samples were placed in an oven for heating to a temperature and its radii are measured at different temperatures.
2. The purposed samples were heated up and kept constant from 25 °C to 30 °C, 40 °C, 50 °C, 60 °C, 70 °C, 80 °C, 90 °C, 100 °C, 110 °C, 120 °C, 130 °C, 140 °C, 150 °C, 160 °C, 170 °C, 175 °C, 176 °C, 177 °C, 178 °C, 179 °C and180 °C.
3. The radius corresponding to each temperature was recorded and analyzed using Digimser (refer 2.2.1) and graphs were plotted to analyze the exact the temperature at which the samples flattens. The procedure mentioned above was done for three different samples that are Sample 1A, Sample 1B, and Sample 3B.

3.3.3 Results and discussion

Shrinkage test was performed to find to the effect of shrinkage on the curvature of the samples. This is done by heating up the samples until the cure temperature and checking for its radius of curvature. Graphs were plotted between Average radius (cm) vs. Temperature (C) to determine the variation in radius of curvature with an increase in temperature. Figures 3.30 to 3.32 show the Average radius (cm) vs. Temperature (C) for Sample 1A, Sample 1B, and Sample 3B respectively.

The radius values corresponding to the temperature for the respective samples are shown in Appendix D

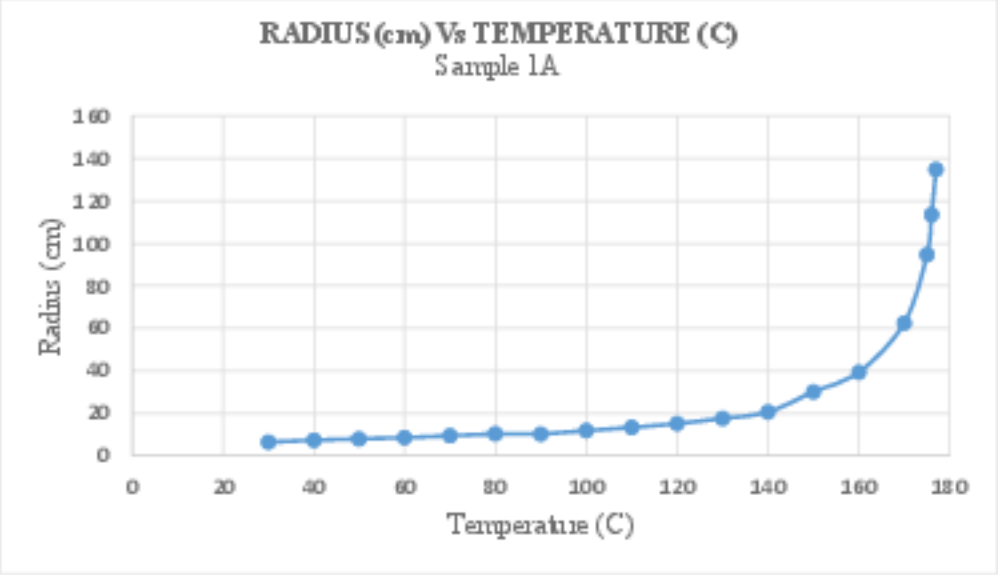

Figure 3.30 Radius (cm) Vs Temperature (C) for Sample 1A

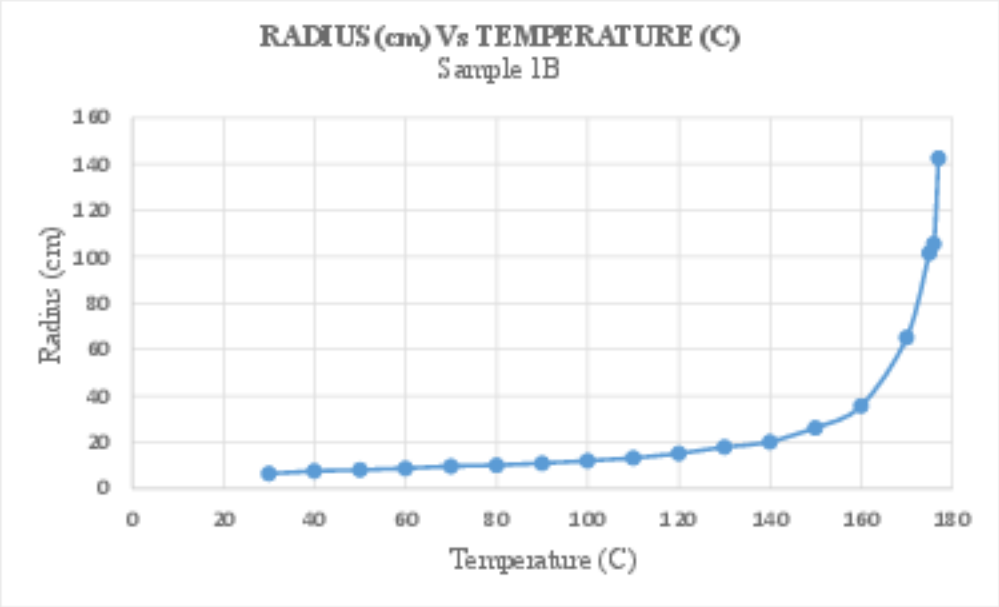

Figure 3.31 Radius (cm) Vs Temperature (C) for Sample 1B

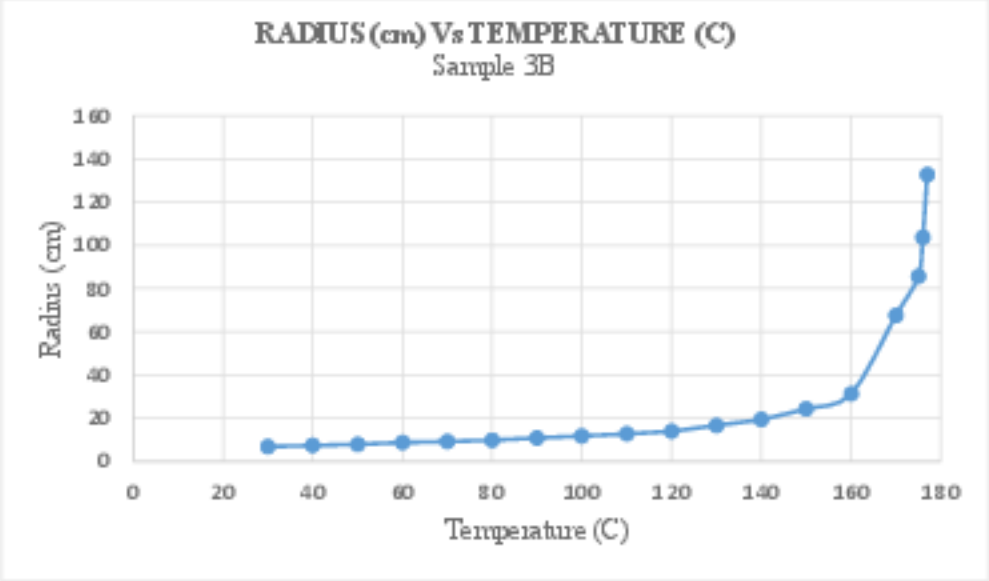

Figure 3.32 Radius (cm) Vs Temperature (C) for Sample 3B

From the above experiments on all the samples above, it was found that the samples appear to be flat at 178°C, but one cannot conclude that the samples are completely flat because they can still have a larger radius and look like flat for this sample size. This is similar to the case of earth being round on a global scale but appears to be flat at the local scale.

After comparing three different samples, a combined graph was plotted as shown in figure 3.33.

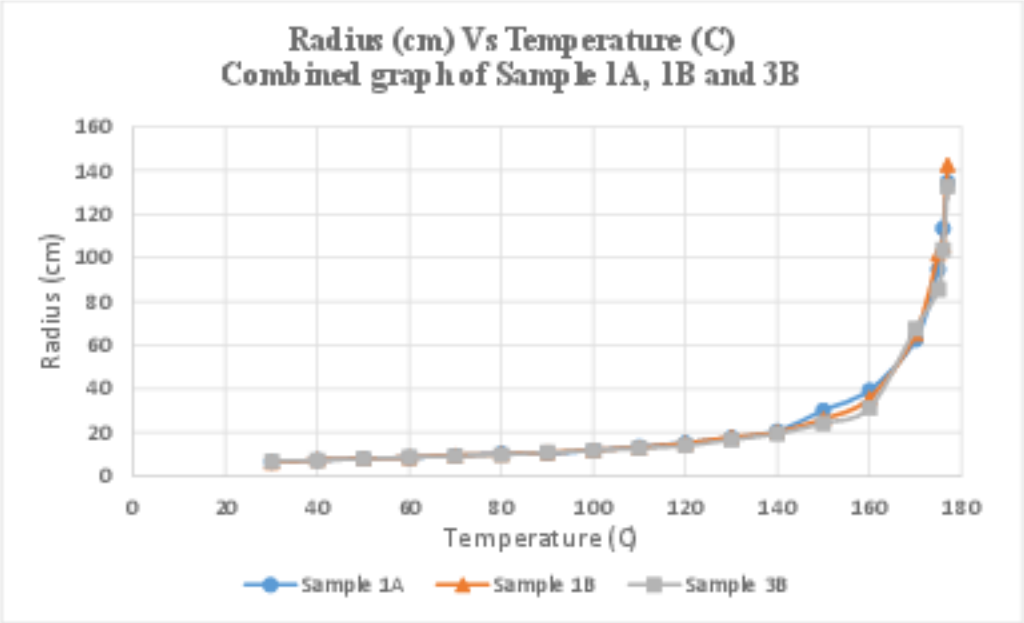

Figure 3.33 Radius (cm) Vs Temperature (C). The combined graph for Sample 1A, 1B, and 3B

All the samples follow the same pattern as shown in temperature cycling which is a 5th-degree polynomial equation (refer 3.1. The sample shows the same variation as a theoretical variation which is verified using MATLAB program (explained in section 3.2).

The radius at 177°C is 136.68 cm and the radius at a temperature greater than 177°C appear to be infinity (sample looked like flat piece) but it also can be a very large radius of curvature which cannot be determined using this technique. The flattening of the sample at various temperature is shown in figure 3.34. So to calculate the shrinkage strain at 177°C, the curvature is calculated using equation 3.1, where K is the curvature of the sample and R is the radius of the sample.

$$K = \frac{1}{R} \qquad \ldots\ldots\ldots\ldots (3.1)$$

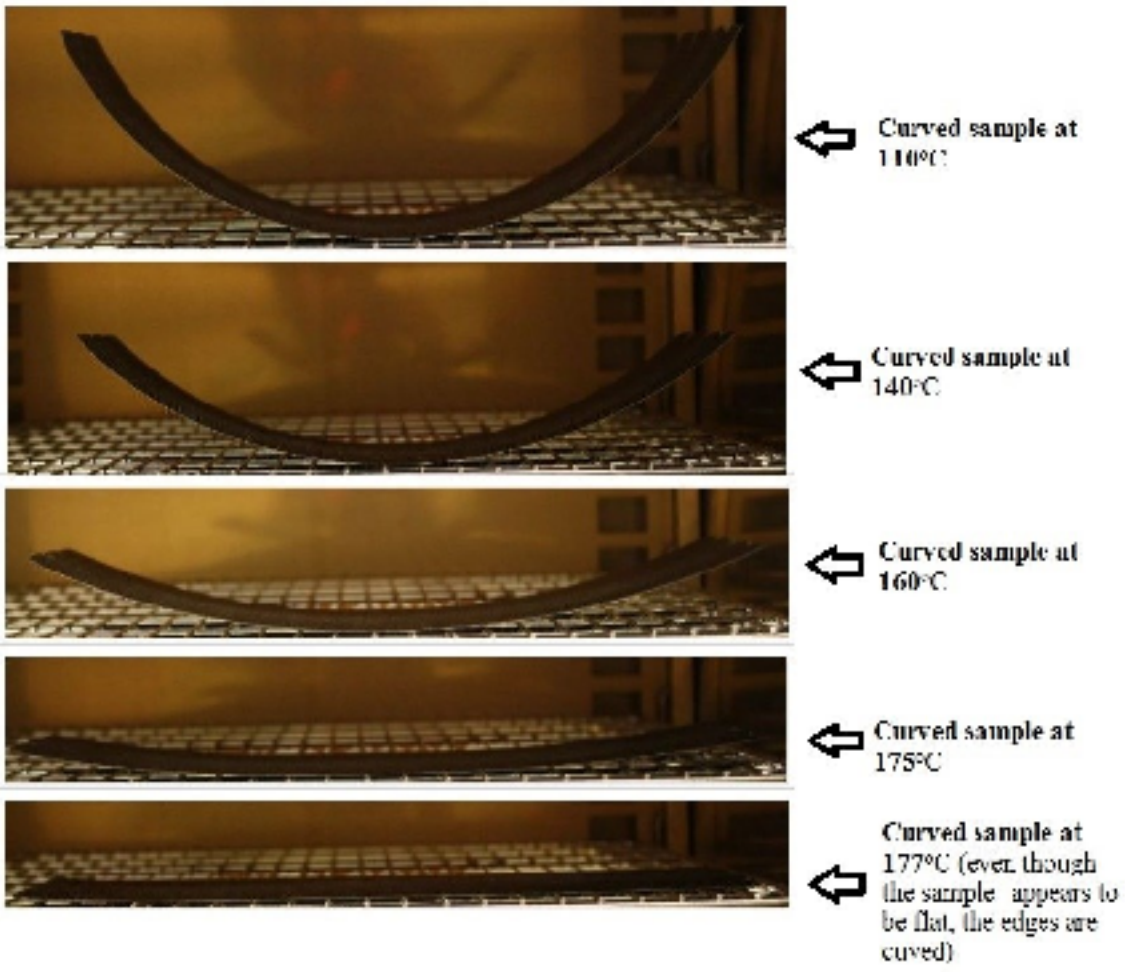

Figure 3.34 Curved samples at different temperatures

After calculating the curvature of the sample K_1 substituting the value in equation 1.13, since all the other values are zero we get the moment due to shrinkage in the x-direction is given as equation 3.2

$$M_x^S = \quad D_{11}\, K_x \qquad \ldots\ldots\ldots (3.2)$$

The moment due to shrinkage in terms of shrinkage strain is given by equation 1.18

$$M_x^S = \int_{\frac{-H}{2}}^{\frac{H}{2}} (\bar{Q}_{11}\varepsilon_x^s + \bar{Q}_{12}\varepsilon_y^s + \bar{Q}_{16}\varepsilon_{xy}^s) z\, dz \qquad \ldots\ldots\ldots (1.18)$$

Where ε_x^s , ε_y^s, ε_{xy}^s are the off-axis strains due to resin shrinkage and are given as,

$$\varepsilon_x^s = \varepsilon_1^s m^2 + \varepsilon_x^s n^2 \;\; , \;\; \varepsilon_y^s = \varepsilon_1^s n^2 + \varepsilon_2^s m^2 \;\; , \varepsilon_{xy}^s = 2(\varepsilon_1^s - \varepsilon_2^s)mn \qquad \ldots\ldots\ldots (1.21)$$

Where ε_1^s and ε_2^s are the strains due to shrinkage of a unidirectional layer, along the fiber direction, and transverse to the fiber direction respectively and m= cos θ and n= sin θ. [2][18]

From the above two equations, the value for the shrinkage strain was calculated as $\varepsilon^s = \varepsilon_2^s = 6.4 \times 10^{-5}$

Different values of ε^s were used for calculation of radius (obtained theoretically) using MATLAB program. The shrinkage strain values used for theoretical calculations are $\varepsilon^s = 6.6 \times 10^{-4}$ [2] , $\varepsilon^s = 3.3 \times 10^{-4}$ (which is half of 0.00066) and $\varepsilon^s = 0.000064$ (value of strain obtained from experimental radius at 177 °C). Using laminate theory, the radii for different values of shrinkage strain for different temperature were plotted as shown figure 3.35. For comparison, the experimental radius obtained for different temperatures (shown in figure 3.35 blue line with error bars) is also incorporated in figure 3.35.

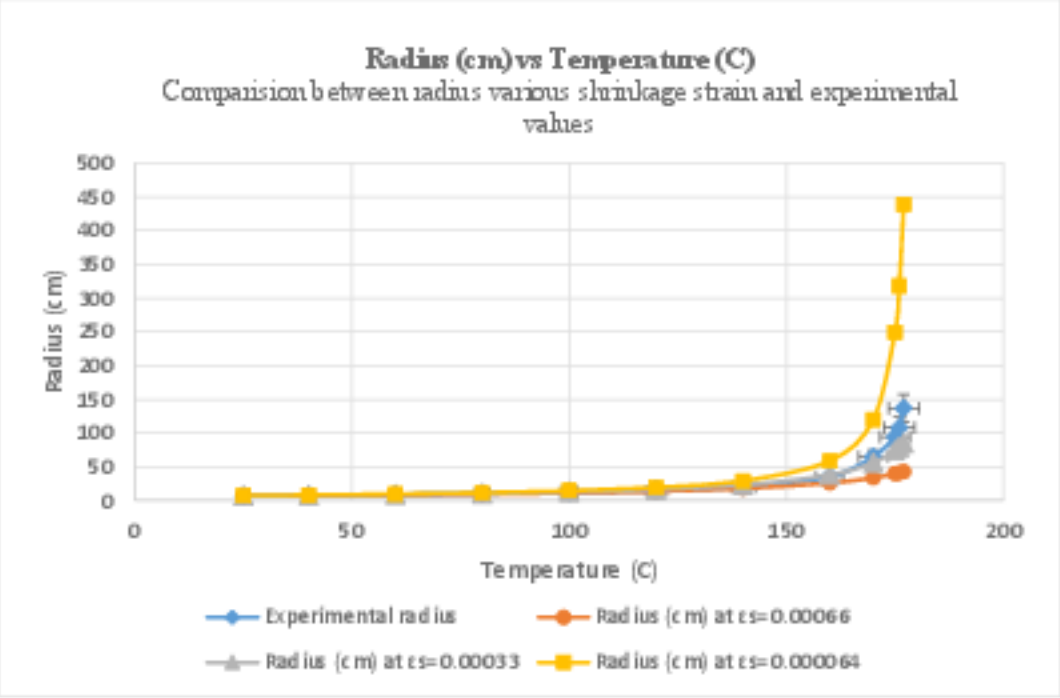

Figure 3.35 Radius (cm) vs Temperature (C). Comparison between radius various shrinkage strain and experimental values

From figure 3.35, it can be seen that good agreement between all the shrinkage strain values with the experimental result is obtained until 120 °C. There is no significant difference in all curves in figure 3.35 until 120 °C. The radius due to shrinkage strain $\varepsilon^s = 6.4 \times 10^{-5}$ shows a higher value than the

experimental radius for all the temperature higher than 140°C whereas the radius due to shrinkage strain $\varepsilon^s = 3.3 \times 10^{-4}$ seems to agree with experimental data until 160°C. This difference in radius values (when compared to experimental radius) for $\varepsilon^s = 3.3 \times 10^{-4}$ at higher temperature can be attributed to the reduction in elastic properties of the composite material (reduction in E_2 and G_{12}). The value of E_2 and G_{12} were reduced to be a percentage value at room temperature.

To check for a decrease in elastic properties, a graph for radius of the sample at 100%, 80%, 60%, 50%, 40%, 20% and 10% of elastic properties (Values of E_2 and G_{12}) mentioned in input parameter in Table 3.1 with temperature (C) was plotted as shown in figure 3.36.

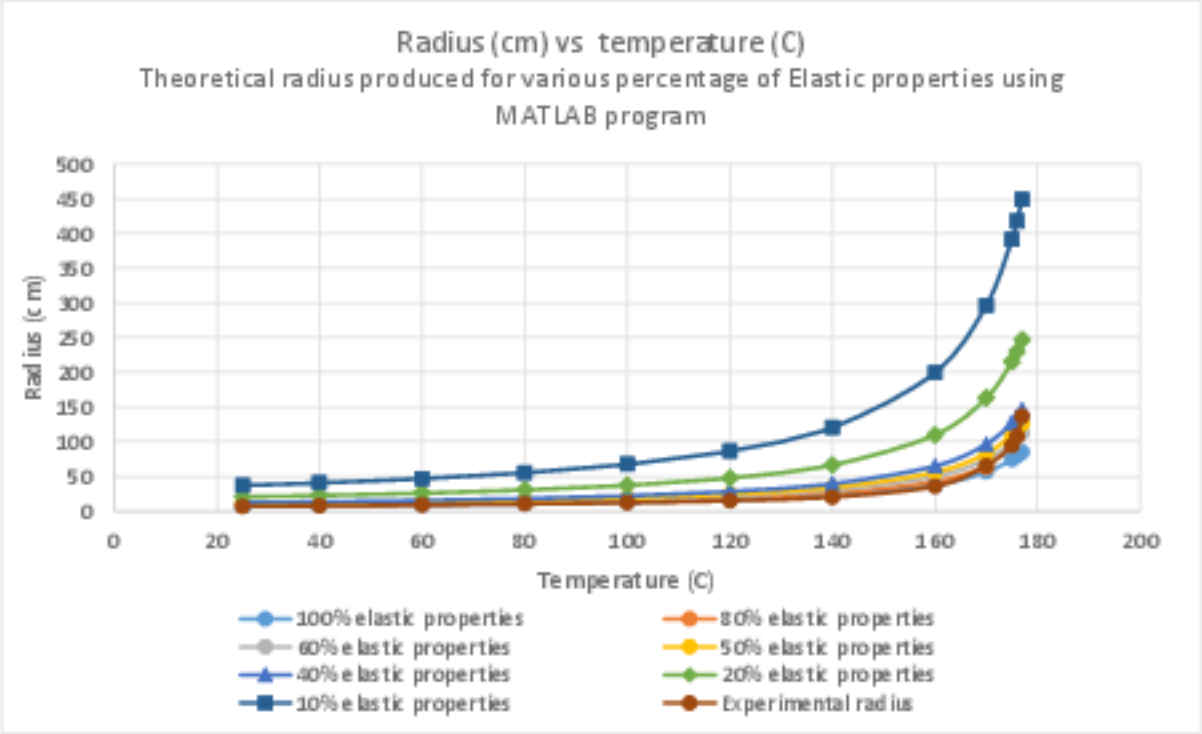

Figure 3.36 Radius (cm) vs. Temperature (C). Theoretical radius produced for different percentage of Elastic properties using MATLAB program

From the graph, theoretically, as the samples tend to be soft (sample have low elastic properties), they tend to open up more (large radius). From the graph (figure 3.36), it is seen that the samples have

elastic properties similar to 100% of elastic properties at a lower temperature (<160°C), whereas at a higher temperature (temperature higher than 160°C) the samples tend to have lower elastic properties. This drop in elastic properties can be seen in the graph as the samples tend to drop from 100% elastic properties to 40% or more when the temperature is greater than 160 °C.

From figure 3.36, for the reduction of elastic constants to about 40% or more of the values at room temperature, there is no significant difference in the radius of curvature at low temperature. For temperature greater than 160 °C, the change in radius becomes more pronounced.

By using the values of E_2 and G_{12} to be 50% those at room temperature, and the linear shrinkage strain of 3.3×10^{-4}, the value of the radius at cure ($\Delta T = 0$) is indeed equal to 1.37 cm, which agrees with the experimental value.

From figure 3.35, a graph plotted for calculated values of the radius at different temperatures and different values of assumed ε^0. It seems that the best fit of shrinkage strain to the experimental radius is linear shrinkage strain corresponding to 3.3×10^{-4}. A linear shrinkage strain of 3.3×10^{-4} corresponds to a volumetric strain of 1×10^{-3}.

It is also observed that at low temperature (temperature less than 100 °C) the radius does not change with the amount of shrinkage. This is because at low temperature, the difference in actual temperature and cure temperature (ΔT) (refer to equations 1.6-1.11) is high and this makes the contribution of thermal coefficient of expansion much more dominant than the contribution of resin shrinkage. At higher temperatures (temperature greater than 160 °C) ΔT is small, and this makes the relative contribution from resin shrinkage more significant than contribution due to the coefficient of thermal contraction.

CHAPTER 4: EFFECT OF MOISTURE

4.1 Opening up of the sample

The samples after curing, when placed in room conditions were observed to be opening up. This can be seen by physically tracing and measuring the radius of curvature of the samples using method explained in section 2.3.

The radii were measured for every 1 h for the first 6 h and then for every 6 h time interval until 24 h. Later time interval was increased to 24 h, 48 h and 72 h until 168 h, 288 h, and 840 h respectively. The total duration of measurements of the radius was 840 h. This procedure was done for three samples.

Radius values were plotted against their respective time in hours (figures 4.1, 4.2 & 4.3). The radii for the upper and lower side of the same sample are plotted in the same graph for comparison.

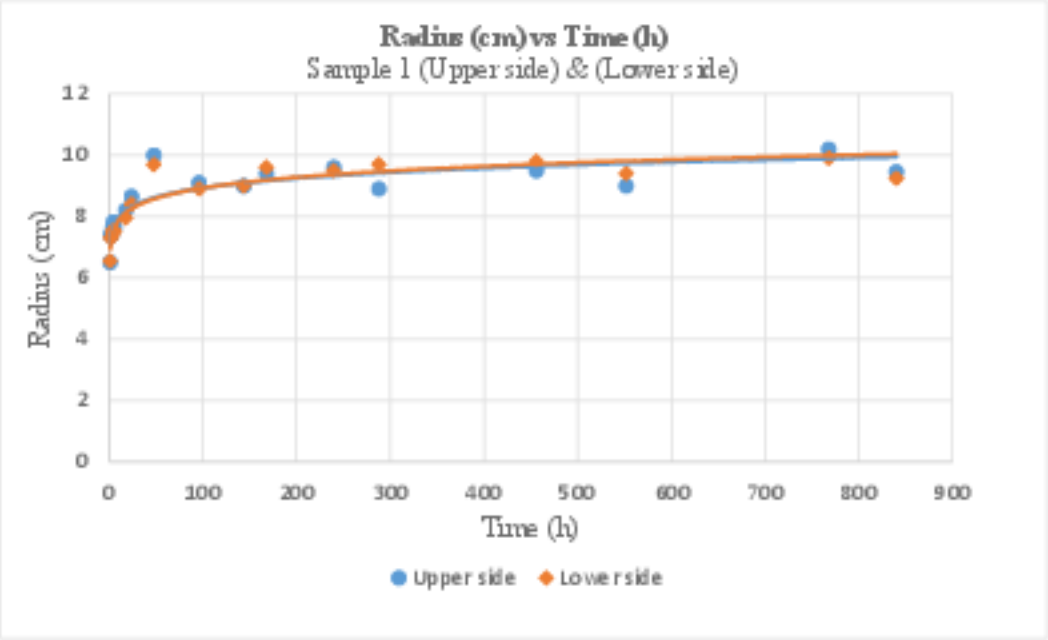

Figure 4.1 Radius (cm) vs Time (h) for Sample 1 (Upper side) & (Lower side)

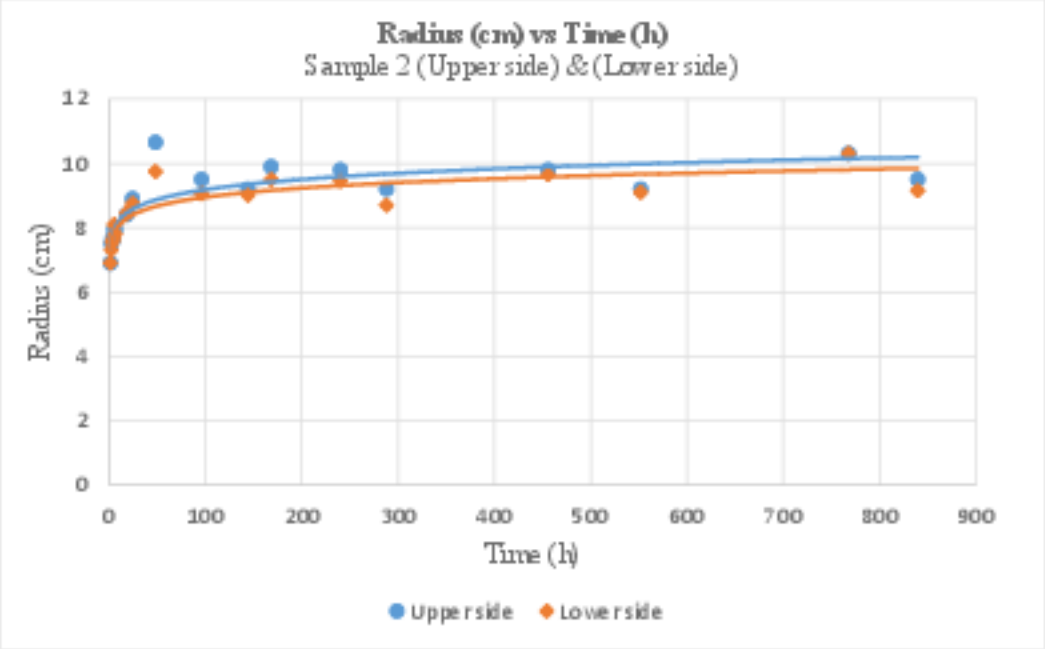

Figure 4.2 Radius (cm) vs Time (h) for Sample 2 (Upper side) & (Lower side)

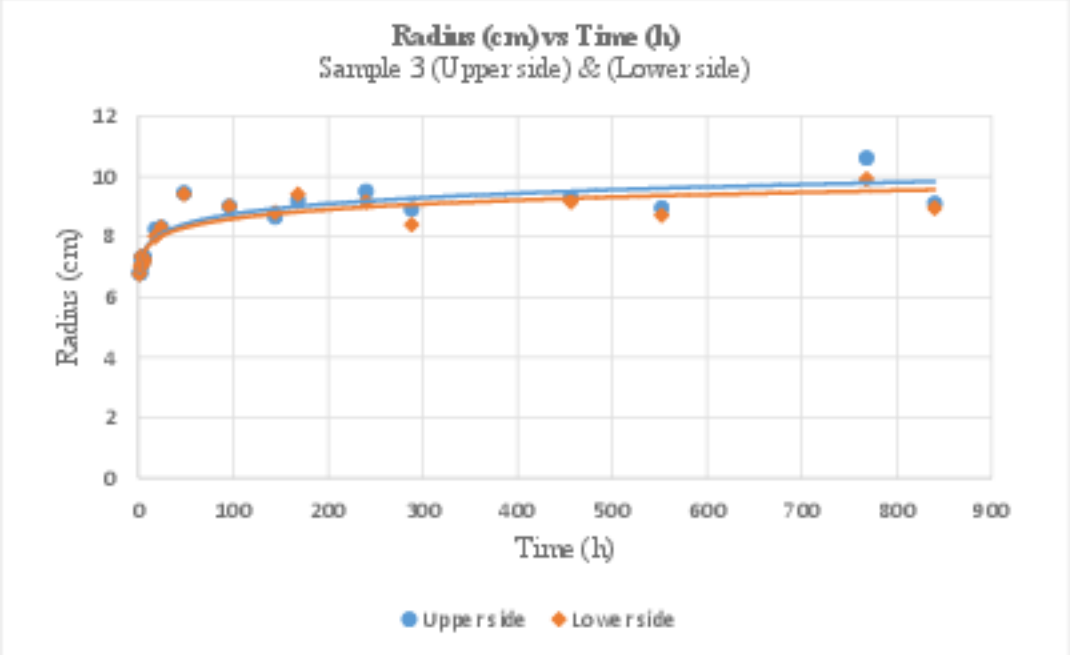

Figure 4.3 Radius (cm) vs Time (h) for Sample 3 (Upper side) & (Lower side)

From the figures shown above, it is clearly evident that the samples tend to change their radii of curvature as they are left at room conditions. Since from DSC test, it is concluded that the samples are after completely cured, so the only reason for opening is because of the moisture absorption from the surrounding. This can be concluded by analyzing the effect of moisture absorption on the samples.

4.2 Moisture Absorption

The primary aim of performing a moisture absorption test is to find the effect of moisture on the opening up of the sample. In order to do so, it is necessary to calculate the stress resultants and moment resultants due to moisture. This is done by using the coefficient of moisture expansion β_H. Along with the calculation of stress and moment resultants, the samples are also checked to see if the moisture absorption follows the Fickian law of diffusion. Fick's second law of diffusion is given by equation 4.1

$$\frac{\partial \Delta C}{\partial t} = D\frac{\partial^2 \Delta C}{\partial z^2} \qquad \ldots\ldots\ldots (4.1)$$

ΔC= Moisture content (%). (Refer to equation 1.30)

D = diffusion coefficient.

t = conditioning time.

z = length in the thickness direction.

The Fick's second law equation (4.1) can be derived into form as shown in equation (4.2) [22]. Fick's second law of diffusion helps to understand the process of moisture absorption and desorption in a material with the help of a diffusion coefficient [25].

$$\Delta C = \frac{4M_m}{h\sqrt{\pi}}\sqrt{t}\sqrt{D} \qquad \ldots\ldots\ldots (4.2)$$

M_m = Maximum moisture content.

D = diffusion coefficient.

t = conditioning time.

h= thickness of the sample.

So to check the samples, whether they follow Fick's law of diffusion, a graph between moisture content (ΔC) and the square root of time needs to be plotted. Figure 4.4 shows a schematic representation of the Fickian curve i.e. the curve which follows the equation 4.2.

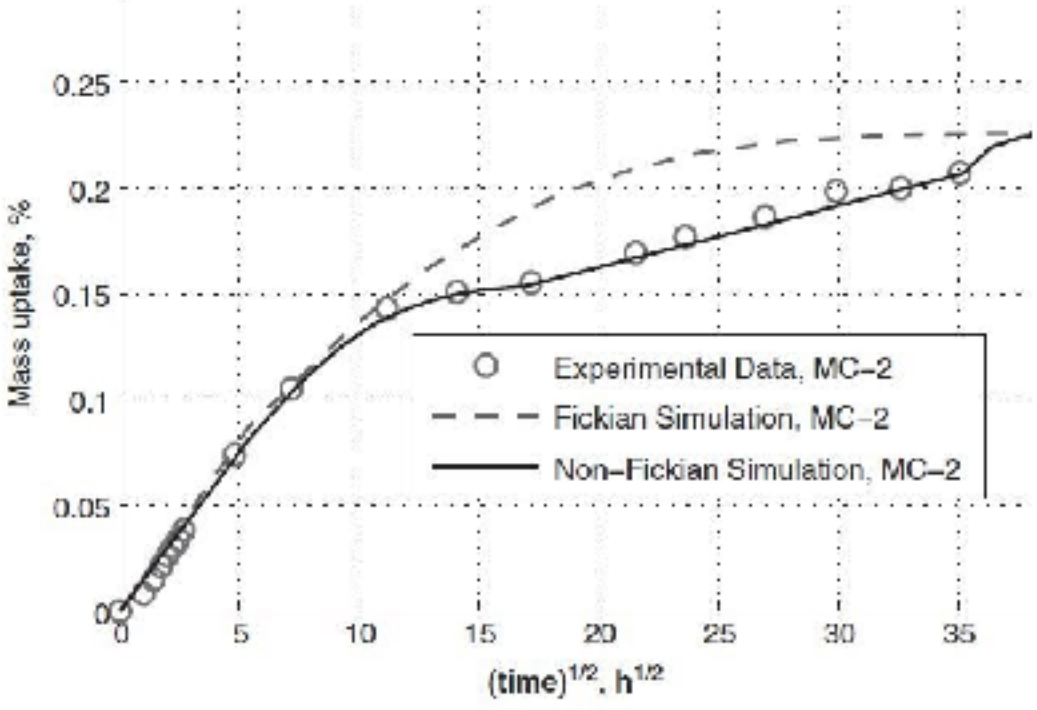

Figure 4.4 Schematic representation of Fickian curve [25]

4.2.1 Sample preparation

Two samples of carbon epoxy (CYCOM 922) material with the layup sequence and dimensions shown in figure 4.5 were manufactured using 4DPC. The samples were labeled as samples 1 and sample 2 along with marking the upper and lower surfaces (as shown in figure 4.6) for measuring the radius and the weight of the samples.

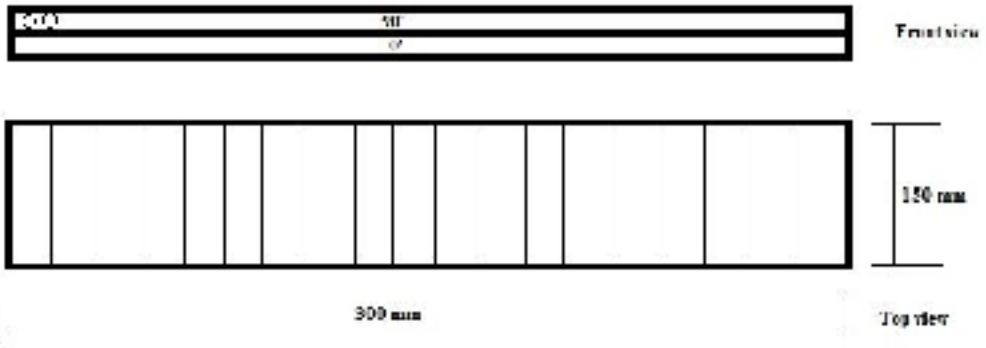

Figure 4.5 Layup sequence of material for Moisture Absorption

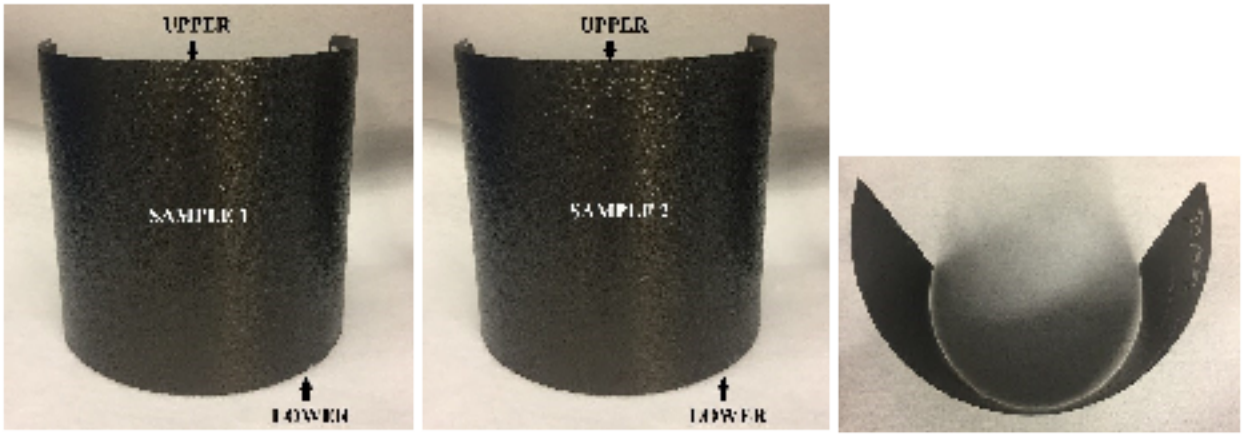

Figure 4.6 Moisture Absorption samples

4.2.2 Experimental Procedure

1. After preparing new samples for moisture absorption (refer 4.1.1). The samples were left in relative humidity averaging about 30% and a temperature of 22°C (72°F) for moisture absorption through diffusion from the surroundings.

2. During this moisture absorption, the relative humidity recorded by using humidity and temperature logger (DICKSON TP125).

3. The Radius & Weight measurements of dry samples were recorded, using the techniques and devices mentioned in the sections 2.2.1 and 2.2.3. Both the weight and radius were recorded at time intervals of every 1 h. for the first 5 h, then for an every 5 h until 53 h of exposure to surroundings. Later the readings were taken every 12 h. until 161 h. of total time after curing. Eventually, this time interval between the readings was increased to 24 h until the weight of the sample attained a constant weight.

4. The weights of the sample were measured using a weighing scale of 0.1mg of accuracy (shown in figure 2.17)

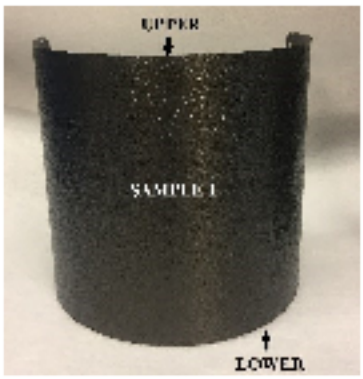

Figure 4.7 Schematic representation of a sample for Moisture Absorption

5. After calculating both the radius and weight, graphs were plotted between Radius (cm) vs. Time and Weight (gm) vs. Time. The process mentioned above is repeated for both Sample 1 and Sample 2.

4.2.3 Results and Discussion

The humidity and temperature logger recorded the Relative humidity and temperature of the room at which the samples were placed, for every 15 min during the whole course of the experiment. The range of relative humidity and temperature change is shown in figure 4.8.

From data's plotted in a humidity and temperature logger (figure 4.8), It is observed that change in temperature at which the samples were placed was fairly consistent and the relative humidity change is not

very significant. This variation in relative humidity does not have a large impact on the change in radius as the diffusion is a very slow process.

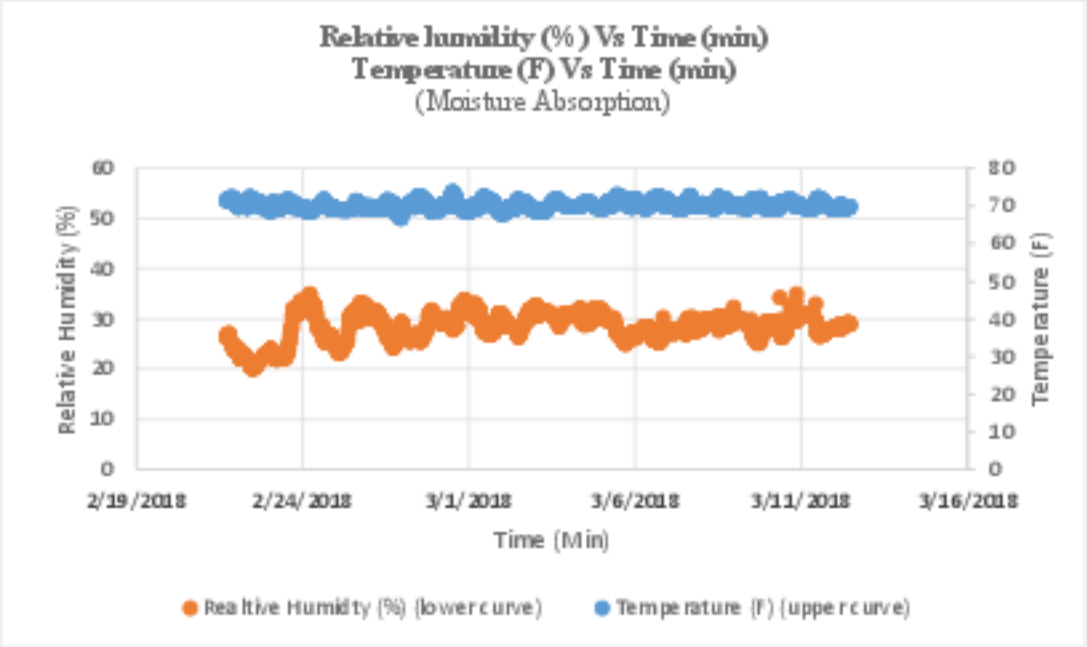

Figure 4.8 Relative humidity (%) & Temperature (C) Vs Time (min) during Moisture Absorption

A. Radius Calculations

The graph between Radius (cm) Vs. Time (min) is plotted for both sample1 and sample 2. The graphs were plotted for both the upper and lower side of each sample as shown in figures 4.7 & 4.8.

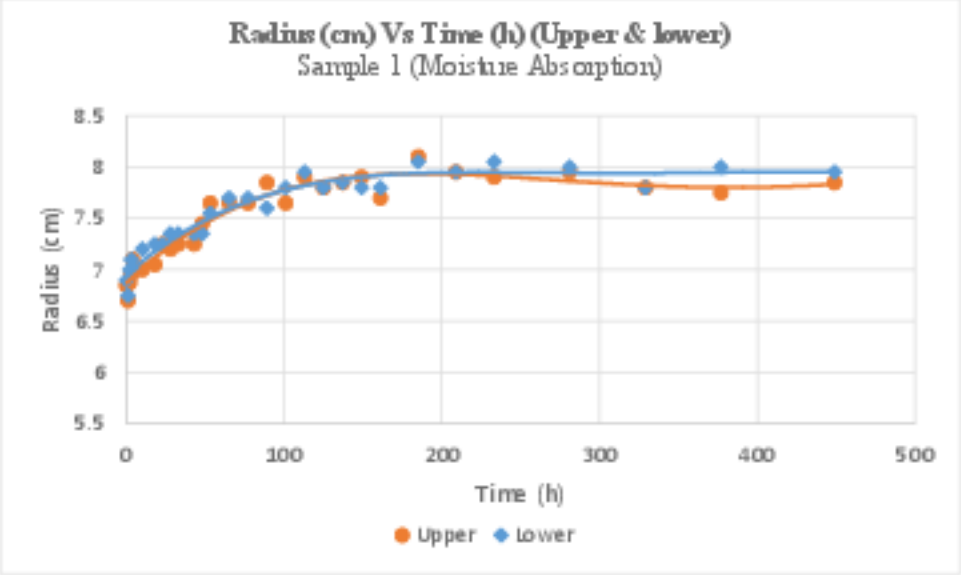

Figure 4.9 Radius (cm) Vs Time (h) (Upper & lower). Sample 1 (Moisture Absorption)

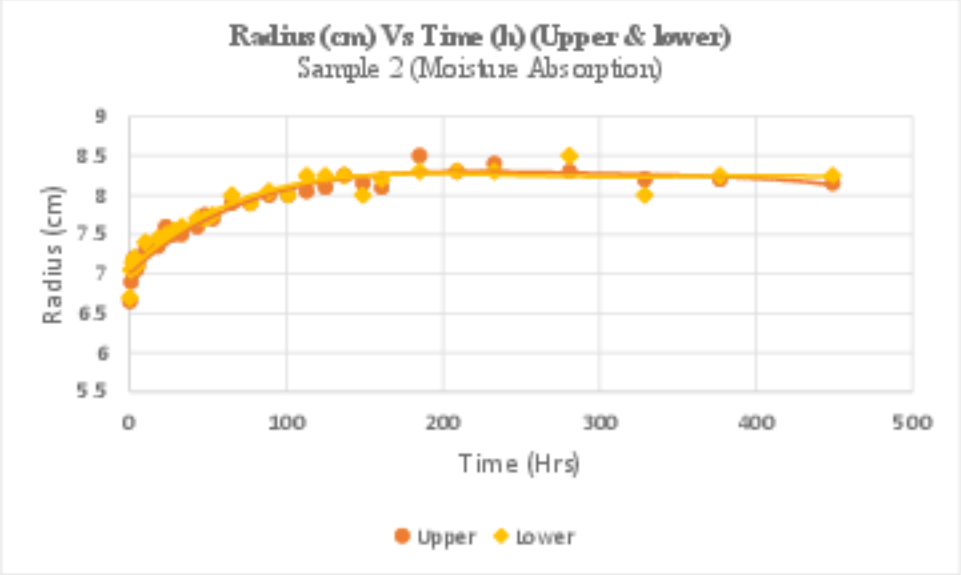

Figure 4.10 Radius (cm) Vs Time (h) (Upper & lower). Sample 2 (Moisture Absorption)

From figures 4.9 and 4.10, it is clear that there is is there is a significant change in radius for the first 0-100 h. This is the period at which the rate of moisture diffusion into the material is maximum, and this can be validated using a Weight (g) vs. Time (h) (shown in figure 4.11 - 4.12), and finding the moisture diffusion into the sample for 0-100 h.

The final average radius of the sample obtained at the end of the experiment is shown in table 4.1

Samples Name	Final Average Radius (cm)
Sample 1	7.94 ± 0.16
Sample 2	8.28 ± 0.20

Table 4.1 Final radius of the sample after Moisture Absorption

The difference between the values of the radius (Table 4.1) is due to the difference amount of moisture diffused into the samples. The moisture content (ΔC) in sample 1 at the end of the experiment is found to be 0.31% whereas in Sample 2 the moisture content (ΔC) was found to have 0.29%. This difference in moisture content is very small but the initial weight of sample 2 is larger than sample 1 (refer figure 4.9 & 4.10), sample 2 has more moisture present in it. Hence moisture weight present in sample 2 is slightly larger than sample 1. This is the reason for the samples having different final average radius.

B. Weight determination

During this experiment weights of samples were recorded and plotted against time (shown in figure 4.9 and 4.10). This was done to analyze the change in weight of the samples due to the moisture diffusion.

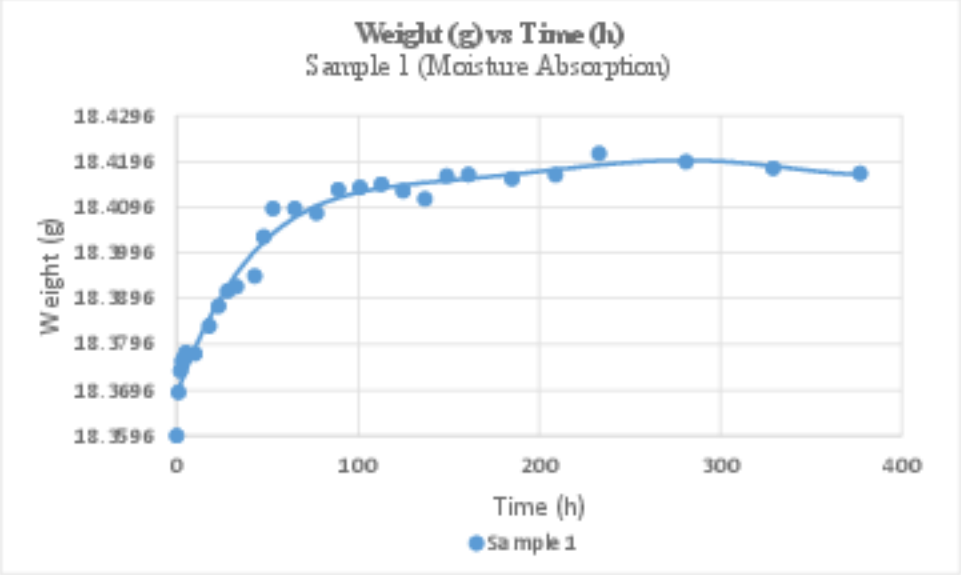

Figure 4.11 Weight (g) vs. Time (h) for Sample 1 during Moisture Absorption

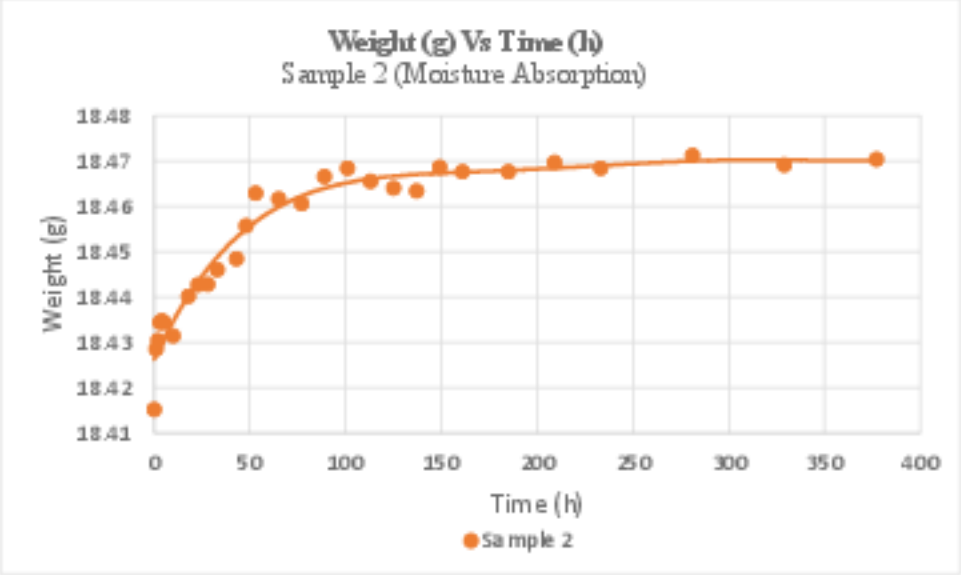

Figure 4.12 Weight (g) vs. Time (h) for Sample 2 during Moisture Absorption

From figures 4.11 & 4.12, it is clear that the moisture absorption for first 0 – 100 h is very high and later on the moisture absorption reach an asymptotic value. To observe the diffusion of the moisture into the samples, the moisture content (ΔC) (as explained in equation 1.30) is plotted against the Square root of time to check for the Fick's second law of diffusion as explained in equation 4.2

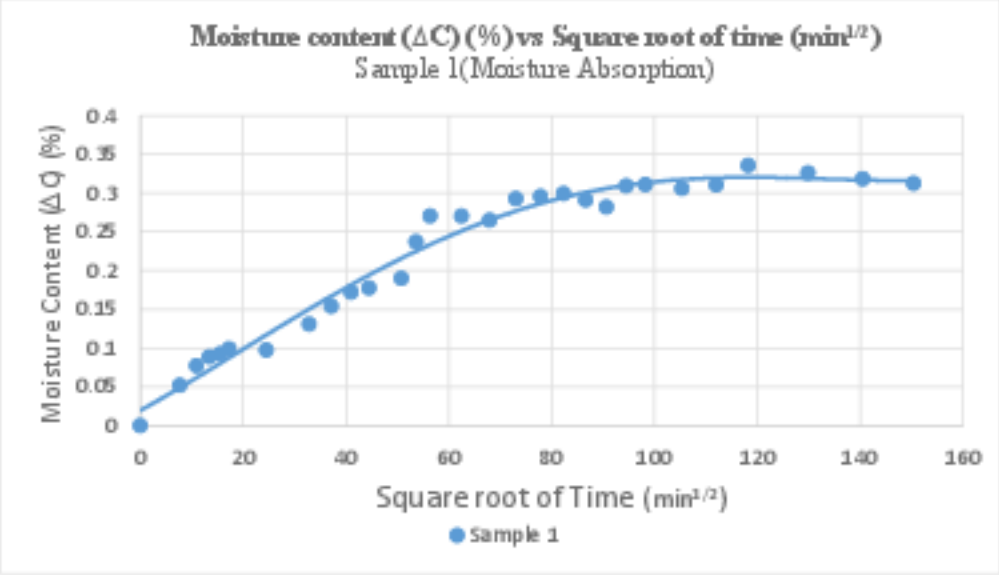

Figure 4. 13 Moisture content (ΔC) (%) vs. Square root of time (min1/2) for Sample 1 (Moisture Absorption)

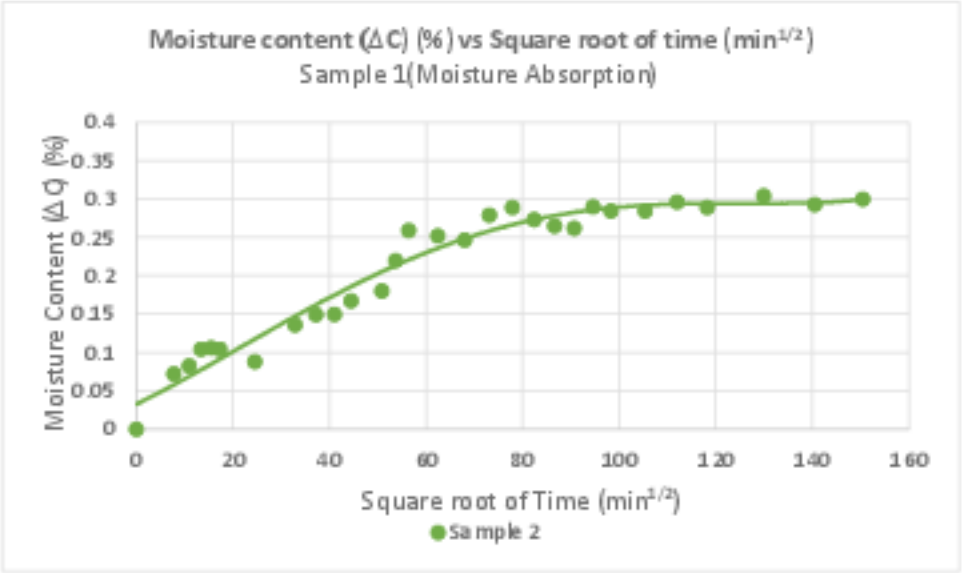

Figure 4. 14 Moisture content (ΔC) (%) vs. Square root of time (min1/2) for Sample 2 (Moisture Absorption)

From figures 4.13 and 4.14, it is observed that both samples follow good relation with Fick's second law of diffusion (refer figure 4.4). This means the composite made by 4D printing absorb moisture from the surrounding through diffusion explained by the equation 4.1 & 4.2. This conclusion is made by comparing

the figure 4.15 with figure 4.4. This is done to understand the moisture diffusion pattern in composite samples made by 4DPC.

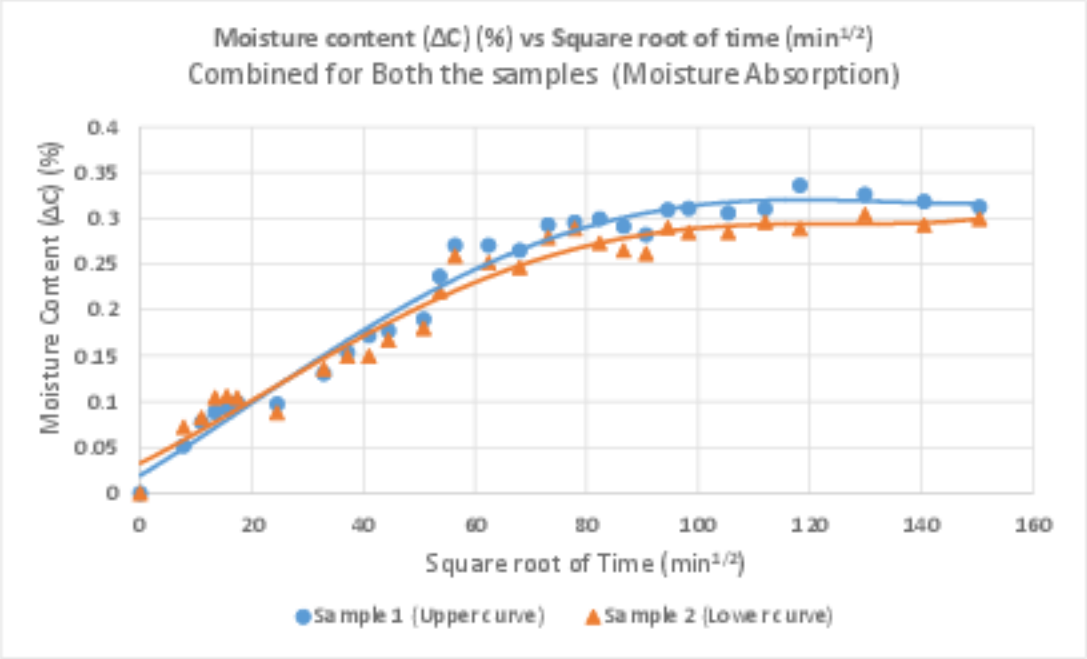

Figure 4.15 Moisture content (ΔC) (%) vs. Square root of time (min1/2) for both the samples (Moisture Absorption)

To observe the variation in radius for the change in moisture content (ΔC) (given by equation 1.30) present in the sample, a graph is plotted between Average radius (cm) vs. Moisture content (ΔC) as shown in figure 4.16.

From the graph shown in figure 4.13, it is clear that the radius change in the sample is linearly proportional to the moisture content (ΔC). Since the radius is the average value, they are represented with error bars in the graph.

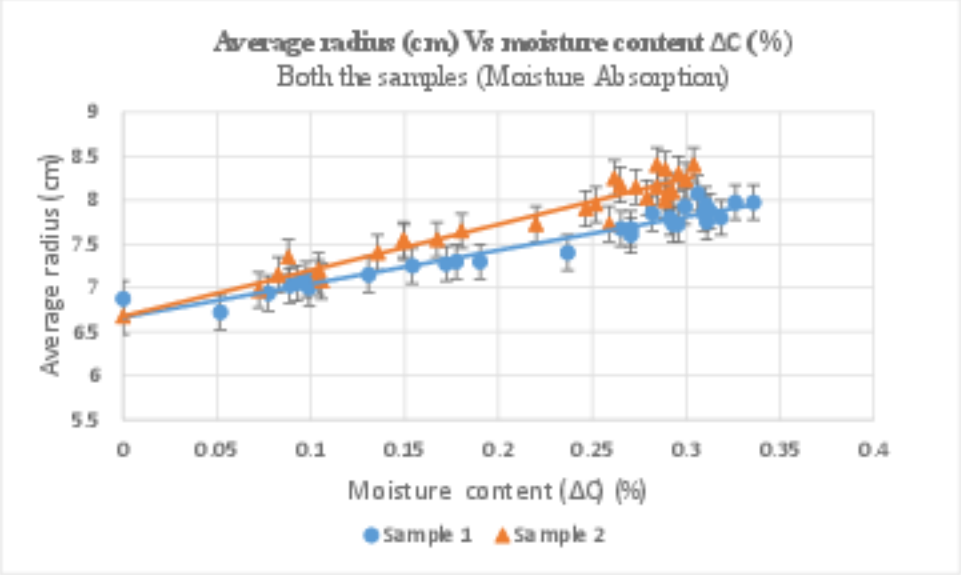

Figure 4.16 Average radius (cm) vs. moisture content ΔC (%) for both the samples (Moisture Absorption)

The change in radius with moisture content is linear. Validating this result with the theoretical analysis is necessary.

So to calculate the effect of moisture on samples made by 4D PC theoretically, it is necessary to refer the value of the coefficient of moisture expansion (β_H) of the laminate to calculate the stress resultants and moment resultants. Since the coefficient of moisture expansion (β_H) of a composite is a material property, it is dependent on various properties such as moisture expansion coefficient of the matrix, fiber volume fraction, the elastic modulus of composite and the elastic modulus of the matrix. Hence while calculating the coefficient of moisture expansion the above-mentioned parameter was taken into consideration.

All the above-mentioned parameters are referred from various references as shown below follows:

β_m = Isotropic matrix moisture expansion coefficient (β_m = 0.004 [20])

v_f = fiber volume fraction (Assumed to be 0.6).

E_m = modulus of the isotropic matrix [26].

E_2 = Elastic modulus of the unidirectional composite [26].

4.3 Calculation of stress resultants and moment resultants due to Moisture Absorption

Analogous to the coefficient of thermal contraction, the stress resultant and the moment resultant due to moisture absorption is given by the equation 1.22-1.29.

The stress resultants and moment resultants due the difference in coefficient of thermal contraction between the layers during cooling and resin shrinkage is responsible for the curvature of the laminate (laminate attains smaller radius) during curing. Whereas the stress resultants and moment resultants due to moisture absorption are responsible for the opening up of the laminate (laminate attains higher radius). Hence we can conclude that the effect of moisture absorption is opposite when compared to the effect of the difference in coefficients of thermal contraction and resin shrinkage.

The total stress resultant due to the difference in coefficient of thermal contraction, shrinkage strain and coefficient of moisture expansion, considering the directions for the stress resultants is given by equation 4.3.

$$\textbf{Total Stress resultants} = N^T + N^S + (-N^H) \qquad \ldots\ldots\ldots (4.3)$$

The total moment resultant due to the difference in coefficient of thermal contraction, shrinkage strain and coefficient of moisture expansion, considering the directions for the moment resultants is given by equation 4.4.

$$\textbf{Total Moment resultants} = M^T + M^S + (-M^H) \qquad \ldots\ldots\ldots (4.4)$$

The above equations are applicable for samples whose reference or initial state is flat piece at cure temperature (Tc).

The following equation gives the contributions of the difference in coefficients of thermal contraction between the layer, resin shrinkage and coefficient of moisture expansion in the radius of the sample [2].

$$R_x = \frac{1}{K_x} \quad \ldots\ldots\ldots (4.5)$$

$$R_y = \frac{1}{K_y} \quad \ldots\ldots\ldots (4.6)$$

$$K_x = \frac{1}{B_{11}}[N_x^T + N_x^s - N_x^H - A_{11}\varepsilon_x^\circ - A_{12}\varepsilon_y^\circ] \quad \ldots\ldots\ldots (4.7)$$

$$K_y = \frac{1}{B_{22}}[N_y^T + N_y^s - N_x^H - A_{12}\varepsilon_x^\circ - A_{22}\varepsilon_y^\circ] \quad \ldots\ldots\ldots (4.8)$$

$$\varepsilon_x^\circ = \frac{Y_2(M_x^T + M_x^S - M_x^H - X_3) - X_2(M_y^T + M_y^s - M_y^H - Y_3)}{Y_2X_1 - Y_1X_2} \quad \ldots\ldots\ldots (4.9)$$

$$\varepsilon_y^\circ = \frac{Y_1(M_x^T + M_x^S - M_x^H - X_3) - X_1(M_y^T + M_y^s - M_y^H - Y_3)}{Y_1X_2 - Y_2X_1} \quad \ldots\ldots\ldots (4.10)$$

Where,

$$X_1 = B_{11} - \frac{D_{11}}{B_{11}}A_{11} - \frac{D_{12}}{B_{22}}A_{12}$$

$$X_2 = -\frac{D_{11}}{B_{11}}A_{12} - \frac{D_{12}}{B_{22}}A_{22} \quad \ldots\ldots\ldots (4.11)$$

$$X_3 = \frac{D_{11}}{B_{11}}(N_x^T + N_x^s - N_x^H) - \frac{D_{12}}{B_{22}}(N_y^T + N_y^s - N_y^H)$$

$$Y_1 = -\frac{D_{11}}{B_{11}}A_{11} - \frac{D_{22}}{B_{22}}A_{12}$$

$$Y_2 = B_{22} - \frac{D_{12}}{B_{11}}A_{12} - \frac{D_{22}}{B_{22}}A_{22} \quad \ldots\ldots\ldots (4.12)$$

$$Y_3 = \frac{D_{12}}{B_{11}}(N_x^T + N_x^s - N_x^H) - \frac{D_{22}}{B_{22}}(N_y^T + N_y^s - N_y^H)$$

Where,

N_x^T, N_y^T & N_{xy}^T= Thermal stress resultants. (Refer equations 1.4 - 1.12)

M_x^T, M_y^T & M_{xy}^T=Thermal moment resultants (Refer equations 1.4 - 1.12)

N_x^S, N_y^S & N_{xy}^S= Stress resultants due to shrinkage. (Refer equations 1.13 - 1.21)

M_x^S, M_y^S & M_{xy}^S=Moment resultants due to shrinkage. (Refer equations 1.13 - 1.21)

N_x^H, N_y^H & N_{xy}^H= stress resultants due to moisture. (Refer equations 1.22 - 1.29)

M_x^H, M_y^H & M_{xy}^H= moment resultants due to moisture (Refer equations 1.22 – 1.29)

ε_x^*, ε_y^* & ε_{xy}^*= In plane strain

K_x, K_y & K_{xy}= curvature.

R_x, R_y = radius of the sample in x and y direction respectively.

A MATLAB program for calculating the radius of curvature due to stress resultants and moment resultants due to difference in coefficient of thermal contractions, resin shrinkage and moisture absorption is developed using the relation 4.3 & 4.4, and equations 4.5 - 4.12 along with the input parameters given in Table 4.2 for various moisture content (ΔC) and different coefficients of moisture expansions (β_H) values.

So to calculate the stress resultant and moment resultants due to moisture absorption, different values of coefficient of moisture expansion (β_H) were referred for generation of radius using MATLAB program. The coefficient of moisture expansion chosen are 0.001 (using β_m = 0.004 [20]), 0.003 & 0.005 (upper limit and lower limit of the coefficient of moisture expansion values suggested by M.Hyer [18]).

Modulus of Elasticity E_1 (GPA)	155
Modulus of Elasticity E_2 (GPA)	12.1
Shear Modulus G_{12} (GPA)	4.40
Poisson's ratio υ_{12}	0.248
On axis coefficient of thermal contraction α_1 (10^{-6} %/°C)	-0.018
On axis coefficient of thermal contraction α_2 (10^{-6} %/°C)	24.3
On-axis shrinkage coefficient ε_1^s (%)	0
On-axis shrinkage coefficient ε_2^s (%)	3.3×10^{-2}
Difference in temperature from cure temperature (ΔT)(°C)	-157
Coefficient of moisture expansion (β_H) (/%)	0.001, 0.003 & 0.005

Table 4.2 Input parameters for calculating the theoretical radius [2]

These theoretical value of radii obtained for different values of coefficient of moisture expansion (β_H) are then compared with the experimental radius obtained for the corresponding moisture content (ΔC) during moisture absorption test (refer section 4.2).

This comparison graph is shown in figure 4.17

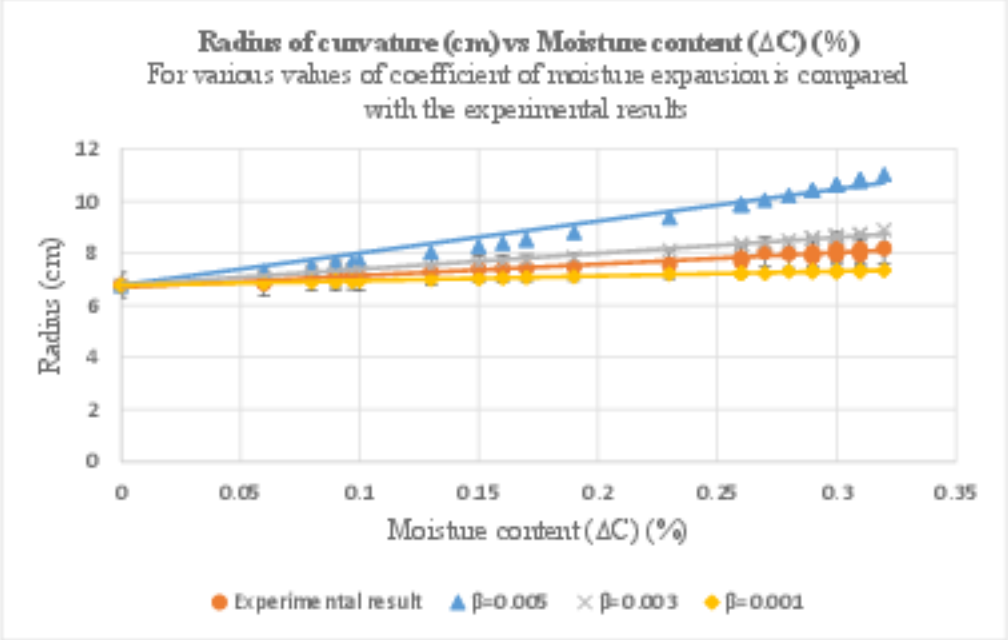

Figure 4.17 Radius of curvature (cm) vs. Moisture content (ΔM) (%) For various values of coefficient of moisture expansion is compared with the experimental results

The experimental radius shows a close relation within a range of theoretical β_H values of 0.001/% - 0.003/%. Since the experimental radius values are an average value, it is shown with error bars. Hence it can be concluded that the value of the coefficient of moisture expansion (β_H) of the thin composite laminate made by 4D printing is in the range of 0.001/% - 0.003/%.

4.3 Prevention of moisture absorption

The opening up of the samples after curing is caused due to moisture absorption. This opening up of the sample can be prevented by covering the sample with aluminum foil tape as shown in figure 4.18.

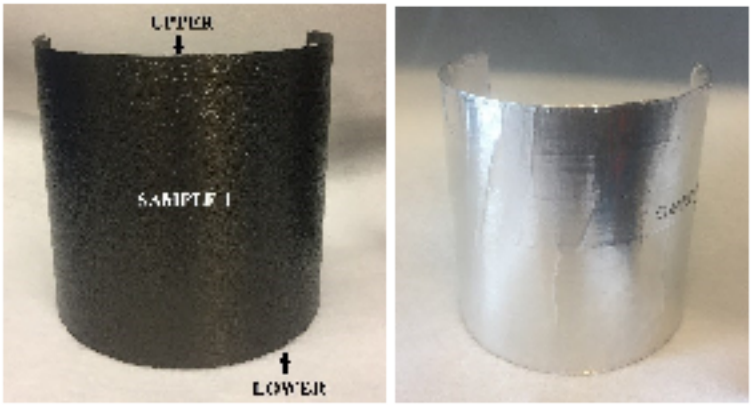

Figure 4.18 Samples before and after aluminum foil covering

This efficiency of avoidance is checked by checking the radius and weight change of both sample 1 and sample 2, before and after covering and over the course of time.

Sample	Average Radius before covering with Aluminum foil tape (cm)	Average Radius right after covering with Aluminum foil tape (cm)	Weight before covering with Aluminum foil tape (g)	Weight right after covering with Aluminum foil tape (g)
Sample 1	6.75 ± 0.05	6.7 ± 0.1	18.3905	31.2815
Sample 2	7 ± 0.05	7.1 ± 0.05	18.4500	30.3215

Table 4.3 Radius and Weight of sample before and after covering with aluminum foil tape

After checking for the change in radius and weight of sample covered with aluminum foil tape (refer Appendix E) for two weeks (as shown in table 4.4), it was found that moisture is absorbed by the samples through the edges of the tape and through the adhesive layer, which accounts for the change in

weight of the sample for 0.15-0.2% of its weight after covering with aluminum foil tape. But the radius of curvature does not vary significantly.

Time	Sample 1		Sample 2	
	Average Radius (cm)	**Weight (g)**	**Average Radius (cm)**	**Weight (g)**
After covering	6.7 ±0.1	31.2815	7 ± 0.05	30.3215
After one week	6.8 ±0.1	31.3264	7.1 ±0.1	30.3826
After two weeks	6.7 ±0.1	31.3408	7.4 ± 0.05	30.4039

Table 4.4 Radius and weight calculation after covering with aluminum foil tape

Hence by applying this method, the opening up of the samples can be prevented.

CHAPTER 5: CONCLUSIONS AND CONTRIBUTIONS

5.1 Conclusions

Thin composite laminates were made by 4DPC by using an AFP machine. The prepregs that are laid up by AFP machine on a flat mold have unsymmetric layup sequence of [0/90]. This was later cured in an autoclave. After curing the sample and cooling to room temperature, it tends to curl up and take curvature. This is due to the difference in the coefficient of thermal contraction between the layers and resin shrinkage. Later when these samples were placed in the room, they were observed to open up, which leads to a change in the radius of curvature of the samples. This is due to absorption of moisture from the atmosphere through diffusion.

So to analyze various factors such as temperature, resin shrinkage, and moisture that affect the radius curvature of a thin composite laminate made by 4D printing, a series of test were performed, and the following conclusions can be made.

1. **The effect of temperature on the curvature of a thin composite laminate made by 4DPC**

   The effect of temperature is due to the difference in coefficient of thermal contraction between the layers and was found that this contribution is agreed with experimental for all the temperatures until 160℃. For temperature above 160℃, the effect of resin shrinkage become more significant whereas at low temperature, the effect is less significant as compared to the coefficient of thermal contraction.

2. **The effect of resin shrinkage on the curvature of a thin composite laminate made by 4DPC**

   It was found that the radius for shrinkage strain $\varepsilon^{s} = 3.3 \times 10^{-4}$ agrees with all experimental radius obtained until 160°C. The change in radius above 160°C was found to be due to the drop in the elastic properties of 50% along with shrinkage strain $\varepsilon^{s} = 3.3 \times 10^{-4}$.

3. **The effect of moisture on the curvature of a thin composite laminate made by 4DPC**

The moisture entering into the laminates was found to increase the radius of the laminate, this was found by calculating the stress resultants and moment resultants due to moisture absorption. For which the coefficient of moisture expansion (β_H) is analyzed for a range of values and was found to be in the range of 0.001/% - 0.003 /%. The opening up of laminate due to the effect of moisture can be limited by covering the laminate with aluminum foil tape.

5.2 Summary

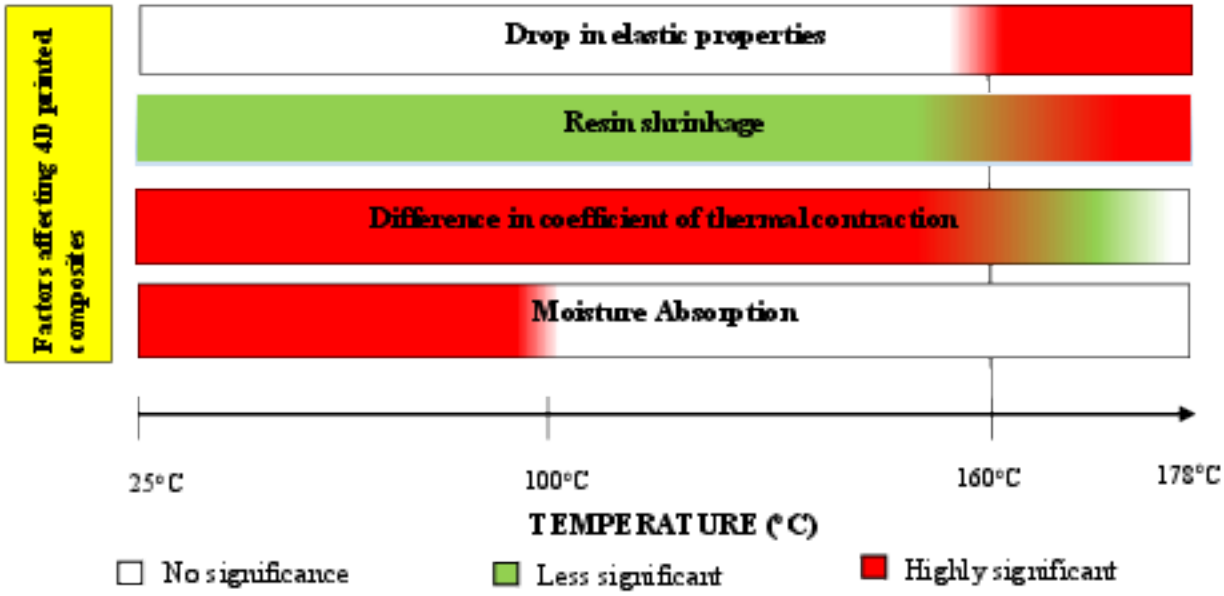

Figure 5.1 Flow chart of factors affecting curvature of a 4D printed composite laminate

Factors affecting curvature of the laminate can be classified into 4 based on the temperature of the samples.

- From room conditions to 100°C, the factors affecting the curvature are the moisture absorption from the surrounding, difference in coefficient of thermal contraction between the layers and resin shrinkage which is less significant when compared to former two factors.

- From 100°C to 160 °C, as the moisture present in sample is evaporated, the primary reason responsible for the curvature is difference in coefficient of thermal contraction between the layers. Here the resin shrinkage is also a small factor responsible for curvature but is less significant when compared to contribution due to difference in thermal contractions coefficients.
- From 160°C to 176°C, the contribution of difference in coefficient of thermal contraction becomes comparable with other significant factors such as resin shrinkage and drop in elastic properties. Hence all the three factors affect the curvature of the sample.
- At 177°C, the cure temperature the primary factors responsible for curvature of the samples are the resin shrinkage and drop in elastic properties. The contribution due to difference in thermal coefficients is zero as the value of ΔT (ΔT = cure temperature – sample temperature) is zero.

5.3 Contributions

1. For the first time, the parametric study of a composite laminate made by 4DPC was performed to find the effect of shrinkage on the curvature of the laminate.
2. The effect of moisture concentration on the curvature of the laminate was determined.

References

[1] Hoa S.V, *Principles of the Manufacturing of Composite Materials*, 2nd ed. DEStech Publications,Inc, 2017.

[2] Hoa S.V, "Factors affecting the properties of composites made by 4D printing (moldless composites manufacturing)," *Adv. Manuf. Polym. Compos. Sci.*, vol. 3, no. 3, pp. 101–109, 2018.

[3] Website, "www.digimizer.com." .

[4] S. G. Taghavi, "Moisture Effects on High Performance Polymer Composites," University of Toronto, 2000.

[5] X. Wang, M. Jiang, Z. Zhou, J. Gou, and D. Hui, "3D printing of polymer matrix composites: A review and prospective," *Compos. Part B Eng.*, vol. 110, pp. 442–458, 2017.

[6] Charles W. Hull, "Apparatus for production of three-dimensional objects by stereolithography," Patent number:4,575,330, 08-Aug-1984.

[7] M. Kamran and A. Saxena, "A Comprehensive Study on 3D Printing Technology A Comprehensive Study on 3D Printing Technology," *Moradabad Inst. Technol. Int. J. Mech. Eng.*, vol. 6, no. 2, pp. 63–69, 2016.

[8] J. Q. Al-maliki and A. J. Q. Al-maliki, "The Processes and Technologies of 3D Printing," *Int. J. Adv. Comput. Sci. Technol.*, vol. 4, no. 10, pp. 161–165, 2015.

[9] B. S. Shahi, "Advanced Manufacturing Techniques (3D Printing)," no. 4, pp. 16–23, 2016.

[10] S. Tibbits, "4D printing: Multi-material shape change," *Archit. Des.*, vol. 84, no. 1, pp. 116–121, 2014.

[11] D. Deng and Y. Chen, "Origami-Based Self-Folding Structure Design and Fabrication Using Projection Based Stereolithography," *J. Mech. Des.*, vol. 137, no. 2, p. 021701, 2015.

[12] F. Momeni, S. M.Mehdi Hassani.N, X. Liu, and J. Ni, "A review of 4D printing," *Mater. Des.*, vol. 122, pp. 42–79, 2017.

[13] D. Raviv, "Active printed materials for complex self-evolving deformations," *Sci. Rep.*, vol. 4, pp. 1–8, 2014.

[14] J. J. Wu, L. M. Huang, Q. Zhao, and T. Xie, "4D Printing: History and Recent Progress," *Chinese J. Polym. Sci. (English Ed.*, vol. 36, no. 5, pp. 563–575, 2018.

[15] S. W. Tsai and H.Hahn, *Introduction to composite materials*. Technomic Publishing Company, Inc, 1980.

[16] V. P. Nikolaev, E. V. Myshenkova, V. S. Pichugin, E. N. Sinitsyn, and A. N. Khoroshev, "Temperature effect on the mechanical properties of composite materials," *Inorg. Mater.*, vol. 50, no. 15, pp. 1511–1513, 2014.

[17] T. A. Bogetti and J. W. Gillespie, "Process-Induced Stress and Deformation in Thick-Section Thermoset Composite Laminates," *J. Compos. Mater.*, vol. 26, no. 5, pp. 626–660, 1992.

[18] M. W. Hyer, *Stress Analysis of Fiber-reinforced Composite Materials*. DEStech Publications,Inc, 2009.

[19] Barbero. E.J, *Introduction to Composite Materials Design*, Second. CRC Press, Taylor & Francis Group, 2011.

[20] D. F. Adams and M. M. Monub, "Moisture expansion and thermal expansion coefficients of a polymer-matrix," *Fibrous Compos. Struct. Des.*, pp. 819–830, 1980.

[21] W. W. Wright, "The effect of diffusion of water into epoxy resins and their carbon-fibre reinforced composites," *Composites*, vol. 12, no. 3, pp. 201–205, 1981.

[22] C.-H. Shen and G. S. Springer, "Moisture absorption and desorption of composite materials,"

Compos. Mater., vol. 10, pp. 2–20, 1976.

[23] M. Li, "Temperature and Moisture Effects on Composite Materials for Wind Turbine Blades," Thesis, Montana State University-Bozeman, 2000.

[24] G. Twigg, A. Poursartip, and G. Fernlund, "Tool-part interaction in composites processing. Part I: Experimental investigation and analytical model," *Compos. Part A Appl. Sci. Manuf.*, vol. 35, no. 1, pp. 121–133, 2004.

[25] M. H. Shirangi and B. Michel, *Moisture Sensitivity of Plastic Packages of IC Devices*. 2010.

[26] Cytec Engineered, "Cycom 977-2 Epoxy Resin System - Technical Data Sheet," *Cytec - Eng. Mater.*, pp. 1–4, 2012.

Appendix

A. DSC test results.

a) DSC results after sample preparation

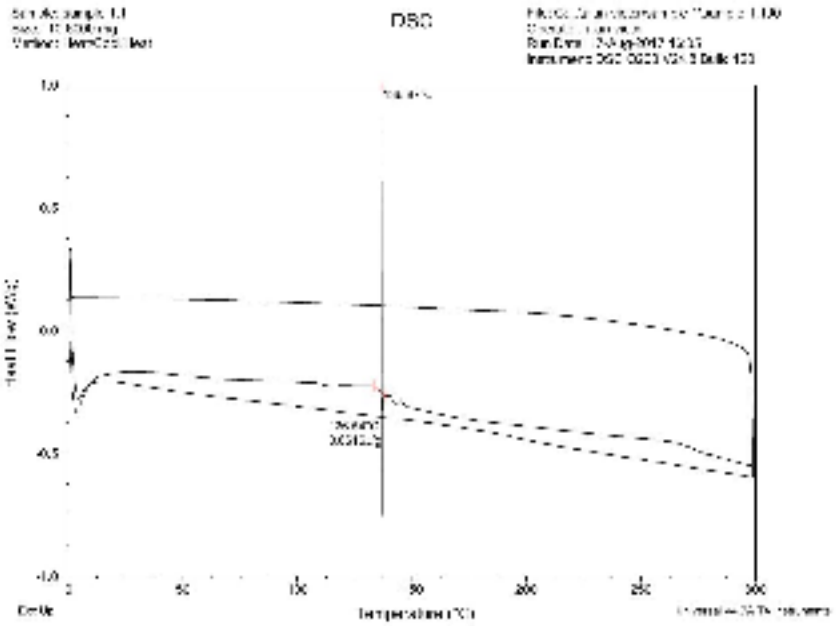

Figure A.1 DSC test result for Sample 1.1

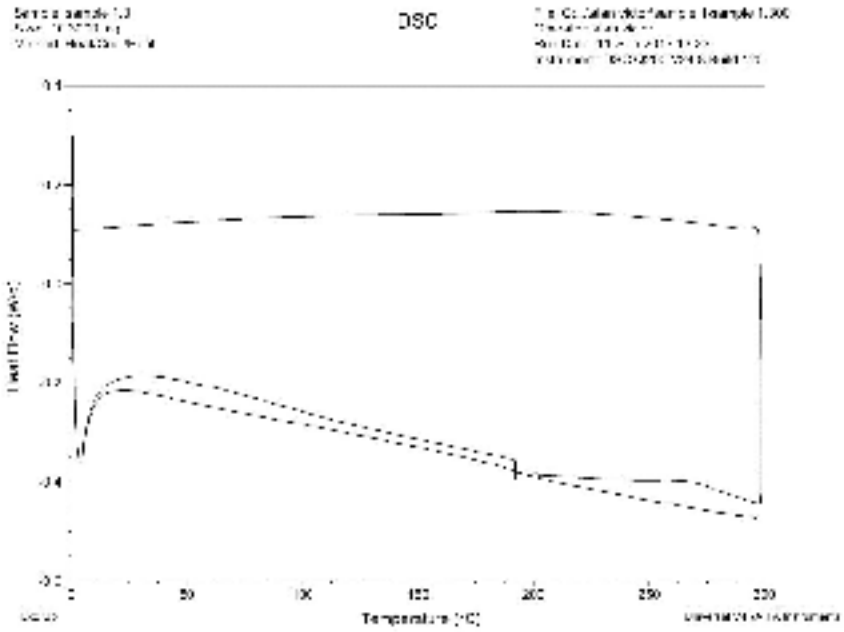

Figure A.2 DSC test result for Sample 1.3

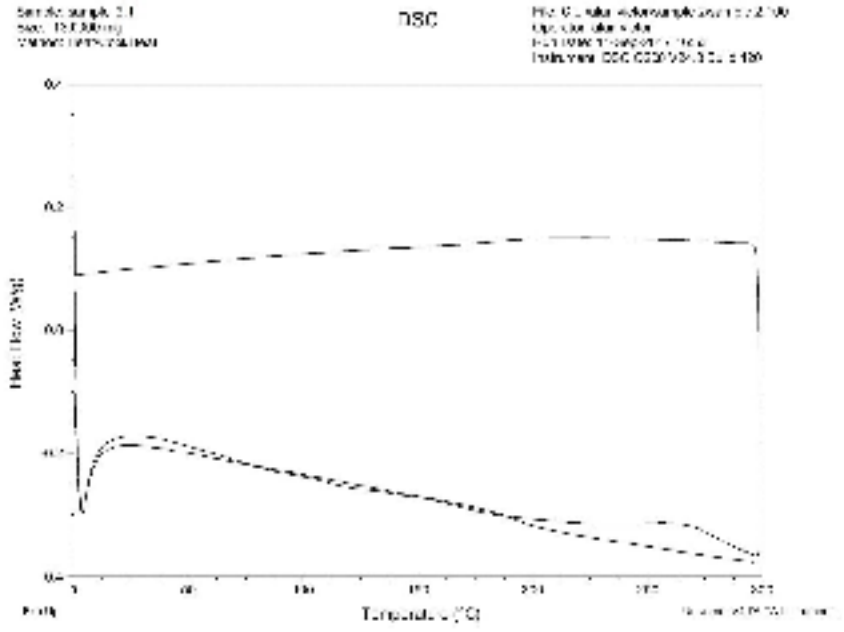

Figure A.3 DSC test result for Sample 2.1

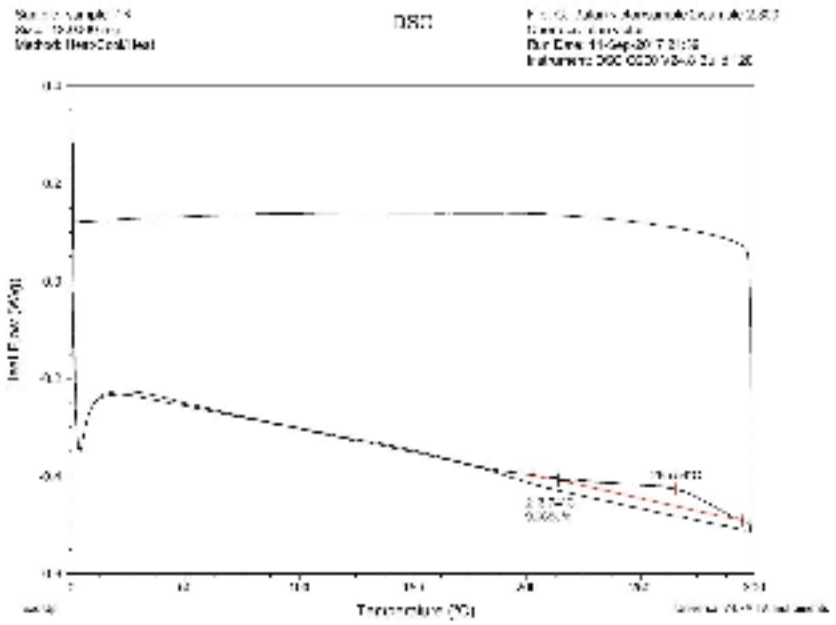

Figure A4 DSC test result for Sample 2.3

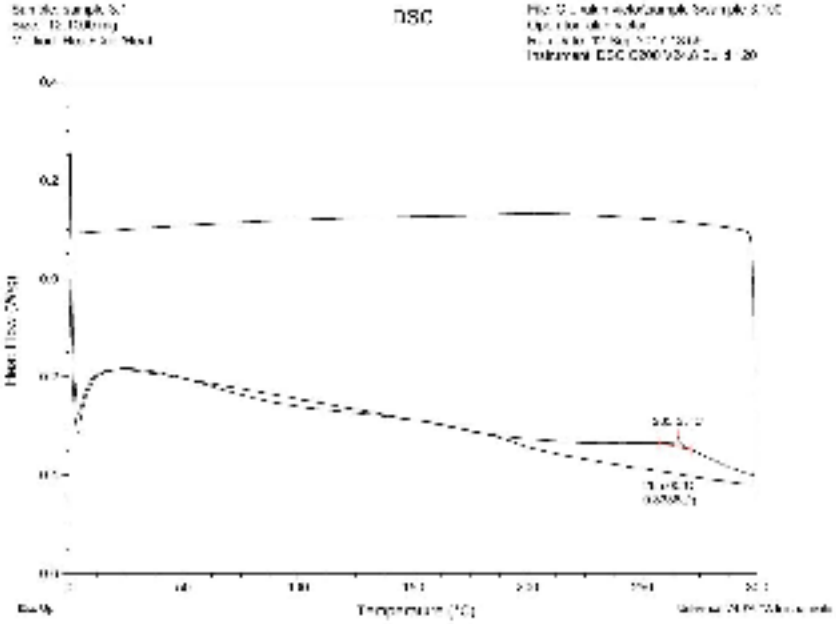

Figure A5 DSC test result for Sample 3.1

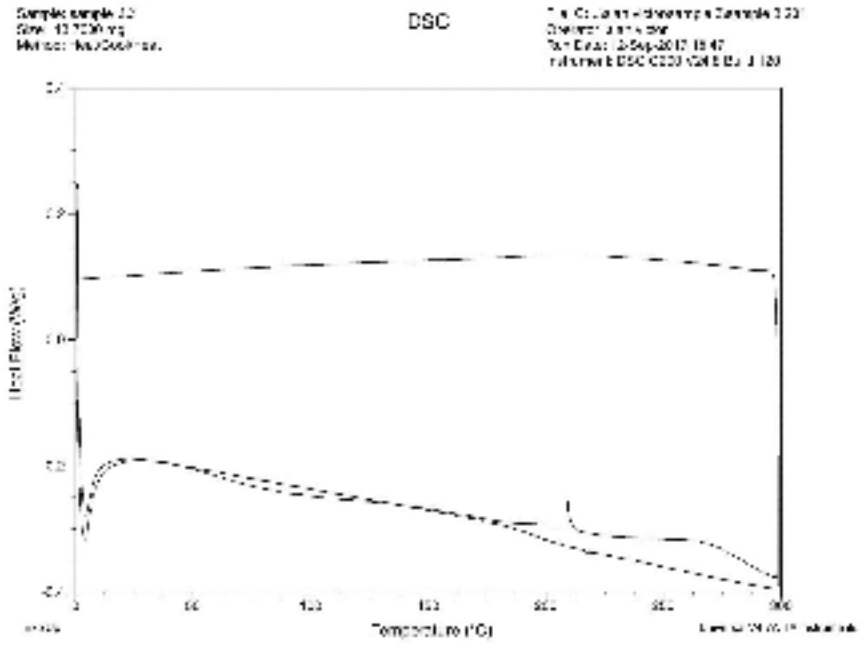

Figure A.6 DSC test result for Sample 3.3

b) Radius observed after sample preparation

	SAMPLE 1		SAMPLE 2		SAMPLE 3	
TIME (H)	Upper side (cm)	Lower side (cm)	Upper side (cm)	Lower side (cm)	Upper side (cm)	Lower side (cm)
1	6.5	6.55	6.9	6.9	6.8	6.75
2	7.4	7.3	7.5	7.3	6.8	7
3	7.4	7.35	7.65	7.55	7.3	7.35
4	7.625	7.5	7.65	7.65	7.1	7.1
5	7.825	7.55	7.95	8.1	7.3	7.1
6	7.65	7.5	7.95	7.8	7.3	7.25
18	8.2	7.95	8.4	8.45	8.25	8
24	8.65	8.4	8.9	8.75	8.3	8.3
48	10	9.7	10.65	9.75	9.45	9.4
96	9.1	8.9	9.5	9.05	9	9
144	9	9	9.2	9	8.65	8.8
168	9.4	9.6	9.9	9.5	9.2	9.4
240	9.6	9.5	9.8	9.45	9.5	9.15
288	8.9	9.7	9.2	8.7	8.9	8.4
456	9.5	9.8	9.8	9.65	9.3	9.15
552	9	9.4	9.2	9.1	8.95	8.7
768	10.2	9.9	10.3	10.3	10.6	9.9

840	9.45	9.25	9.5	9.15	9.1	8.95

B. Moisture Desorption

I. Removal of free moisture

a) Radius Calculation

Sample 1A

Time (h)	Upper side (cm)	Lower side (cm)	Average Radius (cm)
0	8.6	8.6	8.6
10	7.6	7.6	7.6
10.5	7.5	7.65	7.575
12	7.4	7.25	7.325
24	7.05	6.95	7
36	6.85	6.9	6.875
48	6.7	6.9	6.8
60	6.6	6.7	6.65
72	6.6	6.65	6.625
84	6.85	6.55	6.7
96	6.7	6.5	6.6
108	6.45	6.4	6.425
120	6.35	6.5	6.425
144	6.3	6.2	6.25
168	6.55	6.4	6.475
192	6.3	6.25	6.275
216	6.4	6.35	6.375
240	6.3	6.2	6.25
264	6.35	6.35	6.35
294	6.2	6.2	6.2
318	6.2	6.2	6.2
342	6.35	6.2	6.275
366	6.25	6.25	6.25
390	6.25	6.1	6.175
414	6.25	6.15	6.2
438	6.1	6.25	6.175
462	6.15	6.1	6.125
486	6.2	6.2	6.2

Sample 1B

Time (h)	Upper side (cm)	Lower side (cm)	Average Radius (cm)
0	8.6	8.7	8.65
10	7.8	8.05	7.925
10.5	7.8	7.9	7.85
12	7.5	7.65	7.575
24	7	7.2	7.1
36	7.15	6.8	6.975
48	6.8	6.95	6.875
60	6.55	6.65	6.6
72	6.65	6.6	6.625
84	6.65	6.75	6.7
96	6.7	6.75	6.725
108	6.4	6.9	6.65
120	6.55	6.6	6.575
144	6.4	6.6	6.5
168	6.5	6.7	6.6
192	6.4	6.5	6.45
216	6.3	6.6	6.45
240	6.4	6.5	6.45
264	6.3	6.45	6.375
294	6.25	6.3	6.275
318	6.3	6.4	6.35
342	6.35	6.4	6.375
366	6.35	6.4	6.375
390	6.15	6.35	6.25
414	6.4	6.35	6.375
438	6.1	6.25	6.175
462	6.3	6.3	6.3
486	6.35	6.5	6.425

Sample 2A

Time (h)	Upper side (cm)	Lower side (cm)	Average Radius (cm)
0	8.35	8.3	8.325
10	7.45	7.55	7.5
10.5	7.6	7.55	7.575
12	7.2	7.3	7.25
24	6.9	7.1	7
36	6.8	6.85	6.825
48	6.7	6.75	6.725
60	6.65	6.55	6.6
72	6.55	6.65	6.6
84	6.35	6.4	6.375
96	6.5	6.5	6.5
108	6.4	6.4	6.4
120	6.15	6.3	6.225
144	6.25	6.5	6.375
168	6.25	6.35	6.3
192	6.2	6.3	6.25
216	6.25	6.35	6.3
240	6.1	6.3	6.2
264	6.15	6.2	6.175
294	6.1	6.05	6.075
318	6	6.15	6.075
342	6.15	6.25	6.2
366	6.15	6.15	6.15
390	6.05	6.25	6.15
414	6.15	6.3	6.225
438	6.05	6.15	6.1
462	6.1	6.2	6.15
486	6.2	6.2	6.2

Sample 2B

Time (h)	Upper side (cm)	Lower side (cm)	Average Radius (cm)
0	8.05	8.25	8.15
10	7.65	7.45	7.55
10.5	7.5	7.3	7.4
12	7	7.1	7.05
24	6.8	6.85	6.825
36	6.6	6.65	6.625
48	6.5	6.6	6.55
60	6.4	6.35	6.375
72	6.3	6.35	6.325
84	6.4	6.4	6.4
96	6.5	6.25	6.375
108	6.4	6.25	6.325
120	6.1	6.2	6.15
144	6.3	6.25	6.275
168	6.4	6.25	6.325
192	6.2	6.1	6.15
216	6.1	6	6.05
240	6.1	6.1	6.1
264	6.15	6.25	6.2
294	5.95	5.95	5.95
318	6.15	6.15	6.15
342	6.05	6	6.025
366	6.15	6	6.075
390	6.1	6.05	6.075
414	6.05	5.95	6
438	6.1	6	6.05
462	6.1	5.95	6.025
486	6.05	6	6.025

Sample 3A

Time (h)	Upper side (cm)	Lower side (cm)	Average Radius (cm)
0	8.5	8.6	8.55
10	7.7	7.5	7.6
10.5	7.8	7.6	7.7
12	7.4	7.5	7.45
24	7.2	7.1	7.15
36	7.3	6.9	7.1
48	7	6.9	6.95
60	6.55	6.4	6.475
72	6.8	6.6	6.7
84	6.7	6.6	6.65
96	6.6	6.45	6.525
108	6.6	6.5	6.55
120	6.65	6.45	6.55
144	6.5	6.55	6.525
168	6.6	6.55	6.575
192	6.45	6.4	6.425
216	6.3	6.6	6.45
240	6.45	6.2	6.325
264	6.45	6.25	6.35
294	6.45	6.25	6.35
318	6.3	6.2	6.25
342	6.3	6.3	6.3
366	6.45	6.3	6.375
390	6.5	6.45	6.475
414	6.2	6.35	6.275
438	6.3	6.25	6.275
462	6.4	6.2	6.3
486	6.45	6.35	6.4

Sample 3B

Time (h)	Upper side (cm)	Lower side (cm)	Average Radius (cm)
0	8.2	8.5	8.35
10	7.55	7.8	7.675
10.5	7.8	7.75	7.775
12	7.35	7.6	7.475
24	7.15	7.1	7.125
36	7.15	7.05	7.1
48	6.95	6.95	6.95
60	6.6	6.7	6.65
72	6.85	6.8	6.825
84	6.6	6.8	6.7
96	6.65	6.7	6.675
108	6.65	6.65	6.65
120	6.5	6.45	6.475
144	6.6	6.65	6.625
168	6.55	6.65	6.6
192	6.5	6.55	6.525
216	6.3	6.35	6.325
240	6.3	6.5	6.4
264	6.45	6.5	6.475
294	6.3	6.4	6.35
318	6.45	6.5	6.475
342	6.4	6.4	6.4
366	6.4	6.4	6.4
390	6.3	6.5	6.4
414	6.3	6.4	6.35
438	6.35	6.4	6.375
462	6.35	6.4	6.375
486	6.25	6.45	6.35

b) Weight Measurement

Sample 1A

Time (h)	Time (min)	Time sqrt ($min^{1/2}$)	Weight (g)	Moisture content ΔC (%)
0	0	0	19.2088	0.428192755
10	600	24.49489743	19.1883	0.32101386
10.5	630	25.0998008	19.185	0.303760672
12	720	26.83281573	19.1881	0.319968212
24	1440	37.94733192	19.1723	0.23736204
36	2160	46.47580015	19.171	0.230565329
48	2880	53.66563146	19.1674	0.21174367
60	3600	60	19.1596	0.170963408
72	4320	65.7267069	19.1539	0.141162447
84	5040	70.9929574	19.158	0.162598226
96	5760	75.89466384	19.1616	0.181419885
108	6480	80.49844719	19.1549	0.146390685
120	7200	84.85281374	19.1494	0.117635372
144	8640	92.95160031	19.141	0.073718167
168	10080	100.3992032	19.1451	0.095153945
192	11520	107.3312629	19.1419	0.078423581
216	12960	113.8419958	19.1425	0.081560525
240	14400	120	19.1417	0.077377934
264	15840	125.8570618	19.1325	0.029278137
294	17640	132.8156617	19.1308	0.020390131
318	19080	138.1303732	19.1386	0.061170394
342	20520	143.2480366	19.1327	0.030323785
366	21960	148.1890684	19.1289	0.010456478
390	23400	152.9705854	19.1336	0.0350292
414	24840	157.6071064	19.1322	0.027709665
438	26280	162.111073	19.1269	0
462	27720	166.4932431	19.131	0.021435779
486	29160	170.7629936	19.1303	0.017776012

Sample 1B

Time (h)	Time (min)	Time sqrt ($min^{1/2}$)	Weight (gm)	Moisture content ΔC (%)
0	0	0	19.3211	0.395949057
10	600	24.49489974	19.3075	0.325280984
10.5	630	25.09980008	19.3032	0.302937402
12	720	26.83281573	19.306	0.317486711
24	1440	37.94733191	19.2886	0.227073147
36	2160	46.47580021	19.2863	0.215121928
48	2880	53.66563153	19.2747	0.154846219
60	3600	60	19.2764	0.163679728
72	4320	65.72670691	19.271	0.135620346
84	5040	70.99295741	19.2728	0.144973473
96	5760	75.89466382	19.2728	0.144973473
108	6480	80.49844721	19.2703	0.131983019
120	7200	84.85281374	19.2657	0.108080582
144	8640	92.95160031	19.2588	0.072226928
168	10080	100.3992031	19.2615	0.086256619
192	11520	107.3312631	19.2604	0.080540819
216	12960	113.8419961	19.2577	0.066511128
240	14400	120	19.2583	0.069628837
264	15840	125.8570621	19.2479	0.015588546
294	17640	132.8156621	19.251	0.031696709
318	19080	138.1303731	19.256	0.057677618
342	20520	143.2480371	19.2507	0.030137855
366	21960	148.1890681	19.2473	0.012470836
390	23400	152.9705851	19.2534	0.044167546
414	24840	157.6071061	19.2537	0.0457264
438	26280	162.1110731	19.2463	0.007274655
462	27720	166.4932431	19.2492	0.022343582
486	29160	170.7629941	19.2449	0

Sample 2A

Time (h)	Time (min)	Time sqrt ($min^{1/2}$)	Weight (gm)	Moisture content ΔC (%)
0	0	0	19.7026	0.444036604
10	600	24.494897	19.685	0.354311641
10.5	630	25.099801	19.6826	0.342076419
12	720	26.832816	19.6788	0.322703984
24	1440	37.947332	19.6626	0.240116235
36	2160	46.4758	19.6577	0.215135989
48	2880	53.665631	19.6523	0.18760674
60	3600	60	19.6483	0.167214703
72	4320	65.726707	19.6445	0.147842268
84	5040	70.992957	19.6465	0.158038286
96	5760	75.894664	19.6445	0.147842268
108	6480	80.498447	19.645	0.150391272
120	7200	84.852814	19.6357	0.102979786
144	8640	92.9516	19.6307	0.07748974
168	10080	100.3992	19.6335	0.091764166
192	11520	107.33126	19.6322	0.085136754
216	12960	113.842	19.6323	0.085646555
240	14400	120	19.6306	0.076979939
264	15840	125.85706	19.6229	0.037725268
294	17640	132.81566	19.6196	0.020901838
318	19080	138.13037	19.6294	0.070862328
342	20520	143.24804	19.6215	0.030588055
366	21960	148.18907	19.6293	0.070352527
390	23400	152.97059	19.6231	0.03874487
414	24840	157.60711	19.6225	0.035686065
438	26280	162.11107	19.6155	0
462	27720	166.49324	19.6174	0.009686218
486	29160	170.76299	19.6207	0.026509648

Sample 2B

Time (h)	Time (min)	Time Sqrt ($min^{1/2}$)	Weight (gm)	Moisture content ΔC (%)
0	0	0	18.9432	0.421977
10	600	24.49489743	18.9256	0.328675
10.5	630	25.09980088	18.9245	0.322844
12	720	26.83281573	18.9216	0.30747
24	1440	37.94733192	18.9047	0.21788
36	2160	46.47580015	18.9055	0.222121
48	2880	53.66563146	18.8971	0.177591
60	3600	60	18.8932	0.156916
72	4320	65.72670769	18.8898	0.138892
84	5040	70.9929574	18.8926	0.153735
96	5760	75.89466384	18.8895	0.137301
108	6480	80.49844719	18.8904	0.142073
120	7200	84.85281374	18.8824	0.099663
144	8640	92.95160031	18.8756	0.063615
168	10080	100.3992032	18.8799	0.08641
192	11520	107.3312629	18.874	0.055133
216	12960	113.8419958	18.8759	0.065205
240	14400	120	18.8775	0.073687
264	15840	125.8570618	18.8686	0.026506
294	17640	132.8156617	18.867	0.018024
318	19080	138.1303732	18.8744	0.057253
342	20520	143.2480366	18.8694	0.030747
366	21960	148.1890684	18.8663	0.014313
390	23400	152.9705854	18.8704	0.036048
414	24840	157.6071064	18.8686	0.026506
438	26280	162.111073	18.8636	0
462	27720	166.4932431	18.8662	0.013783
486	29160	170.7629936	18.8684	0.025446

Sample 3A

Time (h)	Time (min)	Time sqrt ($min^{1/2}$)	Weight (g)	Moisture content ΔC (%)
0	0	0	19.2142	0.421773
10	600	24.4948974	19.1943	0.317767
10.5	630	25.0998008	19.1912	0.301565
12	720	26.8328157	19.1891	0.29059
24	1440	37.9473319	19.1777	0.231008
36	2160	46.4758002	19.169	0.185538
48	2880	53.6656315	19.1666	0.172995
60	3600	60	19.1602	0.139546
72	4320	65.7267069	19.1599	0.137978
84	5040	70.9929574	19.1587	0.131706
96	5760	75.8946638	19.1629	0.153657
108	6480	80.4984472	19.1588	0.132229
120	7200	84.8528137	19.1507	0.089895
144	8640	92.9516003	19.1433	0.051219
168	10080	100.399203	19.1482	0.076829
192	11520	107.331263	19.1453	0.061672
216	12960	113.841996	19.1451	0.060627
240	14400	120	19.1485	0.078397
264	15840	125.857062	19.1376	0.021428
294	17640	132.815662	19.1385	0.026132
318	19080	138.130373	19.145	0.060104
342	20520	143.248037	19.1397	0.032404
366	21960	148.189068	19.1335	0
390	23400	152.970585	19.1406	0.037108
414	24840	157.607106	19.1398	0.032927
438	26280	162.111073	19.1336	0.000523
462	27720	166.493243	19.1357	0.011498
486	29160	170.762994	19.1375	0.020906

Sample 3B

Time (h)	Time (min)	Time sqrt	Weight (g)	Moisture content ΔC (%)
0	0	0	19.4268	0.435309
10	600	24.49489743	19.406	0.327774
10.5	630	25.09980088	19.4046	0.320536
12	720	26.83281573	19.4034	0.314332
24	1440	37.94733192	19.3868	0.228511
36	2160	46.47580015	19.3827	0.207314
48	2880	53.66563146	19.3796	0.191288
60	3600	60	19.374	0.162336
72	4320	65.72670691	19.3736	0.160268
84	5040	70.9929574	19.372	0.151996
96	5760	75.89466384	19.3736	0.160268
108	6480	80.49844719	19.3753	0.169057
120	7200	84.85281374	19.3586	0.082719
144	8640	92.95160031	19.3564	0.071345
168	10080	100.3992032	19.3617	0.098746
192	11520	107.3312629	19.3551	0.064624
216	12960	113.8419958	19.3559	0.06876
240	14400	120	19.3557	0.067726
264	15840	125.8570618	19.3473	0.024299
294	17640	132.8156617	19.3484	0.029986
318	19080	138.1303732	19.3571	0.074964
342	20520	143.2480366	19.3513	0.044978
366	21960	148.1890684	19.346	0.017578
390	23400	152.9705854	19.3506	0.041359
414	24840	157.6071064	19.3501	0.038775
438	26280	162.111073	19.3426	0
462	27720	166.4932431	19.3472	0.023782
486	29160	170.7629936	19.3488	0.032054

II. Removal of Bound Moisture

a) Weight Calculations

Sample 1A

Time (h)	Weight (gm)
20	19.12
23	19.1212

Sample 1B

Time (h)	Weight (gm)
20	19.24
23	19.2399

Sample 2A

Time (h)	Weight (gm)
20	19.6095
23	19.6083

Sample 2B

Time (h)	Weight (gm)
20	18.8588
23	18.8569

Sample 3A

Time (h)	Weight (gm)
20	19.1299
23	19.1251

Sample 3B

Time (h)	Weight (gm)
20	19.3404
23	19.3368

C. Temperature cycling

Sample 1A (Heating up)

Temperature (C)	Radius 1 (cm)	Radius 2 (cm)	Average radius (cm)
25	6.2	6.2	6.2
40	7.57	7.26	7.41
60	8.55	8.06	8.31
80	9.57	9.26	9.42
100	11.25	11.54	11.39
120	14.74	14.78	14.76
140	22.66	21.88	22.27
160	37.71	41.55	39.63

Sample 3B (Heating up)

Temperature (c)	Radius 1 (cm)	Radius 2 (cm)	Average radius (cm)
25	6.35	6.35	6.35
40	8.22	8.37	8.29
60	9.01	8.94	8.97
80	10.31	10	10.15
100	12.84	12.41	12.63
120	16.10	14.96	15.53
140	21.92	21.83	21.87
160	39.60	36.36	37.98

Sample 1A (Cooling down)

Temperature (c)	Radius 1 (cm)	Radius 2 (cm)	Average radius (cm)
160	38.59	36.41	37.50
140	23.24	21.81	22.52
120	15.54	14.44	15
100	11.61	11.52	11.56
80	8.78	8.70	8.74
60	7.16	7.17	7.17
40	6.56	6.61	6.59
25	6.43	6.40	6.41

Sample 3B (Cooling down)

Temperature (C)	Radius 1 (cm)	Radius 2 (cm)	Average radius (cm)
160	39.60	36.36	37.98
140	22.36	20.96	21.66
120	15.67	15.30	15.48
100	12.19	12.04	12.11
80	9.65	9.50	9.57
60	8.09	7.88	7.98
40	7.04	7.04	7.04
25	6.38	6.49	6.43

D. Shrinkage test

a) Shrinkage test

Sample 1A		Sample 1B		Sample 3B	
Temperature (C)	Radius (cm)	Temperature (C)	Radius (cm)	Temperature (C)	Radius (cm)
30	6.47	30	6.34	30	6.82
40	7.41	40	7.47	40	7.36
50	8.06	50	7.97	50	7.90
60	8.58	60	8.66	60	8.70
70	9.46	70	9.58	70	9.20
80	10.35	80	10.04	80	9.82
90	10.29	90	10.86	90	10.84
100	11.87	100	11.92	100	11.74
110	13.39	110	13.11	110	12.71
120	15.17	120	15.04	120	13.92
130	17.62	130	17.81	130	16.65
140	20.58	140	20.03	140	19.36
150	30.188	150	26.13	150	24.28
160	39.29	160	35.61	160	31.28
170	62.52	170	65.08	170	67.49
175	94.65	175	101.59	175	85.61
176	113.50	176	105.57	176	103.71
177	134.73	177	142.59	177	132.73

b) Radius at different shrinkage strain at different temperature

Temperature (C)	Experimental average radius (cm)	Radius (cm) at εs=-0.00066	Radius (cm) at εs=-0.00033	Radius (cm) at εs=-0.000064
170	65.03	33.53	56.1	119.81
160	35.39	25.98	37.749	58.78
140	19.99	17.91	22.82	29.12
120	14.71	13.67	16.353	19.35
100	11.84	11.05	12.742	14.49
80	10.07	9.27	10.437	11.58
60	8.65	7.99	8.8382	9.64
40	7.41	7.02	7.6642	8.26
25	6.54	6.43	6.9699	7.46

a) Radius for different percentage of elastic properties at different temperature

ΔT (C)	100% elastic properties Radius (cm)	80% elastic properties Radius (cm)	60% elastic properties Radius (cm)	50% elastic properties Radius (cm)	40% elastic properties Radius (cm)	20% elastic properties Radius (cm)	10% elastic properties Radius (cm)	Experimental Radius (cm)
10	48.96	54.755	64.43	72.18	83.81	141.98	258.37	65.03
20	34.38	38.44	45.24	50.68	58.84	99.69	181.4	35.39
40	21.542	24.092	28.35	31.76	36.87	62.47	113.68	19.99
60	15.69	17.54	20.64	23.12	26.85	45.49	82.78	14.71
80	12.33	13.79	16.23	18.18	21.11	35.77	65.08	11.84
100	10.16	11.36	13.37	14.98	17.39	29.47	53.62	10.07
120	8.64	9.66	11.37	12.74	14.79	25.05	45.59	8.64
140	7.51	8.4	9.89	11.08	12.86	21.79	39.66	7.41
160	6.64	7.44	8.75	9.8	11.38	19.28	35.09	6.54

E. Moisture Absorption

a) Radius Calculation

Sample 1

Time (h)	Upper radius (cm)	Lower radius (cm)	Average radius (cm)
0	6.85	6.9	6.88
1	6.7	6.75	6.73
2	6.875	7	6.94
3	6.95	7.1	7.01
4	7.1	7	7.05
5	7	7	7
10	7	7.2	7.1
18	7.05	7.25	7.15
23	7.25	7.25	7.25
28	7.2	7.35	7.28
33	7.25	7.35	7.3
43	7.25	7.35	7.3
48	7.45	7.35	7.4
53	7.65	7.55	7.6
65	7.65	7.7	7.68
77	7.65	7.7	7.68
89	7.85	7.6	7.73
101	7.65	7.8	7.73
113	7.9	7.95	7.93
125	7.8	7.8	7.8
137	7.85	7.85	7.85
149	7.9	7.8	7.85
161	7.7	7.8	7.75
185	8.1	8.05	8.08
209	7.95	7.95	7.95
233	7.9	8.05	7.98
281	7.95	8	7.98
329	7.8	7.8	7.8
377	7.75	8	7.88
449	7.85	7.95	7.9

Sample 2

Time (h)	Upper radius (cm)	Lower radius (cm)	Average radius (cm)
0	6.65	6.7	6.68
1	6.9	7.05	6.98
2	7.15	7.15	7.15
3	7.2	7.2	7.2
4	7.05	7.1	7.08
5	7.1	7.15	7.13
10	7.3	7.4	7.35
18	7.35	7.45	7.4
23	7.6	7.5	7.55
28	7.5	7.55	7.53
33	7.5	7.6	7.55
43	7.6	7.7	7.65
48	7.75	7.7	7.73
53	7.7	7.75	7.73
65	7.9	8	7.95
77	7.9	7.9	7.9
89	8	8.05	8.03
101	8	8	8
113	8.05	8.25	8.15
125	8.1	8.25	8.18
137	8.25	8.25	8.25
149	8.15	8	8.08
161	8.1	8.2	8.15
185	8.5	8.3	8.4
209	8.3	8.3	8.3
233	8.4	8.3	8.35
281	8.3	8.5	8.4
329	8.2	8	8.1
377	8.2	8.25	8.23
449	8.15	8.25	8.2

b) **Weight Calculation**

Sample 1

Time (h)	Time (min)	$\sqrt{t}$ ($min^{1/2}$)	Weight (g)	ΔC 1 (g)	Moisture content ΔC (%)
0	0	0	18.3596	0	0
1	60	7.745967	18.3691	0.0095	0.051744
2	120	10.95445	18.3738	0.0142	0.077344
3	180	13.41641	18.3759	0.0163	0.088782
4	240	15.49193	18.3766	0.017	0.092595
5	300	17.32051	18.3778	0.0182	0.099131
10	600	24.4949	18.3775	0.0179	0.097497
18	1080	32.86335	18.3836	0.024	0.130722
23	1380	37.14835	18.3879	0.0283	0.154143
28	1680	40.9878	18.3912	0.0316	0.172117
33	1980	44.49719	18.3922	0.0326	0.177564
43	2580	50.7937	18.3945	0.0349	0.190091
48	2880	53.66563	18.4031	0.0435	0.236933
53	3180	56.39149	18.4093	0.0497	0.270703
65	3900	62.44998	18.4093	0.0497	0.270703
77	4620	67.97058	18.4083	0.0487	0.265256
89	5340	73.0753	18.4134	0.0538	0.293035
101	6060	77.846	18.4139	0.0543	0.295758
113	6780	82.34076	18.4146	0.055	0.299571
125	7500	86.60254	18.4131	0.0535	0.291401
137	8220	90.66422	18.4114	0.0518	0.282141
149	8940	94.55157	18.4164	0.0568	0.309375
161	9660	98.2853	18.4167	0.0571	0.311009
185	11100	105.3565	18.4158	0.0562	0.306107
209	12540	111.9821	18.4166	0.057	0.310464
233	13980	118.2371	18.4213	0.0617	0.336064
281	16860	129.8461	18.4195	0.0599	0.32626
329	19740	140.4991	18.4181	0.0585	0.318634
377	22620	150.3995	18.417	0.0574	0.312643

Sample 2

Time (h)	$\sqrt{t}$ ($min^{1/2}$)	Weight (g)	ΔC2	Moisture content ΔC (%)
0	0	18.4152	0	0
1	7.745967	18.4285	0.0133	0.072223
2	10.95445	18.4304	0.0152	0.082541
3	13.41641	18.4344	0.0192	0.104262
4	15.49193	18.4347	0.0195	0.105891
5	17.32051	18.4344	0.0192	0.104262
10	24.4949	18.4314	0.0162	0.087971
18	32.86335	18.4402	0.025	0.135757
23	37.14835	18.4427	0.0275	0.149333
28	40.9878	18.4428	0.0276	0.149876
33	44.49719	18.446	0.0308	0.167253
43	50.7937	18.4484	0.0332	0.180286
48	53.66563	18.4557	0.0405	0.219927
53	56.39149	18.4629	0.0477	0.259025
65	62.44998	18.4616	0.0464	0.251966
77	67.97058	18.4606	0.0454	0.246535
89	73.0753	18.4666	0.0514	0.279117
101	77.846	18.4684	0.0532	0.288892
113	82.34076	18.4655	0.0503	0.273144
125	86.60254	18.464	0.0488	0.264998
137	90.66422	18.4634	0.0482	0.26174
149	94.55157	18.4686	0.0534	0.289978
161	98.2853	18.4676	0.0524	0.284548
185	105.3565	18.4676	0.0524	0.284548
209	111.9821	18.4697	0.0545	0.295951
233	118.2371	18.4684	0.0532	0.288892
281	129.8461	18.4712	0.056	0.304097
329	140.4991	18.4691	0.0539	0.292693
377	150.3995	18.4704	0.0552	0.299752

F. MATLAB Program

```
% 4D PRINTING CODING.m

clear; format;
format short g;

% Laminate definition (plies of equal thickness)

Nplies = 2;%input('enter the number of plies =');
thetadt =[90 0];%input('enter the stacking sequence from top in [ ]'); % ply angles in degrees, from top
concentration = input('enter the moisture content in %');
thetadb = fliplr(thetadt); % ply angles in degrees, from bottom
h_ply  = 0.000125;          % SI units, meters
h      = Nplies *h_ply;

for i = 1:Nplies
  zbar(i) = -(h + h_ply)/2 + i*h_ply;
end

% Ply engineering properties (AS/3501)

E1   = 155e9 ; % Pa
nu12 =  .248 ;
E2   = 12.1e9  ; % Pa
G12  = 4.4e9  ; % Pa
nu21 = nu12 * E2 / E1 ;



a1 = -0.018e-6 ; % coefficients of thermal expansion
a2 = 24.3e-6 ;
deltaT = - 157 %input('enter delta t');

% Q matrix (material coordinates)
 denom = 1 - nu12 *nu21 ;
Q11 = E1 / denom       ;
Q12 = nu12 * E2 / denom ;
Q22 = E2 / denom       ;
Q66 = G12              ;

Q = [ Q11 Q12 0; Q12 Q22 0; 0 0 Q66] ;
%Q=[20 .7 0;  .7 2 0; 0 0  .7]
a = [a1 a2 0]' ;
S=inv(Q) ;

% Qbar matrices (laminate coordinates) and contributions to
% ABD matrices

A = zeros(3,3);
B = zeros(3,3);
D = zeros(3,3);
```

```
NT = zeros(3,1);
MT = zeros(3,1);


for i = 1:Nplies
 theta = thetadb(i) *pi / 180; % ply i angle in radians, from bottom
 m = cos(theta);
 n = sin(theta);
 T = [m^2 n^2 2*m*n; n^2 m^2 -2*m*n; -m*n m*n (m^2 - n^2)];
 Qbar = inv(T) * Q *(inv(T))';
 Sbar = inv(Qbar);

  abar = T' *a ;

 A = A + Qbar *h_ply;
 B = B + Qbar *h_ply *zbar(i);
 D = D + Qbar *(h_ply *zbar(i)^2 + h_ply^3 / 12);

 NT = NT + Qbar *abar *h_ply *deltaT ;
 MT = MT + Qbar *abar *h_ply *zbar(i) *deltaT ;
end



Qbar
Sbar
A
B
D


ABD    = [A B; B D];
ABDinv = inv(ABD);
%ASSUMING VOLUME SHRINKAGE OF 3.6%
%e0k = ABDinv *[N T MT]'
%ax = e0k(1:3,1) / deltaT
%CALCULATING THE STRAIN DUE TO SHRINKAGE ACCORDINGLY
vs=0.099;
lin_s=vs/3;
e1=0;
e2=-lin_s/100;

NS=zeros(3,1);
MS=zeros(3,1);
for i=1:Nplies
 theta = thetadb(i) *pi / 180; % ply i angle in radians, from bottom
 m = cos(theta);
 n = sin(theta);
 T = [m^2 n^2 2*m*n; n^2 m^2 -2*m*n; -m*n m*n (m^2 - n^2)];
 Qbar = inv(T) * Q *(inv(T))';
 T_e = [m^2 n^2 m*n; n^2 m^2 -m*n; -2*m*n 2*m*n (m^2 - n^2)];
  if theta==0
```

```
    ebar=[0;e2;0];
  elseif theta==90
    ebar=[e2;0;0];
  else
    ebar=T_e*[e1;e2;0];
  end

  NS=NS+Qbar*ebar*h_ply;
  MS=MS+Qbar*ebar*h_ply*zbar(i);
end

%CALCULATING THE STRAIN DUE TO HYGROSCOPIC SWELLING
SC1=0;
SC2=0.003;

NH=zeros(3,1);
MH=zeros(3,1);

for i=1:Nplies
 theta = thetadb(i)*pi/180; % ply i angle in radians, from bottom
 m=cos(theta);
 n=sin(theta);
 T=[m^2 n^2 2*m*n; n^2 m^2 -2*m*n; -m*n m*n (m^2-n^2)];
 Qbar=inv(T)*Q*(inv(T))';
 T_e=[m^2 n^2 m*n; n^2 m^2 -m*n; -2*m*n 2*m*n (m^2-n^2)];
  if theta==0
    SCbar=[0;SC2;SC2];
  elseif theta==90
    SCbar=[SC2;0;SC2];
  else
    SCbar=T_e*[SC1;SC2;SC2];
  end

  NH=NH+Qbar*SCbar*h_ply*concentration;
  MH=MH+Qbar*SCbar*h_ply*zbar(i)*concentration;
end

%calculating total strain
x1= B(1,1)-(D(1,1)/B(1,1))*A(1,1)-(D(1,2)/B(2,2))*A(1,2);
x2=-(D(1,1)/B(1,1))*A(1,2)-(D(1,2)/B(2,2))*A(2,2);
x3=(D(1,1)/B(1,1))*(NT(1,1)+NS(1,1)+NH(1,1))+(D(1,2)/B(2,2))*(NT(2,1)+NS(2,1)+NH(1,1));

y1=-(D(1,2)/B(1,1))*A(1,1)-(D(2,2)/B(2,2))*A(1,2);
y2= B(2,2)-(D(1,2)/B(1,1))*A(1,2)-(D(2,2)/B(2,2))*A(2,2);
y3=(D(1,2)/B(1,1))*(NT(1,1)+NS(1,1)+NH(1,1))+(D(2,2)/B(2,2))*(NT(2,1)+NS(2,1)+NH(1,1));

ex_total=((y2*(MT(1,1)+MS(1,1)+MH(1,1)-x3))-(x2*(MT(2,1)+MS(2,1)+MH(2,1)-y3)))/(y2*x1-y1*x2);
ey_total=((y1*(MT(1,1)+MS(1,1)+MH(1,1)-x3))-(x1*(MT(2,1)+MS(2,1)+MH(2,1)-y3)))/(y1*x2-y2*x1);

kx=(NT(1,1)+NS(1,1)+NH(1,1)-(A(1,1)*ex_total)-(A(1,2)*ey_total))/B(1,1);
ky=(NT(2,1)+NS(2,1)+NH(2,1)-(A(1,2)*ex_total)-(A(2,2)*ey_total))/B(2,2);

radius_1=1/kx;
radius_2=1/ky;
```

radius_1
radius_2